

UNCLASSIFIED

AD NUMBER
AD905714
NEW LIMITATION CHANGE
TO Approved for public release, distribution unlimited
FROM Distribution authorized to U.S. Gov't. agencies only; Administrative/Operational Use; Sep 1972. Other requests shall be referred to USA Ballistic Research Labs., Aberdeen Proving Ground, MD 21005.
AUTHORITY
USAARDC ltr, 8 Mar 1978

THIS PAGE IS UNCLASSIFIED

*File Copy*

BRL MR 2225

# BRL

AD9057146

MEMORANDUM REPORT NO. 2225

DETERMINATION OF MUZZLE VELOCITY CHANGES  
DUE TO NONSTANDARD PROPELLANT TEMPERATURE  
USING AN INTERIOR BALLISTIC COMPUTER SIMULATION

by

James F. O'Bryon

September 1972

Approved for public release; distribution unlimited.

BALLISTIC RESEARCH LABORATORIES  
ABERDEEN PROVING GROUND, MARYLAND

When this report is no longer needed, Department of the Army organizations will destroy it in accordance with the procedures given in AR 380-5. Navy and Air Force elements will destroy it in accordance with applicable directives. Department of Defense contractors will destroy the report according to the requirements of Section 14 of the Industrial Security Manual for Safeguarding Classified Information. All others will return the report to Director, U. S. Army Ballistic Research Laboratories, Aberdeen Proving Ground, Maryland

Secondary distribution of this report by originating or sponsoring activity is prohibited.

Additional copies of this report may be obtained from the Defense Documentation Center, Cameron Station, Alexandria, Virginia 22314

**This document contains information affecting the national defense of the United States within the meaning of the Espionage Laws, Title 18 U. S. C. Sections 793 and 794. The transmission or the revelation of its contents in any manner to an unauthorized person is prohibited by law.**

The findings in this report are not to be construed as an official Department of the Army position, unless so designated by other authorized documents.

BALLISTIC RESEARCH LABORATORIES

MEMORANDUM REPORT NO. 2225

September 1972

DETERMINATION OF MUZZLE VELOCITY CHANGES  
DUE TO NONSTANDARD PROPELLANT TEMPERATURE  
USING AN INTERIOR BALLISTIC COMPUTER SIMULATION

James F. O'Bryon

Exterior Ballistics Laboratory

Approved for public release; distribution unlimited.

RDT&E Project No. 1T562603A041

ABERDEEN PROVING GROUND, MARYLAND

[REDACTED]

B A L L I S T I C   R E S E A R C H   L A B O R A T O R I E S

MEMORANDUM REPORT NO. 2225

JFO'Bryon/mjm/jah  
Aberdeen Proving Ground, Md.  
September 1972

DETERMINATION OF MUZZLE VELOCITY CHANGES  
DUE TO NONSTANDARD PROPELLANT TEMPERATURE  
USING AN INTERIOR BALLISTIC COMPUTER SIMULATION

ABSTRACT

An interior ballistic computer model is used to study means of simulating the effects of firing weapons using propellants which are not conditioned to 70 degrees F. Functions of burning rate coefficient and propellant force are empirically determined and are used to simulate these effects on muzzle velocity for a wide variety of weapon systems in the current inventory. The simulated velocity changes are compared with data gathered from firings conducted at several discrete propellant temperatures. In the majority of cases, the precision in predicting the changes in muzzle velocity at any given temperature falls within the round-to-round velocity probable error at that same temperature. This method should prove to be sufficiently accurate to permit a significant reduction in the number of rounds fired to determine propellant temperature effects on velocity.

## TABLE OF CONTENTS

	Page
ABSTRACT . . . . .	3
LIST OF FIGURES . . . . .	7
I. INTRODUCTION . . . . .	9
II. STANDARD TEMPERATURE TRAJECTORIES . . . . .	10
III. ITERATION TO DETERMINE ENGRAVING RESISTANCE PRESSURES . . . . .	20
IV. METHODS OF SIMULATING NONSTANDARD PROPELLANT TEMPERATURE . . . . .	22
V. EMPIRICAL DETERMINATION OF PARAMETER TEMPERATURE SENSITIVITY . . . . .	29
VI. DISCUSSION OF RESULTS . . . . .	44
VII. CONCLUSIONS . . . . .	58
REFERENCES . . . . .	60
APPENDIX A: Engraving Pressure Iteration . . . . .	63
APPENDIX B: Standard Interior Trajectory Plots . . . . .	65
APPENDIX C: Propellant Characteristics . . . . .	108
APPENDIX D: Characteristics of 8-Inch Howitzer, M2 . . . . .	109
DISTRIBUTION LIST . . . . .	111

# LIST OF FIGURES

Figure		Page
1	Comparison of Observed and Theoretical Velocity/Time Curves for 105mm Howitzer, M2A2 Firing HE, M1, Zone 1	18
2	Comparison of Observed and Theoretical Velocity/Time Curves for 105mm Howitzer, M2A2 Firing HE, M1, Zone 7	19
3	Engraving Pressure Profile . . . . .	20
4	Propellant Geometries . . . . .	25
5	Effects of Adjustment of Burning Rate Coefficient on Velocity and Maximum Chamber Pressure . . . . .	30
6	Effects of Adjustment of Propellant Force on Velocity and Maximum Chamber Pressure . . . . .	31
7	Comparison of British vs U.S. Propellant Burning Rate Coefficients . . . . .	40
8-13	Propellant Burning Surface Area Variations for a Variety of U.S. Army Weapons . . . . .	43

## I. INTRODUCTION

The standard procedure for obtaining data on the performance of weapons using propellants which are not at a standard temperature of 70 degrees Fahrenheit is to carry out an extensive firing program using propellants conditioned at predetermined temperature levels. For most weapons, this consumes hundreds of rounds as well as much time and effort.

In BRL Report No. 1183<sup>1\*</sup>, a series of equations are presented to describe the interior ballistic performance of a gun. Included in the reference are equations of state, energy, projectile motion and burning rate along with other related formulas.

These equations were used as the primary computer simulation for this report. Its basic assumptions are:

1. The total chemical energy available in the gun is the sum of the chemical energies of the individual propellants being burnt;
2. The total gas pressure is the sum of the "partial pressures" resulting from the burning of the individual propellants;
3. At the time the problem is started the igniter is burned out and all propellants are burning on their exposed surfaces;
4. All of the following energy losses are determined:
  - a. Kinetic energy of projectile, propellant gas, and unburnt propellant;
  - b. Heat energy lost to gun; \*\*
  - c. Energy lost in engraving the rotating band and in overcoming frictional resistance;
  - d. Energy lost in overcoming air shock pressure down the bore; \*\*

---

*\*References are listed on page 60.*

*\*\*These portions of the simulation were added to the model at a later date and are therefore not described in Reference 1.*

5. At any instant in time, the propellants burn at the space-mean pressure determined by the gas temperature and the volume between the breech face and the projectile base;

6. The ratios between the space-mean pressure and the propellant base pressure, and between the projectile base pressure and the breech pressure are constant. These ratios are a function of the propellant weight to projectile weight ratio and the specific heat ratio of the propellant gases.

By using the interior ballistic computer simulation referenced above with a minor modification to determine engraving pressure, the effects of changes in propellant temperature on burning rate coefficient and propellant force are determined empirically by matching the program output of muzzle velocity and maximum chamber pressure with actual firing data at several discrete temperatures.

## II. STANDARD TEMPERATURE TRAJECTORIES

The weapons studied in this report encompass a wide range of those in current use. The velocities range from just over 300 fps for zone 1 of the 81mm Mortar, M29 to velocities in excess of 4800 fps for the 105mm, M68, APDS system. The projectiles vary in weight from 9.12 pounds for the 81mm, M29 Mortar firing HE, M374 to 200 pounds for the 8-inch Howitzer, HE, M106 shell. The projectile shapes include fin- and spin-stabilized mortars, a disposable-sabot round and large and small spin-stabilized artillery. The propellants encompass a wide variety of geometries and chemical compositions.

Most input data necessary to simulate a trajectory are determined statically. These include:

### 1. Projectile

#### a. Fuzed weight

## 2. Propellant

- a. Weight
- b. Geometry (spherical, rectangular, cylindrical)
- c. Chemical properties
  - (1) Force
  - (2) Burning rate coefficient
  - (3) Covolume
  - (4) Density
  - (5) Flame temperature
  - (6) Specific heat ratio

## 3. Igniter

- a. Weight
- b. Force
- c. Specific heat ratio
- d. Flame temperature

## 4. Weapon

- a. Tube length
- b. Chamber volume
- c. Diameter of bore
- d. Maximum design pressure
- e. Surface area of chamber

## 5. Miscellaneous

- a. Air pressure in tube before ignition
- b. Ambient air temperature in tube before ignition
- c. Specific heat ratio of air

The roles of most of these parameters in the model are described in detail in Reference 1.

Several input parameters were not known. These include:

1. Heat loss coefficient;
2. Propellant erosion coefficient;
3. Shot start pressure;
4. Engraving resistance pressure.

Two of the four parameters, heat loss and propellant erosion, were estimated by matching the computer prediction to experimental results for the 8-inch Howitzer, M2 fired at standard propellant temperature. Fixed values of both parameters were subsequently assigned.

A fixed value of .45 was used for the heat loss constant which is used in estimating the amount of energy lost from the propellant gas to the barrel walls. Propellant erosion (dimensionless) which is directly proportional to the velocity of the burning propellant grains is an additive factor to the burning rate equation. It was fixed at 0.00001 for single perforated propellant grains and 0.00004 for all other grain configurations. Shot start pressure was set at zero since its effect is absorbed in the engraving resistance pressure.

Sensitivity studies were performed on these unknown parameters to determine their relative influence during the interior ballistic cycle in the gun. Of these four parameters, adjustment of engraving resistance pressure exerted the greatest influence on the trajectories calculated by the model.

Engraving resistance pressure exerted a major influence on both the chamber pressure/time and chamber pressure/travel curves generated. The energy lost in engraving and overcoming tube friction has been estimated<sup>2</sup> at 4 or 5 percent of the kinetic energy of the shot or approximately 2 percent of the total propellant energy.<sup>3</sup>

It was decided to determine the engraving resistance pressures empirically by adjusting their values until the simulation yielded muzzle velocities and maximum chamber pressures consistent with observed data. In doing so, engraving pressure was absorbing all other energy losses not determined by the model as well as the discrepancies between the estimated and actual energy losses of the other parameters. These include energy lost in recoil, rotational motion of the projectile, expansion of the barrel walls and gas leakage.

Serebryakov<sup>4</sup> suggests that the energy lost in air leakage "can be entirely omitted as a negligible quantity." The total energy lost in rotation of the projectile and translation of recoil parts is approximately 1.0 percent.<sup>5</sup> The strain energy loss in expanding the barrel walls is usually less than 1.0 percent of the energy of the shot.<sup>6</sup>

Some studies<sup>7,8</sup> have been undertaken in attempts to determine experimentally the resistance due to engraving of the band. Static tests where the projectile is hydraulically drawn down the bore have yielded levels of resistance which differ widely from other tests performed under actual firing conditions. This is due, in part, to the fact that the temperatures and pressures in the chamber during the slow hydraulic process are not comparable to those which occur when combustion takes place. Although there is disagreement as to the level of resistance pressure, most authors agree that the position of maximum engraving pressure is near a point where half of the band has undergone engraving. The exact position depends upon the geometry of the band, the geometry of the projectile just behind the band, the degree of ramming, and the composition of the rotating band material itself.

The maximum diameter of most spin-stabilized shells and hence the point of maximum resistance to motion is situated where the rotating band is affixed to the shell body. For most fin-stabilized projectiles, the maximum diameter is located at the obturator band. Table I

contains data for the band configurations on the subject projectiles.

Table I. Band Configurations

Weapon	Band Type	Composition	Band Width Inches	Estimated Travel to Maximum Resistance Inches
8-inch Howitzer, M2 Firing HE, M106	Rotating Band	Gilding Metal	1.000	0.500
175mm Gun, M113 Firing HE, M437	Rotating Band	Gilding Metal	1.067	0.534
155mm Howitzer, M114 Firing HE, M107	Rotating Band	Gilding Metal	0.875	0.438
155mm Howitzer, M109 Firing RAP, M549	Rotating Band	Gilding Metal	1.460	0.730
105mm Gun, M68 Firing APDS, M392A2	Rotating Band*	Fiber	1.650	0.825
4.2-inch Mortar, M30 Firing HE, M329A1	Base Plate	Gilding Metal	0.350	0.350
81mm Mortar, M29 Firing HE, M374	Obturator Band	Delrin	0.200	0.100

*\*The rotating band is located on discarding sabot.*

For this report, the engraving resistance was assumed to increase linearly from the start of engraving achieving a maximum at a point where exactly half of the band had been engraved. It was then assumed to decrease linearly to a point where the projectile had finally traveled the entire width of the band. From this point to the end of the bore, the engraving resistance was assumed to remain constant.

The only exception to this assumption is the 4.2-inch Mortar, M30, Firing HE, M329A1. This projectile uses a base plate rather than a rotating band to impart spin. The shape of the base plate is such that engraving does not occur for the first portion of travel since the plate is made with a slight radius at the edge rather than blunt edges like most rotating band configurations. Hence, engraving for the projectile was assumed to begin when the projectile had traveled half the width of the base plate. From this point, the resistance due to engraving was assumed to increase linearly up to a maximum point occurring where the entire base plate had been engraved. This level was then maintained throughout the remainder of travel.

All engraving resistance levels were first estimated. Then an iteration routine in the model adjusted them until a trajectory yielded, for a propellant temperature of 70 degrees Fahrenheit, a maximum chamber pressure ( $P_m$ ) that was within 100 psi of the experimentally observed value and within 1 fps of the experimentally observed muzzle velocity ( $V_o$ ).

These tolerance levels were chosen because they are consistent with the precision probable errors of the velocity and pressure measuring devices most commonly used for these firings, magnetic coils for velocity measurement<sup>9</sup> and crusher gauges for maximum chamber pressure.<sup>10</sup> The procedure just described was followed for various zones of all systems studied. These include:

1. 8-inch Howitzer, M2 Firing Projectile, HE, M106, Propelling Charge M1 (zones 1-5) (single perforation) and Propelling Charge M2 (zones 5-7) (multiple perforation);
2. 175mm Gun, M113, M107 Firing Projectile, HE, M437 Mods Propelling Charge M86 (zones 1-3) (multiple perforation);
3. 155mm Howitzer, M114 Firing Projectile, HE, M107, Propelling Charge M3 (zones 1-5) (single perforation) and Propelling Charge M4A1 (zones 3-7) (multiple perforation);

4. 155mm Howitzer, M109 Firing Projectile, HE, RAP, M549 Propelling Charge M3A1 (zones 1, 3, 5) (single perforation) and Propelling Charge M4A2 (zones 3, 5, 7) (multiple perforation);
5. 105mm Gun, M68, Firing APDS, M392A2 (multiple perforation);
6. 4.2-inch Mortar, M30, Firing HE, M329A1 (disc and sheet);
7. 81mm Mortar, M29 Firing HE, M374 (disc).

To help clarify the data reduction path taken in this report, a brief summary of the sequence of analyses appears below.

1. Using the iteration routine in the simulation, adjust engraving resistance pressures until the trajectory yielded by the model coincides within 1 fps in muzzle velocity and 100 psi in maximum chamber pressure of experimentally measured values. A distinct engraving resistance profile is determined in this manner for every zone of every system listed above.

2. Use the 8-inch Howitzer, M2 system as a test case to determine the temperature sensitivity of burning rate coefficient ( $\beta$ ) expressed in in/sec/psi and propellant force (F) expressed in ft lb/lb. For every single and multiple perforation zone of this system, adjust ( $\beta$ ) and (F) simultaneously until the changes in muzzle velocity and maximum chamber pressure yielded by the model are the same within 1 fps and 100 psi respectively of those changes observed in test firings at several discrete propellant temperatures.

3. Fit these empirically determined changes in ( $\beta$ ) and (F) with respect to propellant temperature. One pair of fits is made for the single perforated grain zones and another pair for the multiple perforated grain zones of the 8-inch Howitzer system.

4. Take these same fits and examine the model's ability to simulate the effect of propellant temperature change on muzzle velocity for all of the other weapon systems listed above. Use the fits of ( $\beta$ ) and (F) based on the single perforated 8-inch Howitzer zones to simulate propellant temperature changes in all other systems listed above

that use single perforated charges. Likewise, use the fits of ( $\beta$ ) and (F) based on the 8-inch Howitzer multiple perforation zones to simulate propellant temperature changes in all remaining systems listed above.

5. Compare the velocity changes "predicted" by the model with data gathered from actual propellant temperature firings.

The simulation can provide plots of projectile travel, velocity, and chamber pressure versus time for selected trajectories. A comparison of these plots with those from actual range firings indicates that the computer model trajectories are very representative of the experimental data being simulated. Figures 1 and 2 are typical examples of the level of agreement. The simulation velocities shown in these figures agree exactly with firing table velocity standards while the experimental velocities, by virtue of the fact they are individual round observations, disagree slightly with the standard velocities. The curves would be in even closer agreement if the experimental velocities were equivalent to the firing table standards.

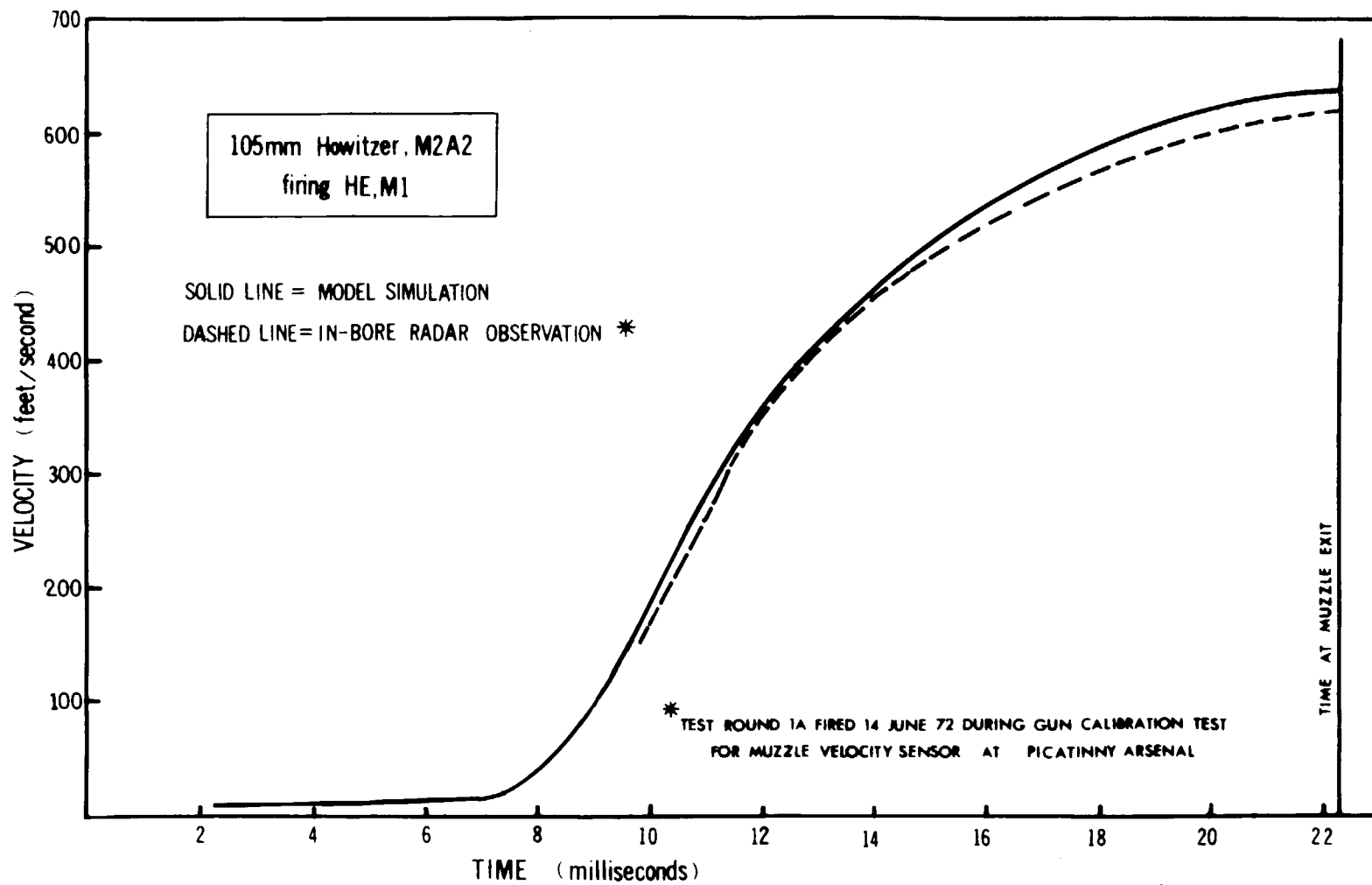


Figure 1. Comparison of Observed vs Theoretical Velocity : Time Curves (Zone 1)

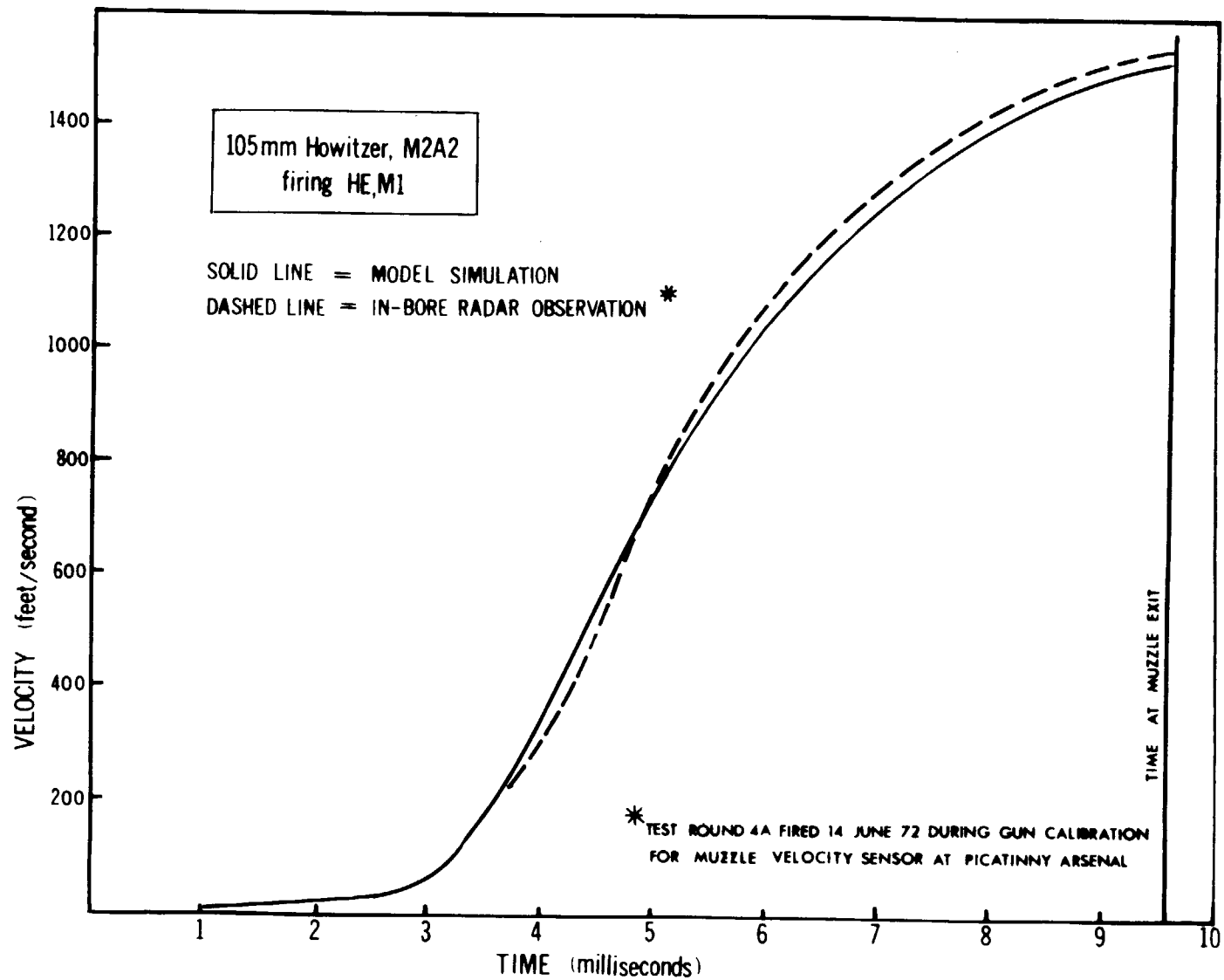


Figure 2. Comparison of Observed vs Theoretical Velocity : Time Curves (Zone 7)

### III. ITERATION TO DETERMINE ENGRAVING RESISTANCE PRESSURES

The interior ballistics computer model is capable of handling a variety of engraving resistance configurations. The data typically are assembled as a series of discrete levels of resistances, each corresponding to a specific projectile travel distance down the bore. Between levels, the program linearly interpolates for the resistance values. For this report the characteristic shape of the engraving profile is assumed to take the form indicated in Figure 3.

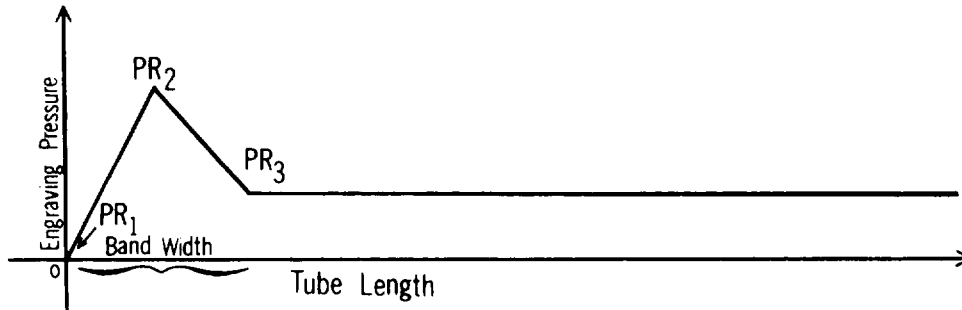


Figure 3. Engraving Pressure Profile

$(PR_1)$  = Initial Engraving Resistance Pressure

$(PR_2)$  = Maximum Engraving Resistance Pressure

$(PR_3)$  = Final Engraving Resistance Pressure Beginning at the Instant the Rotating Band is Completely Engraved and Constant Down Tube

Adjustment of either the maximum engraving resistance or the final engraving resistance, or both, simultaneously affects the muzzle velocity ( $V_o$ ) and maximum chamber pressure ( $P_m$ ) produced by the computer simulation. Since both ( $V_o$ ) and ( $P_m$ ) are readily available from range firings at standard propellant temperature (70 degrees Fahrenheit), an iteration routine was added to the simulation to enable it to adjust the engraving resistance levels until the muzzle velocity and maximum chamber pressure produced fell within specified tolerances.

In the 4.2-inch mortar system, iteration was performed on muzzle velocity alone since only (PR<sub>3</sub>) was adjusted due to base plate configuration. However, when a velocity match with experimental data was achieved, the resultant maximum pressure simulated was also in agreement within 200 psi of experimental data.

The following equations are solved in the iteration algorithm to determine the set of engraving resistances necessary to simulate a firing at 70 degrees Fahrenheit.

$$\Delta V_o = \frac{\Delta V_o}{\Delta PR_2} \cdot \Delta PR_2 + \frac{\Delta V_o}{\Delta PR_3} \cdot \Delta PR_3$$

$$\Delta P_m = \frac{\Delta P_m}{\Delta PR_2} \cdot \Delta PR_2 + \frac{\Delta P_m}{\Delta PR_3} \cdot \Delta PR_3$$

An example of the output from the iteration routine to determine engraving resistance levels is included in Appendix A.

Agreement with experimental data is achieved to within 1 fps for (V<sub>o</sub>) and 100 psi for (P<sub>m</sub>). This same iteration routine is performed on every zone of every weapon system listed on page 14. Once the simulation achieves a "match" with observed data, the engraving profiles are fixed and the iteration routine bypassed.

The plots simulating firings at standard propellant temperature (70 degrees Fahrenheit) for all systems listed on page 14 are contained in Appendix B. Included on each plot are the values of the engraving resistance pressures used to yield each trajectory. Since, it has been pointed out, engraving pressure is absorbing all other energy losses not accounted for in the model, its level changes significantly from zone to zone.

Standard muzzle velocities and maximum chamber pressures to be matched were obtained from reports by Anderson<sup>11</sup> and Heppner.<sup>12</sup>

#### IV. METHODS OF SIMULATING NONSTANDARD PROPELLANT TEMPERATURE

To this point in the analysis, the simulation has produced trajectories matching maximum chamber pressure and muzzle velocity of firings with propellant at 70 degrees Fahrenheit. This has been done for every zone of every weapon included in this report.

Next, a method of representing hot or cold propellant in the model had to be determined. Since propellant temperature itself was not a direct input to the model, other parameters affected by temperature change had to be adjusted to represent this condition.

Propellant surface area is one parameter affected by temperature change. Corner<sup>13</sup> suggests that the area increases approximately 0.17 to 0.22 percent for every 10 degrees Fahrenheit increase in temperature. Trajectory simulations were performed to determine the sensitivity of the model to rates of change of propellant surface area. Since the propellants were of such a variety of geometries and compositions, two types of studies were made; one, assuming that the coefficient of linear expansion was the same in all directions; and two, where the propellants were assumed to be highly anisotropic.

The results indicated that the effects of decreasing the grain surface area were to increase muzzle velocity and maximum chamber pressure rather than decrease them as is observed when firing at low temperatures. The reverse process occurred when burning surface was increased. Hence, adjusting burning surface area as a function of propellant temperature is not adequate in simulating the performance of propellants fired at hot and cold temperatures. It is useful, however, when used in conjunction with other parameters. This aspect is described in more detail on page 55.

Historically, it has been known that propellant burning rate coefficient and propellant force are also affected by temperature conditioning. These parameters shall be referred to extensively throughout the remainder of this report so they are defined below.

$(\beta)$  = propellant burning rate coefficient expressed in  $\frac{\text{in./sec}}{\text{psi}^\alpha}$

$(F)$  = propellant force expressed in inch-pounds/pound

A complete description of the role of these parameters in the mathematical model is contained in Reference 1.

Some interior ballisticians have determined the variations of  $(\beta)$  and  $(F)$  for a given propellant temperature change for a variety of charge geometries and compositions by conducting closed chamber firings. Hunt<sup>14</sup> describes an empirical method of approximating the effect of propellant temperature on muzzle velocity by applying percentage changes in  $(\beta)$  and  $(F)$  for a 10-degree Fahrenheit change in propellant temperature based on closed chamber measurements. Table II is a summary of these effects on a variety of British propellants.

Table II. Rate of Burning and Force Coefficients with Initial Temperature Effects for British Propellants

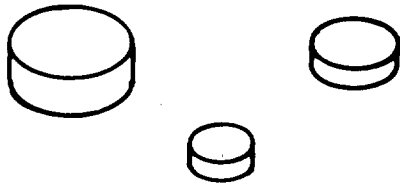
Propellant	Effect of 10 Degrees Fahrenheit Variation in Initial Temperature	
	$d\beta/\beta$ Percent	$dF/F$ Percent
MD	*	0.15
W	1.6	0.15
WM	2.2	0.15
SC	2.0	0.17
HSC	2.0	0.13
A	1.9	0.18
AN	1.8	0.20
ASN	0.9	0.22
N	1.0	0.22
NQ	0.9	0.19
NFQ	1.0	0.22
NCT	*	0.17
NH	0.9	0.17
FNH/P	0.7	0.21

\* *There are no reliable figures available*

Most British propellants are of the "cord" type, long slender cylindrical geometry. Those of the U.S., however, are found in a wide variety of shapes including cylinders (with both single and multiple perforation), spheres, rectangles, sheets, discs and flakes. Appendix C lists the chemical composition, burning rate coefficient and propellant force of each charge studied in this report. Figure 4 shows the relative geometrical sizes and shapes of the grains of these same charges.

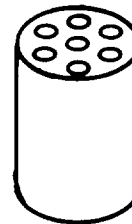
Figure 4. PROPELLANT GEOMETRY

81 MM MORTAR, M29



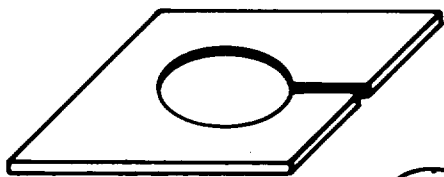
M9 COMPOSITION

105 MM GUN, M68



M30 COMPOSITION

4.2 INCH MORTAR, M30



M8  
COMPOSITION



M9  
COMPOSITION

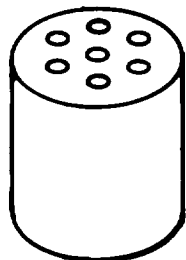
155MM HOWITZER, M114A1



M1 COMPOSITION

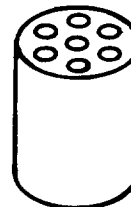


175 MM GUN, M113



M6 COMPOSITION

8 INCH HOWITZER, M2



M1 COMPOSITION



The igniters of the propellants varied in composition and weight from weapon to weapon. Table III summarizes the chemical and physical properties of the igniters used in the subject weapons. Igniter weights are taken from Anderson.<sup>16</sup>

Table III. Igniter Data Summary

Weapon	Igniter Type	Igniter Weight Grains	Igniter Force In.-Lb/Lb	Igniter Gamma	Flame Temperature Degrees K
8-inch Howitzer, M2 Firing HE, M106	Black Powder	2188.	1152000.	1.250	2000.
175mm Gun, M113 Firing HE, M437	Black Powder	6344.	1152000.	1.250	2000.
155mm Howitzer, M114 Firing HE, M107	Black Powder	1312.	1152000.	1.250	2000.
155mm Howitzer, M109 Firing RAP, M549	Clean Burning	1531.	4138200.	1.235	3034.
105mm Gun, M68 Firing APDS, M392A2	Benite Strips	831.	4154160.	1.235	3030.
4.2-inch Mortar, M30 Firing HE, M329A1	Black Powder	130.	1152000.	1.250	2000.
81mm Mortar, M29 Firing HE, M374	Black Powder	1.65	1152000.	1.250	2000.

Studies<sup>17,18</sup> of the performance characteristics of igniters indicate that their combustion is only slightly affected by extreme temperatures. Recent firings<sup>19</sup> were conducted at Aberdeen Proving Ground with the 105mm Howitzer, M2A2 using temperature conditioned black powder and clean burning igniter (CBI). These igniter firings were performed with Projectile, HE, M1 in firing position. The igniters were fired with no propellant occupying the chamber. Table IV summarizes a portion of the results of this test.

Table IV. Igniter Temperature Sensitivity

Igniter Temperature Degrees F	Black Powder			Clean Burning Igniter		
	Mean Pressure psi	Probable Error psi	Igniter Weight Grains	Mean Pressure psi	Probable Error psi	Igniter Weight Grains
- 50	243.4	9.98	306	680.2	69.73	224
70	297.5	8.79	306	735.1	67.27	224
145	264.0	2.78	306	753.0	41.27	224

The weight of the clean burning igniter fired was not equal to that of the black powder because the same weight of clean burning igniter would not fit into the brass primer cylinder.

A linear least-squares fit of ignition pressure versus igniter temperature was performed with the following results.

#### Black Powder

$$\Delta P = .1447 * \Delta T \quad (\text{ERMS} = 23.9 \text{ psi})$$

#### Clean Burning Igniter

$$\Delta P = .3789 * \Delta T \quad (\text{ERMS} = 88.4 \text{ psi})$$

where  $\Delta P$  = change in ignition pressure (psi)

$\Delta T$  = change in igniter temperature (degrees Fahrenheit)

For a temperature span of -50 degrees Fahrenheit to 125 degrees Fahrenheit, black powder igniter pressure varied from 93.7 percent standard up to 103.9 percent standard for the highest temperature, well within the root-mean-square error of the fit itself. Similar results were obtained for the clean burning igniter.

To determine the relative effect of using hot or cold temperature conditioned igniter in the 8-inch Howitzer, these same percentage changes were applied to zones 1 and 7 at both -50 degrees Fahrenheit and 125 degrees Fahrenheit. The model determined that the change in ignition pressure influenced the muzzle velocity and maximum chamber pressure less than 0.5 fps and 50 psi, respectively. The influences of igniter temperature extremes on zone 7 were even less than that for zone 1.

Hence, igniter force and other igniter parameters were not adjusted when simulating firings at temperature extremes. The pressure generated by the ignition cartridge at 70 degrees Fahrenheit was used as the initial condition in integrating the burning rate equations for the propellants for all weapons and temperatures.

## V. EMPIRICAL DETERMINATION OF PARAMETER TEMPERATURE SENSITIVITY

The 8-inch Howitzer, M2 firing HE, M106 projectile was chosen as the first system to examine in simulating the effects of propellant temperature on muzzle velocity and maximum chamber pressure. This system was selected because of its broad velocity span, abundance of available experimental data and the fact that its charge system is composed of both single perforation degressive burning grains and multiple perforation progressive burning grains.

It is an eight zone system with zones 1-5 (M1) single perforated cylinders and zones 5-7 (M2) multiple perforated cylinders. The igniter for these zones is composed of 2188 grains of black powder.

The characteristics of this weapon system are given in Appendix D.

It was not known at first what levels of burning rate coefficient and propellant force would be needed as inputs to the model to enable it to produce ( $V_o$ ) and ( $P_m$ ) comparable to those encountered under actual firing conditions. Experimental data on the 8-inch Howitzer, including those at nonstandard temperatures were gathered from Aberdeen Proving Ground Firing Records No. 19080 (1940), No. 61809 (1955), No. 69187 (1962), and Yuma Test Station Firing Records No. Y4594 (1962), No. Y4657 (1962), No. Y4557 (1962), No. Y4786 (1963), and No. Y2011 (1964).

When firing at nonstandard propellant temperature, both ( $V_o$ ) and ( $P_m$ ) are affected. If only the burning rate is adjusted, nonstandard muzzle velocity can be simulated. However, by simultaneously allowing both ( $\beta$ ) and ( $F$ ) to vary, a match of both muzzle velocity and maximum chamber pressure can be achieved to within specified tolerances. Agreement to within 1 fps in velocity and 100 psi in maximum chamber pressure was considered a "match."

The effects on the interior ballistic trajectory when adjusting ( $\beta$ ) and ( $F$ ) are shown in Figures 5 and 6. They represent firings of the 8-inch Howitzer, M2, zone 1.

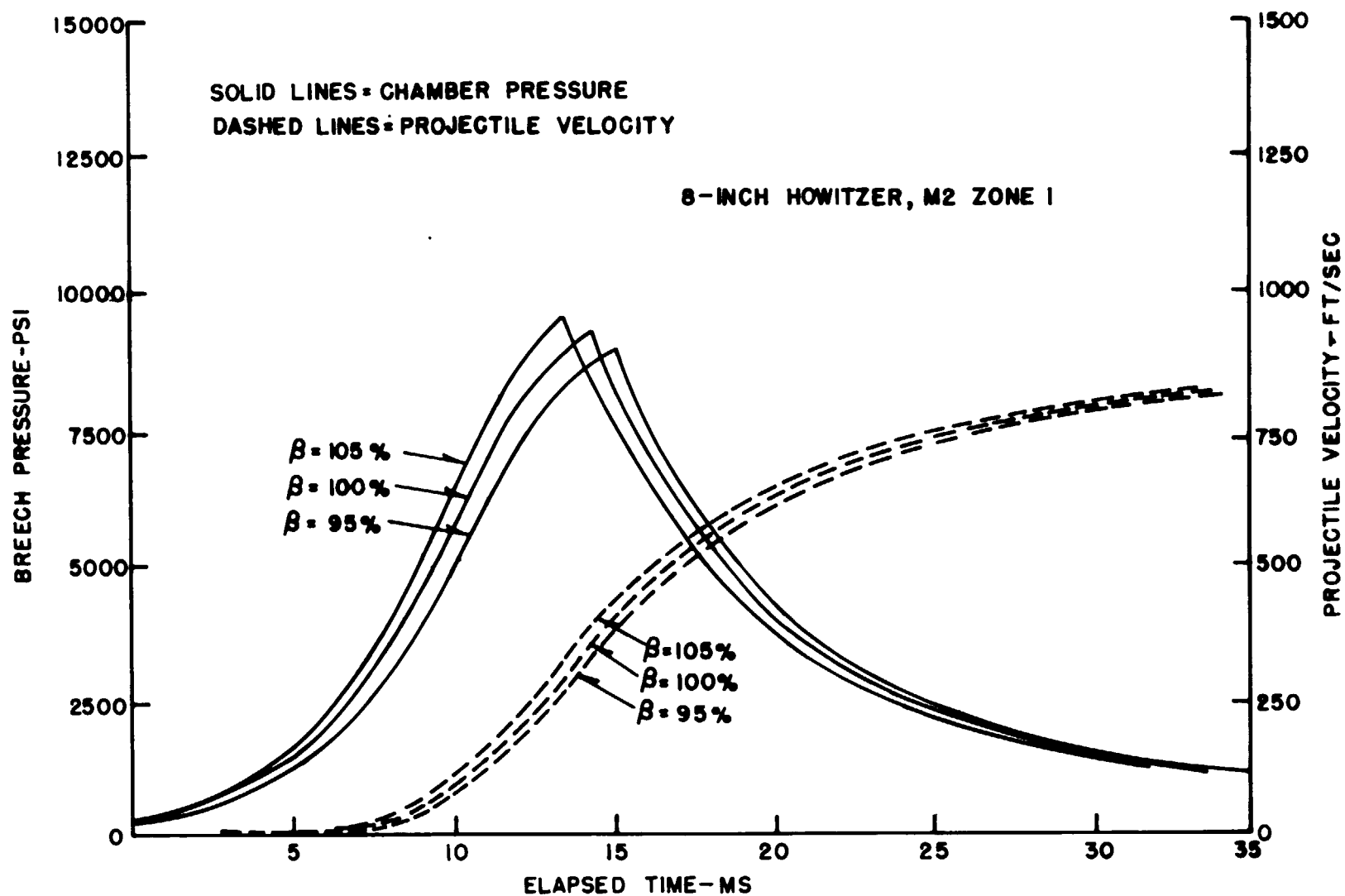


Figure 5. Effects on Projectile Velocity, Chamber Pressure vs Time When Adjusting Burning Rate Coefficient (Propellant Force at 100 % Standard)

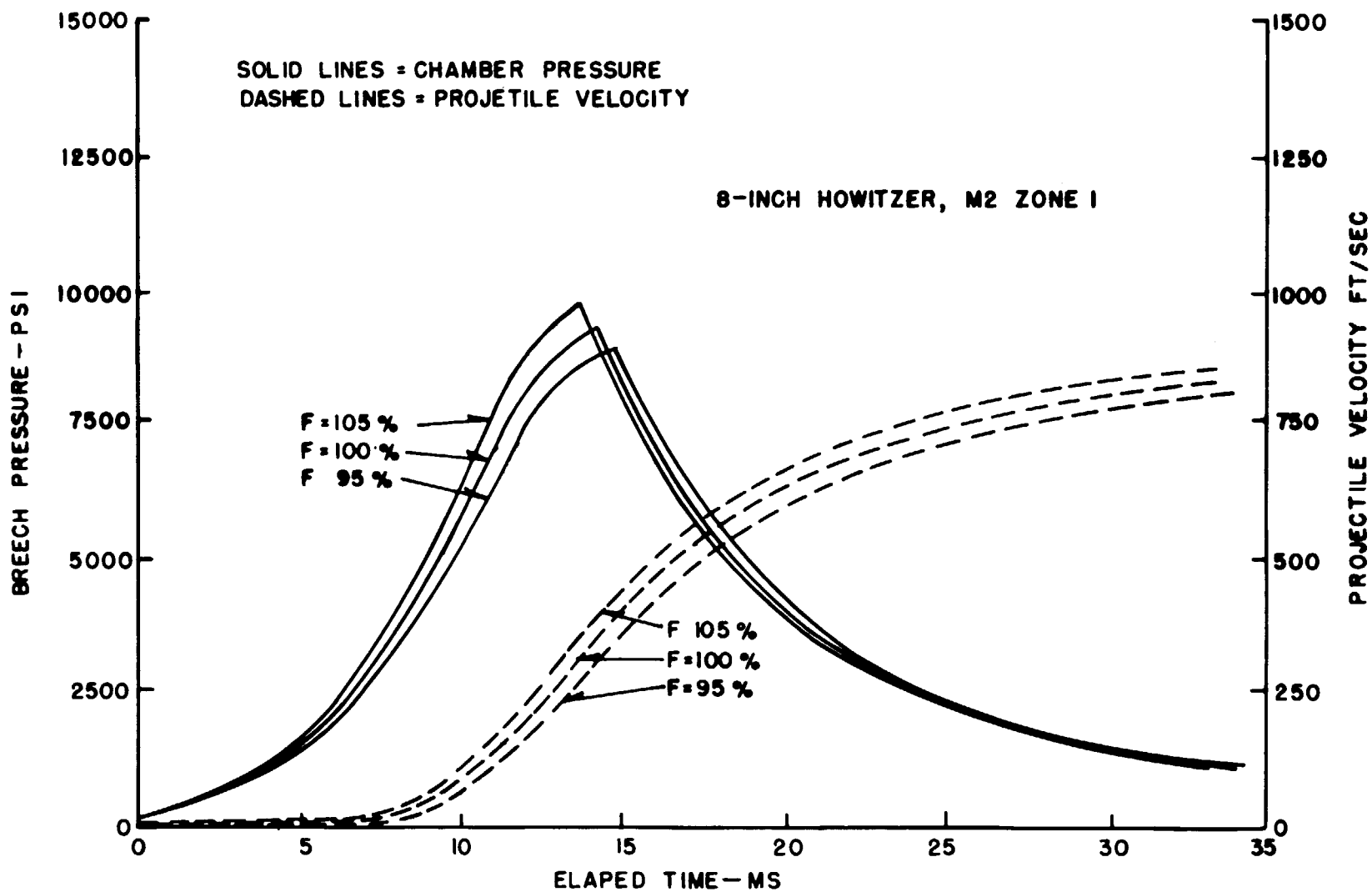


Figure 6. Effects on Projectile Velocity, Chamber Pressure vs Time When Adjusting Propellant Force (Burning Rate Coefficient at 100% Standard)

For every zone of the 8-inch Howitzer system, burning rate coefficient and force were adjusted simultaneously until together the muzzle velocity and maximum chamber pressure produced "matched" experimental data. Table V is a zone-by-zone summary of the results.

Table V. Temperature Sensitivity of ( $\beta$ ) and (F) for the 8-inch Howitzer, M2 Firing HE, M106

Percent Standard ( $\beta$ ) and (F) Needed to Simulate Observed Velocity and Maximum Chamber Pressure Changes at Selected Propellant Temperatures

Propellant Temperature Degrees Fahrenheit	Adjusted Parameter	M1 Single Perforation					M2 Multiple Perforation		
		Zone 1	Zone 2	Zone 3	Zone 4	Zone 5	Zone 5	Zone 6	Zone 7
		Percent Standard					Percent Standard		
- 50	( $\beta$ )	77.5	77.4	76.7	76.5	76.8	89.1	88.3	87.3
	(F)	99.0	99.0	100.1	99.5	99.7	99.8	100.0	100.0
- 10	( $\beta$ )	81.8	81.9	81.7	81.4	81.7	93.4	91.9	90.8
	(F)	99.5	99.4	99.4	99.8	99.9	100.0	99.9	99.9
30	( $\beta$ )	86.8	87.8	87.2	87.7	90.5	97.3	95.6	95.0
	(F)	100.0	99.8	99.8	100.0	99.9	99.9	100.0	100.0
70	( $\beta$ )	100.0	100.0	100.0	100.0	100.0	100.0	100.0	100.0
	(F)	100.0	100.0	100.0	100.0	100.0	100.0	100.0	100.0
100	( $\beta$ )	113.7	114.9	115.1	111.2	110.3	102.8	103.8	104.6
	(F)	100.1	100.0	100.0	100.0	100.0	100.0	100.0	99.9
130	( $\beta$ )	126.8	133.1	133.8	130.0	127.7	105.5	107.3	109.0
	(F)	100.1	100.0	100.1	100.0	100.0	100.0	100.1	100.0

When the  $(\beta)$  and  $(F)$  percentage changes are examined closely, one can readily see that the single perforation zones exhibit one level of sensitivity and the multiple perforation zones another level. Corner<sup>20</sup> points out that "the coefficient is substantially less in shapes that have narrow perforations, such as multitubular grains. This is believed to be due to the erosion process in the perforations having different temperature coefficients from the normal burning mechanism."

The percentage nominal  $(\beta)$  and  $(F)$  needed to match each temperature fluctuated slightly from zone-to-zone. These minor variations could be the result of a combination of factors.

First, the firing table data being matched are the results of smooth fits of change in velocity over the entire temperature span and not simply the mean observed velocity change at each specific propellant temperature.

Secondly, the convergence tolerances for the simulation of 1 fps in muzzle velocity and 100 psi in maximum chamber pressure were generally smaller than the probable errors in the observed data itself.

Finally, there may be influences on  $(V_o)$  and  $(P_m)$  not isolated in the simulation itself. Such things as density of loading, propellant burning surface area, igniter weight, and tube cross-sectional area were examined. These influences and others were studied using multiple regression techniques summarized later in this report.

The zone-to-zone fluctuations were minimal enough, however, to permit use of a fixed set of  $(\beta)$  and  $(F)$  functions across zones.

Tables VI and VII are summaries of the muzzle velocities and maximum chamber pressures achieved when using the percent standard changes in  $(\beta)$  and  $(F)$  listed in Table V. The velocity and pressure changes agree with data found in the referenced firing records as well as firing table FT 8-J-4 dated 1967.

Table VI. Muzzle Velocity Using Percent Standard Changes in Table V  
8-Inch Howitzer, M2 Firing HE, M106

Propellant Temperature Degrees Fahrenheit	Single Perforation					Multiple Perforation		
	Zone 1	Zone 2	Zone 3	Zone 4	Zone 5	Zone 5	Zone 6	Zone 7
	fps	fps	fps	fps	fps	fps	fps	fps
- 50	804.2	882.6	982.4	1131.6	1359.5	1329.8	1583.4	1888.3
- 10	809.6	887.8	988.0	1137.5	1365.9	1351.0	1602.8	1907.0
30	814.6	893.1	993.5	1143.4	1374.1	1368.4	1621.7	1928.8
70	820.3	899.3	1000.1	1150.6	1380.5	1381.0	1639.8	1950.0
100	825.0	904.1	1005.3	1155.3	1385.6	1392.4	1653.3	1966.2
130	830.3	909.7	1010.6	1161.7	1392.0	1402.5	1665.9	1982.2

Table VII. Maximum Chamber Pressure Using Percent Standard Changes in Table V  
8-Inch Howitzer, M2 Firing HE, M106

Propellant Temperature Degrees Fahrenheit	Single Perforation					Multiple Perforation		
	Zone 1	Zone 2	Zone 3	Zone 4	Zone 5	Zone 5	Zone 6	Zone 7
	psi	psi	psi	psi	psi	psi	psi	psi
- 50	7450	9250	11950	15750	25350	13800	20400	32400
- 10	7850	9800	12650	16800	26750	14400	21250	33750
30	8300	10450	13350	17950	28950	15000	22100	35400
70	9350	11550	14750	19900	31950	15450	23050	37300
100	10250	12600	16050	21000	33300	15900	23850	39150
130	11000	13900	17350	23100	35400	16350	24600	41150

The force coefficients in Table V are very close to nominal. However, ( $\beta$ ) cannot be sufficiently adjusted to absorb simultaneously the change in ( $V_o$ ) and ( $P_m$ ) being taken up by the nonstandard force. Velocity is more sensitive to small changes in ( $F$ ) than to changes in ( $\beta$ ), while pressure is almost equally sensitive to changes in ( $F$ ) and ( $\beta$ ). Table VIII is based on selected zones of the 8-inch Howitzer, M2, firing HE, M106.

Table VIII. Sensitivity of ( $\beta$ ) and ( $F$ ) for Selected Charges of 8-inch Howitzer

Zone	Change in ( $V_o$ ) For a 1% Change in		Change in ( $P_m$ ) For a 1% Change in	
	( $\beta$ )	F	( $\beta$ )	F
	f/s	f/s	psi	psi
1 (M1)	0.4	4.4	70	100
5 (M1)	0.6	7.2	600	600
5 (M2)	4.2	7.5	150	150
7 (M2)	3.9	9.6	400	300

As a result, simultaneous agreement of ( $V_o$ ) and ( $P_m$ ) with experimental data cannot be accomplished without adjusting both ( $F$ ) and ( $\beta$ ).

The unit changes in Table VIII are approximate and were obtained by simulating trajectories using plus and minus 1 percent standard ( $\beta$ ) and plus and minus 1 percent standard ( $F$ ). They are listed to show only their relative levels of sensitivity.

For example, Table V indicates that 77.5 percent standard burning rate coefficient and 99.0 percent standard propellant force were needed to simulate the velocity and maximum pressure changes that occur when firing zone 1 of the 8-inch Howitzer at -50 degrees Fahrenheit.

If it was desired to absorb this entire velocity and maximum chamber pressure change by adjusting only ( $\beta$ ), keeping propellant force at 100 percent standard, then at -50 degrees Fahrenheit, ( $\beta$ ) would have to absorb the extra 4.4 f/s velocity change and 100 psi chamber pressure that the 1 percent change in propellant force had contributed.

Based on Table VIII, (4.4/0.4) or approximately 11.0 percent ( $\beta$ ) must be subtracted from the already adjusted ( $\beta$ ) of 77.5 percent to a new level of 66.5 percent.

Turning to the resultant effect on pressure, an 11.0 percent change in ( $\beta$ ) will change ( $P_m$ ) by 770 psi where all that was desired was a change of 70 psi resulting in a mismatch of 700 psi in maximum chamber pressure from actual experimental data.

Corner<sup>21</sup> states that "the dependence of the rate of burning on the initial temperature is usually fairly linear over the range 0 to 120 degrees Fahrenheit." Hunt's<sup>22</sup> temperature coefficients were also linear over the temperature span from 35 to 125 degrees Fahrenheit. Linear fits were performed on the empirically determined data in Table V but since the temperature span encompassed was much broader, the linear fits of ( $\beta$ ) were poor, especially at the very low temperatures. Hence, a cubic form was chosen for ( $\beta$ ) and the least square equations are listed below. A linear fit for (F) provided sufficient accuracy over the temperature span. These equations are also given below.

For  $-50 \leq PT \leq 130$  degrees Fahrenheit

Single Perforation Grains

$$\Delta_{\beta_{PT}} = .3647138 (PT - 70) + .0020509 (PT - 70)^2 + .000005 (PT - 70)^3$$

$$\Delta_{F_{PT}} = .00386 (PT - 70)$$

Multiple Perforation Grains

$$\Delta_{\beta_{PT}} = .1094232 (PT - 70) + .0001751 (PT - 70)^2 + .0000007 (PT - 70)^3$$

$$\Delta_{F_{PT}} = .000621 (PT - 70)$$

where  $\Delta_{\beta}$  = Percent change in nominal burning rate coefficient necessary to simulate the performance of a propellant temperature equal to PT.

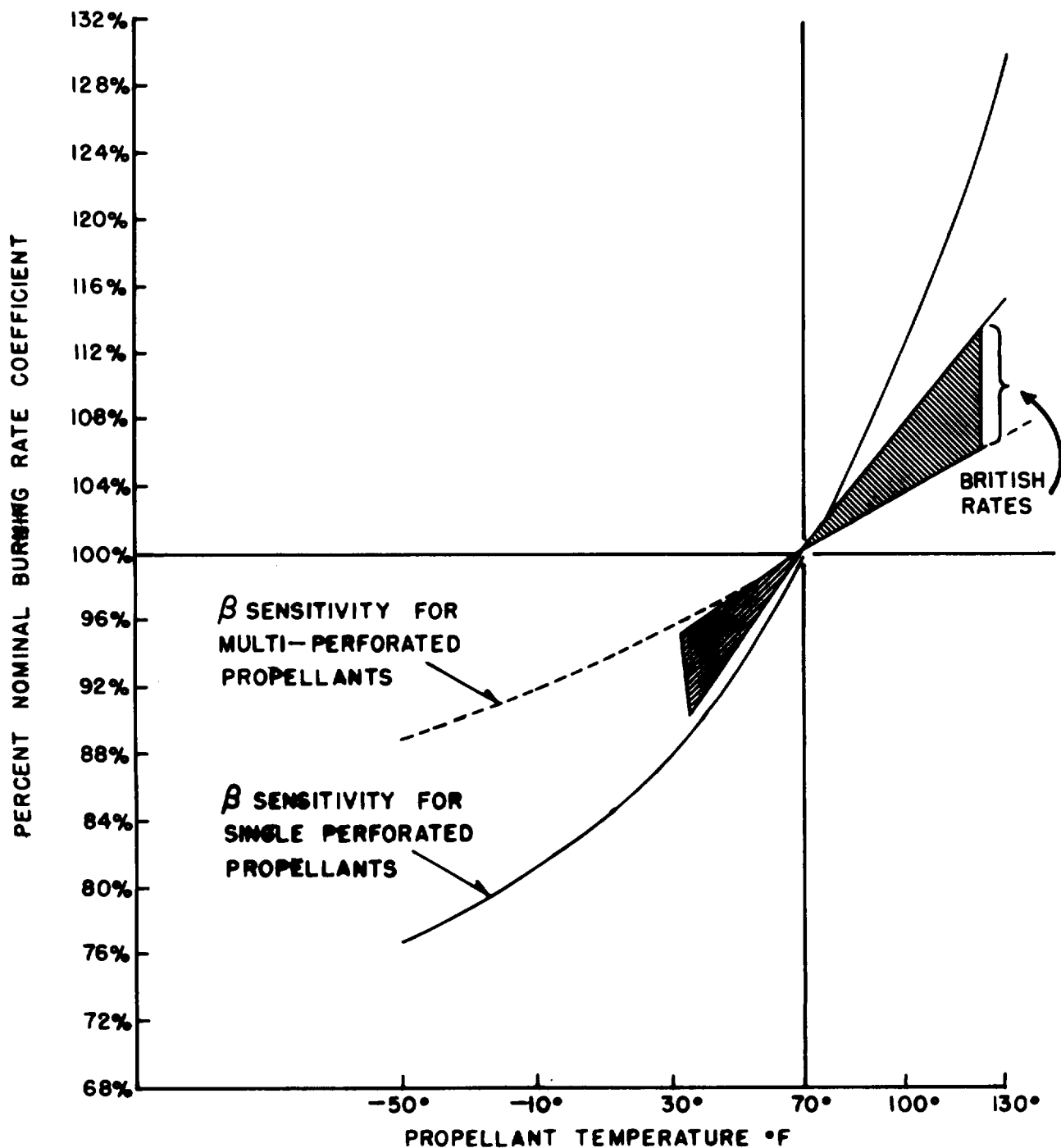
$\Delta_F$  = Percent change in nominal propellant force necessary to simulate the performance of a propellant temperature equal to PT.

PT = Propellant temperature expressed in degrees Fahrenheit.

The values of  $(\Delta_{\beta})$  and  $(\Delta_F)$  for a 10 degree Fahrenheit propellant temperature change are comparable to those of the British propellants listed in Table II.

Figure 7 shows the relative magnitude of the British temperature coefficients and the empirically determined percentage changes of all of the U.S. propellants included in this report.

Figure 7. COMPARISON OF BRITISH BURNING RATE COEFFICIENTS VS. EMPIRICALLY DETERMINED BURNING RATE COEFFICIENTS FOR U.S. PROPELLANTS



The data in Table IX are evaluations of the least squares fits of the 8-inch Howitzer data on page 38.

Table IX. Percent of Standard Propellant Force and Burning Rate Coefficients Used to Simulate Nonstandard Propellant Temperature

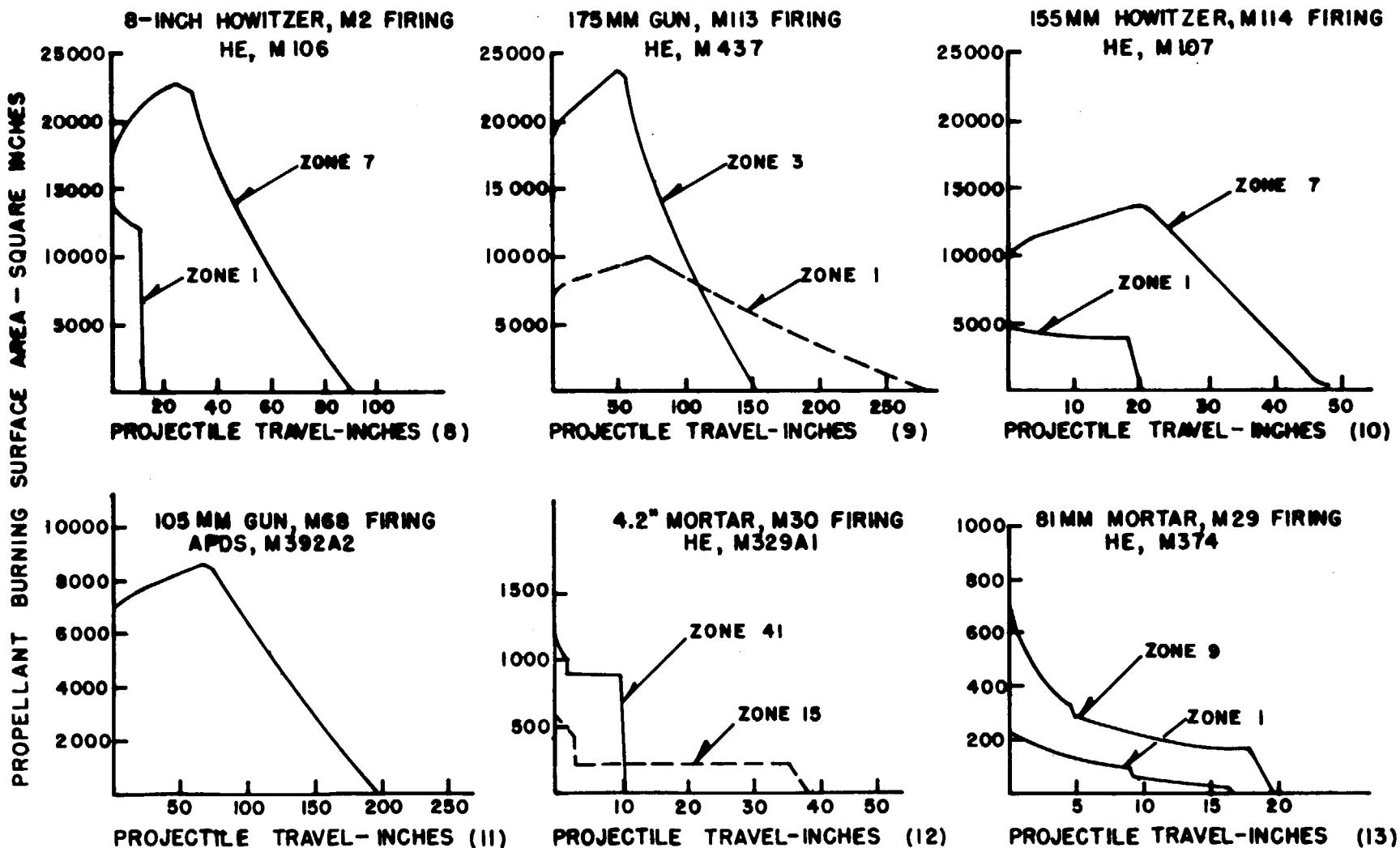
Single Perforation Propellant			Multiple Perforation* Propellant	
Propellant Temperature Degrees Fahrenheit	Percent Standard Burning Rate	Percent Standard Propellant Force	Percent Standard Burning Rate	Percent Standard Propellant Force
-50	77.0	99.5	88.2	99.9
-40	78.0	99.6	89.1	99.9
0	82.8	99.8	92.8	100.0
70	100.0	100.0	100.0	100.0
125	126.6	100.1	106.7	100.0

*\*The multiple perforation values were also used for disc and sheet configurations.*

It is obvious that the propellant force percentages listed in Table IX above do not influence the muzzle velocity and chamber pressure in the same manner and degree as do the burning rate coefficients. Both of these nonstandard conditions were retained and used simultaneously in the analysis because

1. It is a physical fact that both ( $\beta$ ) and ( $F$ ) are influenced by propellant temperature,
2. A simultaneous match of both ( $V_o$ ) and ( $P_m$ ) required at least as many degrees of freedom to compensate for them,
3. It facilitated a better match with experimental data across all weapons than when using a technique attributing all of the velocity changes to a nonstandard ( $\beta$ ).

Examination of the variety of charge shapes found in Figure 4 reveals that some of the propellants have degressive burning geometries (single perforated cylinders), some are progressive burning (multiple perforated grains), and still others exhibit constant burning surface. Figures 8-13 show the burning surface area as a function of travel for representative charges of the systems in this report.



Figures 8-13. PROPELLANT BURNING SURFACE AREA VARIATIONS FOR A VARIETY OF U. S. ARMY WEAPONS

For the mortar systems, which have a variety of disc and sheet propellants, it was found that the percentage changes of burning rate coefficient and force for the multiple perforated grains gave satisfactory results for both mortar systems examined.

No specific reason is known why the mortars which use degressive burning propellants should be successfully simulated using the empirical constants based on progressive burning multiple perforated grains.

One explanation could be related to the web sizes of the systems examined. The average web size of the mortar systems is closely aligned with those of the multiple perforated grains as illustrated in Appendix C.

## VI. DISCUSSION OF RESULTS

If a different family of empirical coefficients existed for  $(\beta)$  and  $(F)$  for every zone and weapon, this simulation technique would be no more effective than to show that it can compensate for one nonstandard condition by adjusting other nonstandard conditions. However, for any model to predict accurately the performance of a system with a prescribed set of initial conditions, there must be a systematic means of representing in the model the phenomena which are to be simulated. There must be a "common denominator".

Corner<sup>23</sup> suggests that the burning coefficients do not vary greatly from one propellant to another. This gives an indication that the coefficients generated from the 8-inch Howitzer (Table IX) might be adequate to simulate the muzzle velocity changes due to change in initial propellant temperature for the other weapon systems listed in Table III.

The computer model contains a parametric option feature which permits the ballistic model to run trajectories with various combinations of nonstandard burning rate coefficients and propellant forces. This feature was used in generating propellant temperature effects for all of the subject weapons using the same coefficients derived from the 8-inch Howitzer found in Table IX.

If fixed functions of ( $\beta$ ) and (F) were found to successfully simulate velocity change over a wide range of weapons, then the model and procedure described in this report could be used for 'predictive' purposes for other similar systems.

Tables X through XIX show the level of prediction precision of the model when using the same percent standard values in Table IX.

Traditionally, U.S. propellant temperature data used to generate firing table corrections are derived from experimental data which have been fitted using a general least-squares technique. Typically, it has the form

$$\Delta V_o = A(PT - 70) + B(PT - 70)^2$$

where  $\Delta V_o$  is the change in velocity from standard.

This form forces the fit through the 70 degrees Fahrenheit point with no correction to muzzle velocity at that temperature.

In some of the following tables, where, as the result of fitting, the firing table values are quite different from the actual observed mean velocity changes at specific temperatures, the unfitted mean observed values are also included for comparison. Since for the mortar systems, the firing table corrections are based on one fit for all zones rather than specific fits for each zone, the unfitted mean observed velocity changes for these specific zones and temperatures are also included for comparison.

Table X. Muzzle Velocity Corrections For Nonstandard Propellant  
Temperature 8-inch Howitzer, M2, Firing  
Projectile, HE, M106

Single Perforation Propellant					
Propellant Temperature Degrees Fahrenheit	1	2	Zone 3	4	5
	M/S	M/S	M/S	M/S	M/S
-50	-4.9* (-4.3)	-5.1 (-4.4)	-5.4 (-4.6)	-5.8 (-5.8)	-6.4 (-6.8)
0	-3.1 (-2.7)	-3.2 (-2.8)	-3.3 (-2.8)	-3.5 (-3.7)	-3.9 (-4.3)
70	S T A N D A R D				
125	2.8 ( 2.2)	2.9 ( 2.4)	2.9 ( 2.4)	3.1 ( 2.9)	3.2 ( 3.3)

Table XI.

Multiple Perforation Propellant			
Propellant Temperature Degrees Fahrenheit	5	Zone 6	7
	M/S	M/S	M/S
-50	-15.6* (-16.7)	-17.2 (-17.2)	-18.8 (-17.2)
0	- 8.7 (-10.0)	- 9.8 (- 9.8)	-11.1 (- 9.6)
70	S T A N D A R D		
125	6.0 ( 7.9)	7.3 ( 7.0)	9.0 ( 7.6)

\*Firing Table corrections, FT 8-J-4, June 1967.

Values in parentheses are predicted using single and multiperforation percentage changes respectively found in Table IX.

Table XII. Muzzle Velocity Corrections For Nonstandard Propellant  
 Temperature 175MM Gun, M113, M107 Firing  
 Projectile, HE, M437 Mods

Multiple Perforation Propellant			
Propellant Temperature Degrees Fahrenheit	1	Zone 2	3
	M/S	M/S	M/S
-50	-12.0* (-11.4)	-18.1 (-20.6)	-29.7 (-28.7)
0	- 7.1 (- 6.1)	-12.6 (-11.5)	-17.2 (-16.5)
70	S T A N D A R D		
125	5.7 (6.7)	14.2 (10.7)	13.1 (13.3)

*\*Firing Table corrections, FT 175-A-0, Revision III, February 1965.*

Values in parentheses are predicted values using multiperforation percentage changes found in Table IX.

Table XIII. Muzzle Velocity Corrections For Nonstandard Propellant  
Temperature 155MM Howitzer, Medium, Towed, M114  
Firing Projectile IIE, M107

Single Perforation Propellant					
Propellant Temperature Degrees Fahrenheit	1	2	Zone 3	4	5
	M/S	M/S	M/S	M/S	M/S
-50	-3.1* (-4.8)	-4.4 (-3.4)	-5.6 (-4.3)	-5.7 (-5.5)	-5.7 (-7.3)
0	-1.8 (-3.8)	-2.6 (-2.0)	-3.3 (-3.2)	-3.3 (-3.8)	-3.3 (-4.6)
70	S T A N D A R D				
125	1.4 (3.8)	2.0 (3.1)	2.6 (3.2)	2.6 (3.1)	2.6 (3.0)

Table XIV.

Multiple Perforation Propellant					
Propellant Temperature Degrees Fahrenheit	3	4	Zone 5	6	7
	M/S	M/S	M/S	M/S	M/S
-50	-6.4* (-6.4)	-8.7 (-6.2)	-11.0 (-10.1)	-13.6 (-12.5)	-16.7 (-13.4)
0	-4.1 (-3.4)	-5.1 (-3.6)	- 6.4 (- 6.0)	- 8.0 (- 7.2)	- 9.8 (- 7.7)
70	S T A N D A R D				
125	3.3 (2.4)	3.9 (3.7)	5.1 (5.2)	6.2 (5.9)	7.7 (6.4)

\*Firing Table corrections, FT 155-Q-4, March 1968.

Values in parentheses are predicted using single and multiperforation percentage changes respectively found in Table IX.

Table XV. Muzzle Velocity Correction For Nonstandard Propellant  
 Temperature 155MM Howitzer, Self-Propelled, M109  
 Firing Projectile, HE, M549 RAP

Propellant Temperature Degrees Fahrenheit	Single Perforation Zone			Multiple Perforation Zone		
	1	3	5	3	5	7
	M/S	M/S	M/S	M/S	M/S	M/S
-50	-4.8* [-4.9] (-2.3)	-5.5 [-4.7] (-3.0)	-5.7 [-7.9] (-7.7)	-9.8 [-4.3] (-3.7)	-14.2 [- 6.3] (- 7.1)	-21.1 [-13.9] (- 9.3)
0	-2.4 [-3.8] (-1.5)	-3.0 [-3.2] (-2.6)	-3.4 [-5.2] (-6.8)	-5.0 [-0.5] (-2.5)	- 8.1 [- 1.6] (- 4.2)	-12.1 [- 6.7] (- 5.4)
70	S T A N D A R D			S T A N D A R D		
125	1.0 [ 2.2] ( 1.7)	2.0 [ 2.5] ( 2.1)	2.8 [ 2.3] ( 3.9)	2.6 [ 1.4] ( 2.5)	5.9 [ 4.4] ( 3.6)	9.0 [ 6.8] ( 4.8)

\*Firing Table correction values, FT 155-AH-2, July 1965.

Values in brackets are unfitted mean observations at the specific temperature changes listed in Table IX.

Values in parentheses for single perforation zones are predicted using single perforation percentage changes found in Table IX.

Values in parentheses for multiple perforation zones are predicted using multiple perforation percentage changes found in Table IX.

Table XVI. Muzzle Velocity Correction For Nonstandard Propellant  
Temperature 105MM Gun, M68 Firing APDS, M392A2

Propellant Temperature Degrees Fahrenheit	MV Correction M/S
-50	-87.8* (-76.3)
0	-51.2 (-44.7)
70	S T A N D A R D
125	53.6 ( 39.2)

\*Correction derived from  $(\Delta V_o)/\text{Deg F}$  value found in DPS Report No. 2005, dated June 1966.

Values in parentheses are predicted values using multiperforation percentage changes found in Table IX.

Table XVII. 4.2-Inch Mortar, M30 Firing HE, M329A1 Muzzle Velocity  
Corrections Due to Nonstandard Propellant Temperature

Propellant Temperature Degrees Fahrenheit	Without Extension				With Extension		
	Zone				Zone		
	5	11	15	19	27	35	39
	M/S	M/S	M/S	M/S	M/S	M/S	M/S
-50	-5.5* [-1.1] (-2.0)	-5.5 [-8.8] (-6.8)	-5.5 [-6.4] (-9.4)	-5.5 [-6.7] (-9.5)	-6.1 [-5.5] (-8.9)	-6.1 [-6.6] (-8.5)	-6.1 [----] (-8.4)
0	-3.4 [-1.7] (-1.3)	-3.4 [-3.8] (-4.5)	-3.4 [-4.5] (-6.0)	-3.4 [-3.8] (-5.9)	-4.0 [-3.7] (-5.7)	-4.0 [-3.2] (-5.3)	-4.0 [-4.4] (-5.3)
70	S T A N D A R D				S T A N D A R D		
125	2.4 [ 1.0] ( 0.9)	2.4 [ 2.0] ( 4.0)	2.4 [ 2.9] ( 4.3)	2.4 [ 2.9] ( 4.3)	3.5 [-3.3] ( 4.2)	3.5 [-3.4] ( 4.0)	3.5 [-3.5] ( 3.9)

\*Firing Table correction values (FT 4.2-H-2, August 1968).

Values in brackets are unfitted mean observations at the specific temperatures.

Values in parentheses are predicted using multiple perforation percentage changes found in Table IX.

Table XVIII. 81MM Mortar, M29 Firing HE, M374

Propellant Temperature Degrees Fahrenheit	Zone			
	1	2	6	9
	M/S	M/S	M/S	M/S
-50	-8.0* [-3.0] (-2.7)	-8.0 [-6.7] (-4.5)	-8.0 [-10.3] (-8.0)	-8.0 [-10.5] (-9.4)
0	-4.5 [-1.5] (-1.3)	-4.5 [-3.5] (-2.5)	-4.5 [-5.3] (-4.5)	-4.5 [-5.5] (-5.0)
70	S T A N D A R D			
125	2.6 [2.4] (1.1)	2.6 [2.9] (2.0)	2.6 [7.3] (3.5)	2.6 [6.4] (3.7)

\*Firing Table (FT 81-AI-2) correction values (Extrapolated for -50 degrees Fahrenheit)

Values in brackets are unfitted mean observations at the specific temperatures.

Values in parentheses are predicted values based on multiperforation percentage changes found in Table IX.

Now looking at the overall prediction performance of this technique from Tables XI - XVIII, it is interesting to note that in the majority of cases, the precision in predicting the changes in muzzle velocity at any given temperature falls within the round-to-round velocity probable error<sup>24</sup> at that same temperature. (See Table XIX.)

Table XIX. Precision of Predicted Values of Muzzle Velocity Changes  
For Nonstandard Propellant Temperature

Probable Error of Predicted Velocity Change From Experimental  
Measurement For All Data in Tables X - XVIII

Propellant Temperature	Perforation	
	Single	Multiple*
Degrees Fahrenheit	M/S	M/S
-50	0.70	1.18
0	0.60	0.83
70	S T A N D A R D	
125	0.66	0.99

*\*This also includes Mortar data.*

After all 'predictions' of propellant temperature effects for all of the subject weapons were carried out using the percentage generated and fitted from the 8-inch Howitzer propellant temperature firing data, each weapon and charge was again examined.

The unfitted mean observations at each propellant temperature were gathered for the remaining systems included in this report and the ( $\beta$ ) (F) levels were adjusted until the resultant muzzle velocity and maximum chamber pressure yielded from the model fell within the same tolerances (1 f/s and 100 psi respectively) specified for the 8-inch Howitzer system.

Examination of the zone-to-zone ( $\beta$ ) and (F) levels found in Table V indicates that there exists a slight trend in the levels of ( $\beta$ ) and (F) as zone increases. For example, ( $\beta$ ) decreases from a level of 89.1 percent at zone 5 (M2) to 87.3 percent standard at zone 7 at -50 degrees Fahrenheit. A similar trend exists at -10 degrees Fahrenheit, +30 degrees Fahrenheit with the trend reversing itself when propellant temperature exceeds standard 70 degrees Fahrenheit. Other trends, although not as pronounced, also seem to exist across the single perforation charges of the 8-inch Howitzer.

These trends were at first thought to be due to the density of loading ( $\delta$ ) which increases as more propellant occupies a fixed sized chamber.

Multiple regression analyses<sup>25</sup> were performed on the parameters of the subject weapons in an attempt to isolate the one or more parameters which might be causing this apparent trend across charge.

The following parameters were examined,

1. Tube Cross Sectional Area,
2. Charge Weight,
3. Density of Loading
4. Chamber Area,
5. Chamber Volume,
6. Projectile Weight,
7. Igniter Weight,
8. Igniter Pressure.

The results of the multiple regression analyses indicated that density of loading ( $\delta$ ) and igniter energy did generate regression cross-products that showed correlation to the levels of (F) and ( $\beta$ ). Igniter energy is defined as the product of igniter force and igniter weight divided by gamma of igniter minus one.

However, when the root-mean-square-error of the regression analysis was examined, it was apparent that the added precision that might be achieved by incorporating fits for density of loading and igniter energy were significantly less than the round-to-round probable errors of the data being studied. Hence, these functions were not generated.

Earlier in this report (Page 22) in describing possible ways of representing propellant temperature change in the model, it was pointed out that initial burning surface area decreases at low temperatures and increases at elevated temperatures. Most single based U.S. propellants have a coefficient of linear expansion similar to that of celluloid. The expansion takes the following form:

$$\text{Fraction unit change in grain dimension} = 1 + \alpha (\Delta T)$$

Where  $\alpha = 6.056 \times 10^{-5}$  inches/inch degrees Fahrenheit

$\Delta T$  = Change in propellant temperature

Most propellants, with the exception of some rocket propellants which are highly anisotropic, expand linearly in all directions. Linear expansion in all dimensions was assumed for the propellants studied herein.

Trajectories were run with the model adjusting all of the propellant grain dimensions using the above form to represent propellant temperatures of -50 and 125 degrees Fahrenheit.

At -50 degrees Fahrenheit, all grain dimensions would decrease by 0.73 percent, resulting in a decrease in burning surface area of 1.46 percent, a decrease in grain volume of 2.19 percent and a proportional increase in the chamber free-space contributed by the decrease in grain volume.

Changing the temperature from standard to 125 degrees Fahrenheit required grain dimension increases of 0.33 percent, increase in burning surface area of 0.66 percent, decrease in grain density of 0.99 percent and an increase in grain volume by a proportionate percentage.

The thermodynamic efficiencies of the charges and weapons examined increased at low temperatures, since the place and time of maximum chamber pressure were delayed resulting in a larger area under the pressure time curve. Hence, the contraction of the propellant at low temperatures actually tends to increase muzzle velocity and maximum chamber pressure since the ratio of propellant burning surface area to volume of unburnt propellant increases.

Since the effects of expansion and contraction of propellant grains on velocity and chamber pressure are generally proportional to the quantity of propellant in the chamber, it was thought that incorporating this phenomena into the model along with changes in (B) and (F) might 'damp out' the slight trend across zones (see Table V) in the levels of (B) necessary to simulate any given temperature and a corresponding trend in velocity prediction (Tables X and XI) of one of overprediction at low zones and underprediction at the higher zones.

Table XX shows the new ( $\beta$ ) and (F) levels necessary to match muzzle velocity and maximum chamber pressure changes when compensating for the expansion and contraction of propellant grains due to initial propellant temperature levels.

Table XX. Percent Standard ( $\beta$ ) and (F) Needed to Simulate Observed Velocity and Maximum Chamber Changes When Compensating For Propellant Grain Expansion and Contraction

8-inch Howitzer, M2 Firing HE, M106			
Propellant Temperature Degrees Fahrenheit	Adjusted Parameter	All Single Perforation Zones	All Multiple Perforation Zones
		Percent Standard	Percent Standard
-50	$\beta$	75.2	87.9
	F	99.5	99.6
70	$\beta$	100.0	100.0
	F	100.0	100.0
125	$\beta$	128.9	107.2
	F	100.1	100.0

Comparing these levels with those in Table IX indicates that the general trend is to increase the amount that ( $\beta$ ) and (F) must be adjusted to compensate for propellant temperature changes.

Trajectories were run using the percentage standards in Table XX to examine the validity of this assumption. The computer predictions are compared with observed data in Table XXI below.

Table XXI. Muzzle Velocity Corrections For Nonstandard Propellant Temperature For 8-inch Howitzer,  
M2 Firing HE, M106

Propellant Temperature Degrees Fahrenheit	Single Perforation					Multiple Perforation		
	Zone					Zone		
	1	2	3	4	5	5	6	7
-50	-4.9* (-4.6)	-5.1 (-4.7)	-5.4 (-4.8)	-5.8 (-6.1)	-6.4 (-7.2)	-15.6 (-16.6)	-17.2 (-17.6)	-18.8 (-17.4)
70	S T A N D A R D					S T A N D A R D		
125	2.8 ( 2.5)	2.9 ( 2.9)	2.9 ( 2.7)	3.1 ( 3.3)	3.2 ( 3.7)	6.0 (8.1)	7.3 (7.0)	9.0 (7.6)

\*Firing Table corrections, FT 8-J-4, June 1967.

Values in parentheses are predicted using single and multiple perforation percentage changes respectively found in Table XX.

The data in the table indicate that incorporating the fluctuation in grain size into the model does not improve the predictive capability significantly. The variance between the predicted and observed velocity change is improved only slightly in most instances. For example, the variance in prediction error for the single perforated charges of the 8-inch Howitzer (Table X) is .41 M/S. When propellant surface area fluctuations are included and new levels of burning rate coefficients and propellant forces are computed (Table XX) the variance in prediction error becomes .33 M/S. The improvement at 125 degrees Fahrenheit for the same single perforated zones change from a level of .23 M/S to a level of .10 M/S. The multiple perforation zones of the same weapon show a slight improvement in matching experimental data at -50 degrees Fahrenheit but some degradation occurs at 125 degrees Fahrenheit.

## VII. CONCLUSIONS

Results of the study indicate that for the great variety of weapon systems, charges, and propellant compositions in current use, the velocity of a projectile fired using propellant at nonstandard temperature can be simulated fairly well, using propellant forces and burning rate coefficients as fixed functions of propellant temperature.

One set of functions is applicable to single perforation charges and another set for disc, sheet, and multiple perforation charges.

Firing data at standard propellant temperature (70 degrees Fahrenheit) are necessary for each zone to establish the engraving resistance levels. Once these 'standard cases' are established, nonstandard propellant temperature firings can be simulated using empirically determined functions of burning rate coefficient and propellant force.

With this model, the muzzle velocity corrections for a 7 zone system can be generated in less than 10 minutes on the BRLESC I computer of the Ballistic Research Laboratories.

Studies are currently in progress to determine the feasibility of applying a similar technique to weapons which have multiple granulation charges.

On the basis of the present performance of the interior ballistics simulation program in the prediction of muzzle velocity effects due to propellant temperature, the model should be sufficiently accurate to permit either a discontinuance of propellant temperature firings or a significant reduction in the number of rounds required for such a firing.

#### ACKNOWLEDGMENTS

The author wishes to acknowledge the many contributions made by members of the Interior Ballistics Laboratory to the success of the work described in this report. The basic interior ballistic computer program and invaluable advice relating to its use and application were provided by Mr. P. G. Baer. It should be noted that the suggestion to use the empirical method of simulating change in propellant temperature by varying burning rate coefficient described in reference 2 was made by Mr. Baer and Mr. J. M. Frankle. Detailed information on burning characteristics of solid propellants was given by Mr. B. B. Grollman.

The help of Mr. James Matts and Mr. Patrick Ward of the Firing Tables Branch of the Exterior Ballistics Laboratory in preparing and programming the engraving pressure iteration routine is also very much appreciated.

## REFERENCES

1. Paul Baer and Jerome M. Frankle, "The Simulation of Interior Ballistic Performance of Guns By Digital Computer Program," Ballistic Research Laboratories Report No. 1183, 1962, Aberdeen Proving Ground, Maryland.
2. F.R.W. Hunt, Chairman Editorial Panel, Internal Ballistics, New York Philosophical Library, (1951), Chapter VI, p. 72.
3. AMCP 706-150, Engineering Design Handbook, Ballistic Series, Interior Ballistics of Guns, February 1965, pp. 1-4.
4. M.E. Serebryakov, Interior Ballistics, translated by V.A. Nekrassoff, The Catholic University, 1949, p. 242.
5. AMCP 706-150, Engineering Design Handbook, (1965), pp. 1-4.
6. F.R.W. Hunt, Internal Ballistics, p. 72.
7. J.A. Petersam, H.G. McGuire and T.E. Turner, "Measurement of Projectile Motion During the Engraving Process," Ballistic Research Laboratories Memorandum Report No. 1070, 1967, Aberdeen Proving Ground, Maryland.
8. M.E. Serebryakov, Interior Ballistics, p.267.
9. L.D. Heppner, "Final Report on Special Study of Setback and Spin For Artillery, Mortar, Recoilless Rifle, and Tank Ammunition," DPS Report No. 2611, 1968, Aberdeen Proving Ground, Maryland.
10. H.B. Anderson, "Artillery Ammunition Master Calibration Chart," MTD Report No. 1375, 1969, Aberdeen Proving Ground, Maryland.
11. Ibid, pp. 4-51.
12. L.D. Heppner, "Final Report on Special Study of Setback and Spin For Artillery, Mortar, Recoilless Rifle, and Tank Ammunition," pp. 11-19.
13. J. Corner, Theory of the Interior Ballistics of Guns, John Wiley and Sons New York, (1950), p. 69.
14. F.R.W. Hunt, Internal Ballistics, pp. 134-135.
15. Ibid, p. 226.
16. H.B. Anderson, "Artillery Ammunition Master Calibration Chart," pp. 4-48.

17. E.E. Ekstedt, D.C. Vest, E.V. Clarke and D.L. Wann, "Pressure Studies of Artillery Fired Statically," Ballistic Research Laboratories Report No. 938, 1955, Aberdeen Proving Ground, Maryland.
18. D.C. Vest, E.V. Clarke, W.W. Shoemaker and W.F. Baker, "On the Performance of Primers For Artillery Weapons," Ballistic Research Laboratories Report No. 852, 1953, Aberdeen Proving Ground, Maryland.
19. USATECOM Project No. 2-MU-005-067-008, FR P-80532, April 1971, Aberdeen Proving Ground, Maryland.
20. J. Corner, Theory of the Interior Ballistics of Guns, p. 73.
21. Ibid, p. 73.
22. F.R.W. Hunt, Internal Ballistics, p. 226.
23. J. Corner, Theory of the Interior Ballistics of Guns, p. 73.
24. H.B. Anderson, "Effects of Environment on Safe Operating Limits For Artillery Weapons," DPS Report No. 2005, June 1966.
25. H.J. Breaux, L.W. Campbell and J.C. Torrey, "Stepwise Multiple Regression Statistical Theory and Computer Program Description," Ballistic Research Laboratories Report No. 1330, 1966, Aberdeen Proving Ground, Maryland.

# APPENDIX A

## 155MM M114 FIRING HE, M107 ZONE 1 ENGRAVING PRESSURE ITERATION

PROJ. WT. BARREL CHAMBER BORE AREA P-K(POLY) SS PRESS MAX GUN PRESSURE  
95.00000 114.0C0C0 795.00000 29.7C572 3.00643 0. 75000.

CHARGE FORCE(F) GAMMA PROPELLANT COVOLUME FLAME TEMP DENSITY IGNITER  
.18750 1152000. 1.2500 2000.  
1.95000 3670150. 1.2640 31.080 2433. .056700 M1

D/DP OR W/T RATIO 2.5000000 L/D OR L/W RATIO 4.5000000  
BETA( ) ALPHA WEB OD-WIDTH DP-THICK LENGTH NO.PERF. GEOMETRY  
.00050790 .84970C00 .0165C0C0 .055C00C0 .02200000 .24750000 1.0 C

RESISTANCE  
PROJ. TRAVEL PRESSURE ESTIMATES  
.000 0. (PR1)  
.438 2200. (PR2)  
.875 200. (PR3)

MISCELLANEOUS  
PT NO. PROP. KV KX EST. MUZ. VEL. DIAMETER  
283.98 1. .0000200 .000CC00 974. 6.1500

GAS AHEAD OF PROJECTILE  
PRESSURE TEMP. MOL.WT. GAMMA IND.  
14.7000 300.0C0C0 28.96C0 1.40C0 AIR

HEAT LOSS PARAMETERS  
C.SUR.A BORE TEMP. K1 K2  
546.77889 300.0C0C0 1.2500CC0 .50CC0000

OPTIONS  
REG INPUT SUMOUT2 OMIT X-PR TABLSFFOPT3 HL OPT2

CONVERGE ON 680 F/S (V0) AND 5400 PSI (PM)

INITIAL GUESS  
PR2 PR3 (VC) (PM) Δ(V0) Δ(PM)  
2800.0 200.0 694.5 5644.5 -14.5 -244.5  
2800.0 307.9 680.0 5693.6 0.0 -293.6 END OF (V0) LCOP  
2454.2 307.9 675.7 5390.1 4.3 9.9 END OF (PM) LCOP  
2491.6 274.9 680.5 5398.9 .5 1.1

CONVERGENCE  
PR2 PR3  
2491.6 274.9 680.5 5398.9 -.5 F/S 1.1 PSI

# ITERATION

## SUMMARY OF RESULTS

RUN NO= 1

X-IN	T-MS	PBR-PSI	PB-PSI	V-F/S	AKG	Z1	Z2	Z3	Z4	Z5
.00000	.00000	.000000	.000000	.00000	.00000000	.0000	.0000	.0000	.0000	.0000
5.0000	17.643	7184.51	7104.70	245.49	2.6568693	.8935	.0000	.0000	.0000	.0000
10.000	19.013	6615.26	6541.78	362.03	2.4799540	1.000	.0000	.0000	.0000	.0000
15.000	20.050	5565.88	5504.05	440.02	2.1548111	1.000	.0000	.0000	.0000	.0000
20.000	20.937	4774.74	4721.70	498.59	1.9096510	1.000	.0000	.0000	.0000	.0000
25.000	21.734	4162.14	4115.90	545.64	1.7197830	1.000	.0000	.0000	.0000	.0000
30.000	22.471	3674.77	3633.95	585.07	1.5686960	1.000	.0000	.0000	.0000	.0000
35.000	23.163	3279.90	3243.47	619.00	1.4462552	1.000	.0000	.0000	.0000	.0000
40.000	23.820	2953.01	2920.20	648.88	1.3448644	1.000	.0000	.0000	.0000	.0000
45.000	24.449	2679.19	2649.43	675.57	1.2599129	1.000	.0000	.0000	.0000	.0000
50.000	25.055	2446.90	2419.72	699.70	1.1878256	1.000	.0000	.0000	.0000	.0000
55.000	25.641	2247.59	2222.62	721.75	1.1259516	1.000	.0000	.0000	.0000	.0000
60.000	26.210	2074.91	2051.86	742.09	1.0723299	1.000	.0000	.0000	.0000	.0000
65.000	26.765	1923.85	1902.48	760.99	1.0254049	1.000	.0000	.0000	.0000	.0000
70.000	27.306	1790.87	1770.98	778.65	.98408151	1.000	.0000	.0000	.0000	.0000
75.000	27.835	1673.08	1654.49	795.25	.94746379	1.000	.0000	.0000	.0000	.0000
80.000	28.354	1568.10	1550.68	810.92	.91481794	1.000	.0000	.0000	.0000	.0000
85.000	28.863	1474.03	1457.65	825.78	.88555029	1.000	.0000	.0000	.0000	.0000
90.000	29.364	1389.29	1373.86	839.93	.85917625	1.000	.0000	.0000	.0000	.0000
95.000	29.856	1312.55	1297.97	853.44	.83528110	1.000	.0000	.0000	.0000	.0000
100.00	30.340	1242.72	1228.92	866.38	.81352918	1.000	.0000	.0000	.0000	.0000
105.00	30.818	1179.09	1165.99	878.81	.79369814	1.000	.0000	.0000	.0000	.0000
110.00	31.289	1120.88	1108.43	890.77	.77554680	1.000	.0000	.0000	.0000	.0000

MUZZLE VELOCITY (V0) = 899.992 F/S      MAXIMUM PRESSURE (PM) = 7188.08 PSI

MUZZLE PRESSURE = 1066.21 PSI      TIME AT MAXIMUM PRESSURE = 17.9698 MS

COUNT = 1      TRAVEL AT MAXIMUM PRESSURE = 6.01753 IN

VELOCITY AT MAXIMUM PRESSURE 273.648 F/S      TIME AT MUZZLE 31.7327 MS

MAXIMUM PROJECTILE ACCELERATION 2.65777 KILO-GS

PROPELLANT NO. 1

TIME AT BURNOUT = 18.6235 MS      PROJECTILE TRAVEL AT BURNOUT = 8.38455 IN

BALLISTIC PARAMETERS

C/M = .022500      EXPANSION RATIO = 5.25969

THERMODYNAMIC EFFICIENCY = .512574      PIEZOMETRIC EFFICIENCY = .589031

PROJECTILE BASE/BREECH PRESSURE RATIO = .988891

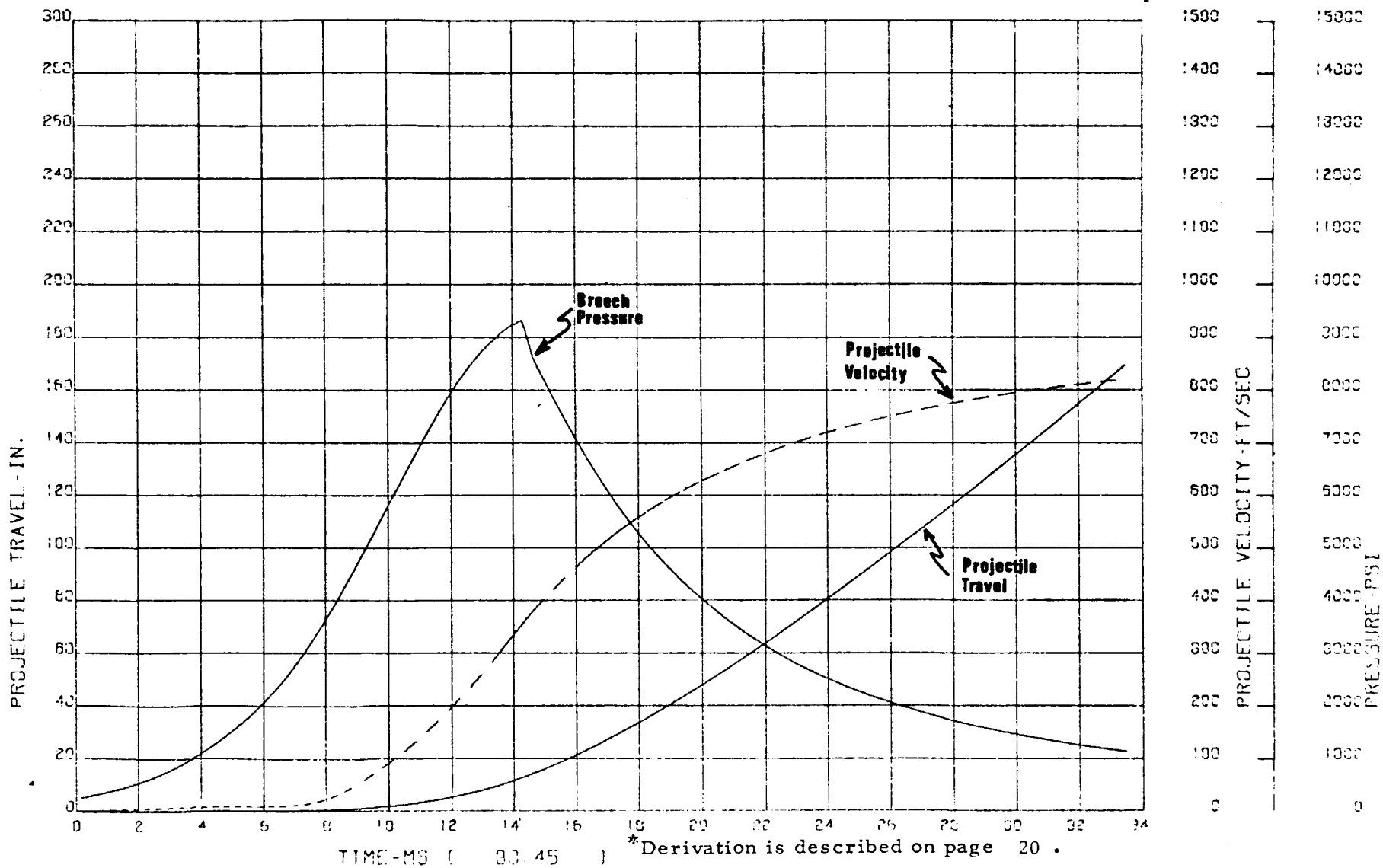
ELAPSED TIME= 55.2000 SEC

# APPENDIX B

8-INCH HOWITZER, M2 FIRING HE, M106 ZONE 1 (M1)

\* Engraving Pressures  
PR2 = 2225 psi  
PR3 = 370 psi

PROJECTILE TRAVEL, VELOCITY, BREECH PRESSURE, VS TIME.

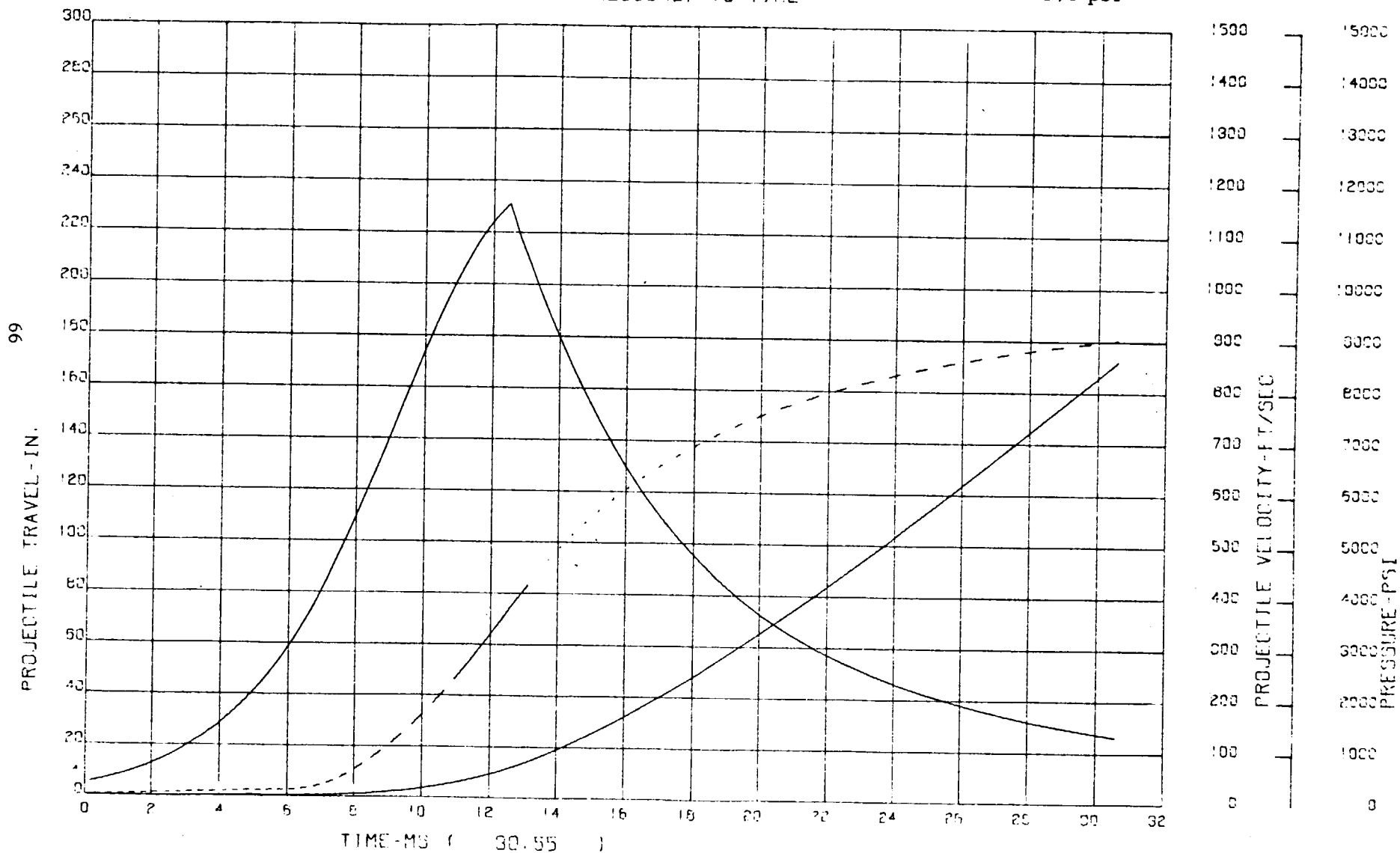


# 8-INCH HOWITZER, M2 FIRING HE, M106 ZONE 2 (M1)

PR2 = 2575 psi

PR3 = 395 psi

PROJECTILE TRAVEL, VELOCITY, BREACH PRESSURE, VS TIME

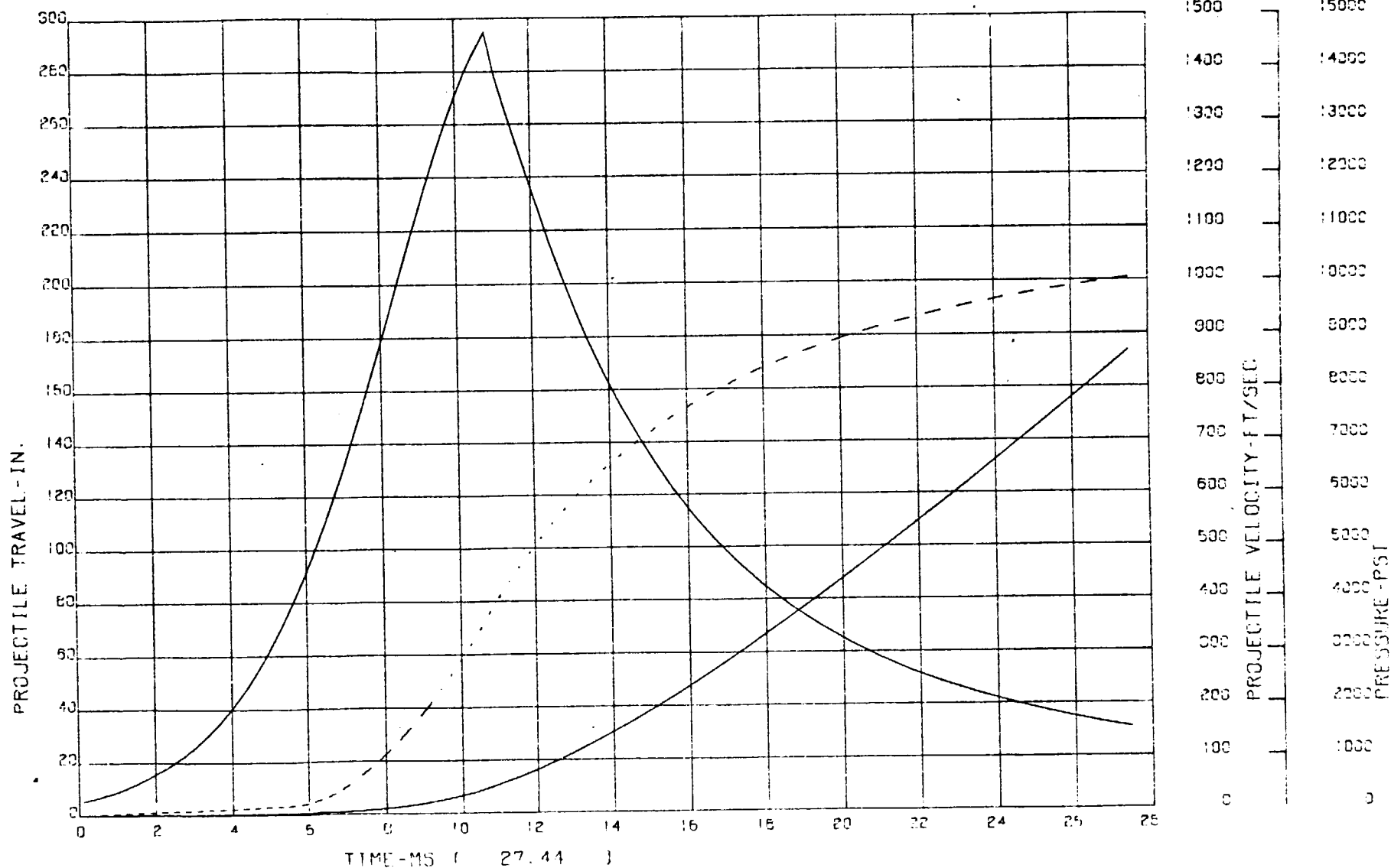


8-INCH HOWITZER, M2 FIRING HE, M106 ZONE 3 (M1)

PR2 = 3110 psi

PR3 = 385 psi

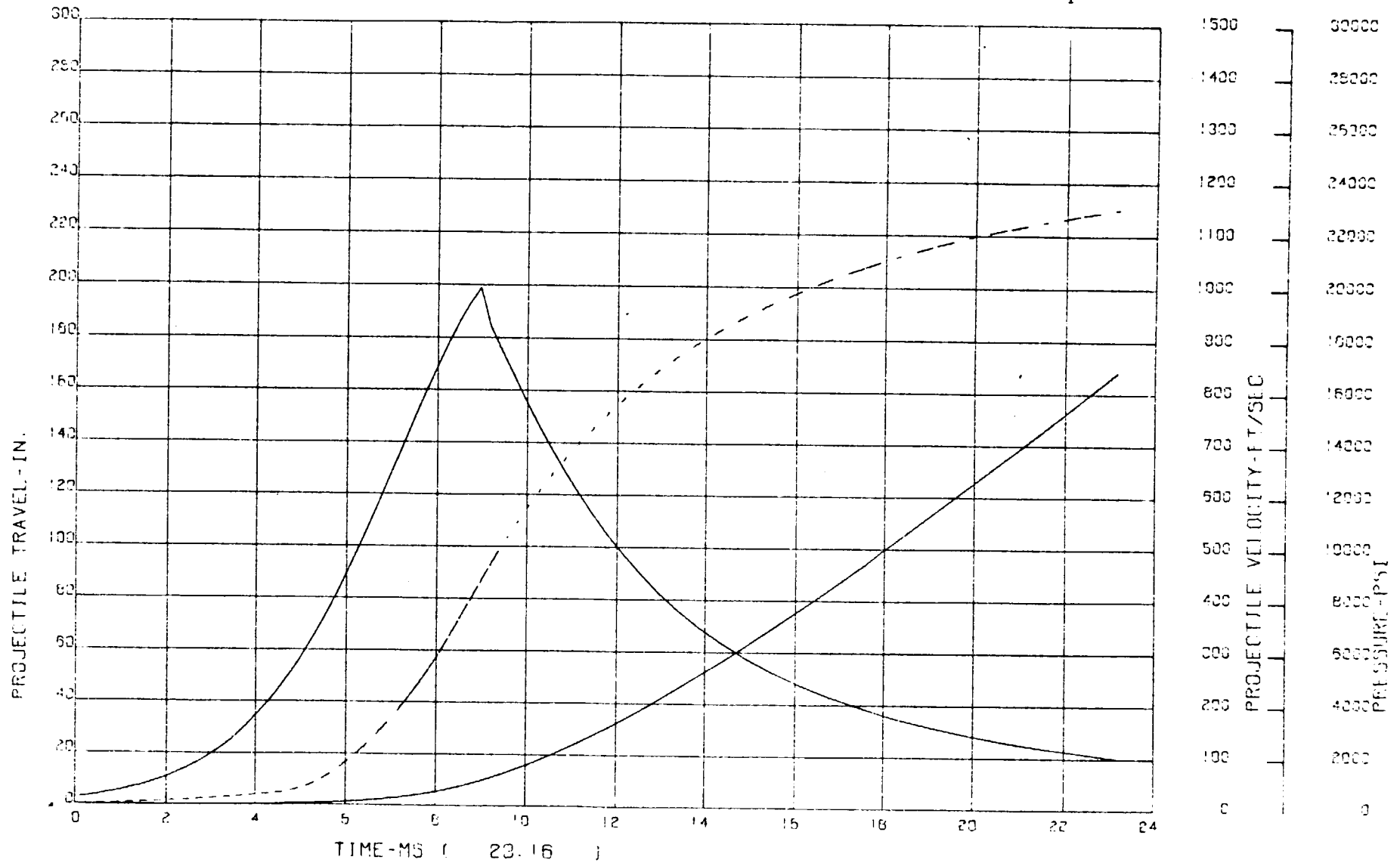
PROJECTILE TRAVEL, VELOCITY, BREACH PRESSURE, VS TIME



# 8-INCH HOWITZER, M2 FIRING HE, M105 ZONE 4 (M1)

PR2 = 3175 psi  
PR3 = 310 psi

PROJECTILE TRAVEL, VELOCITY, BREACH PRESSURE, VS TIME

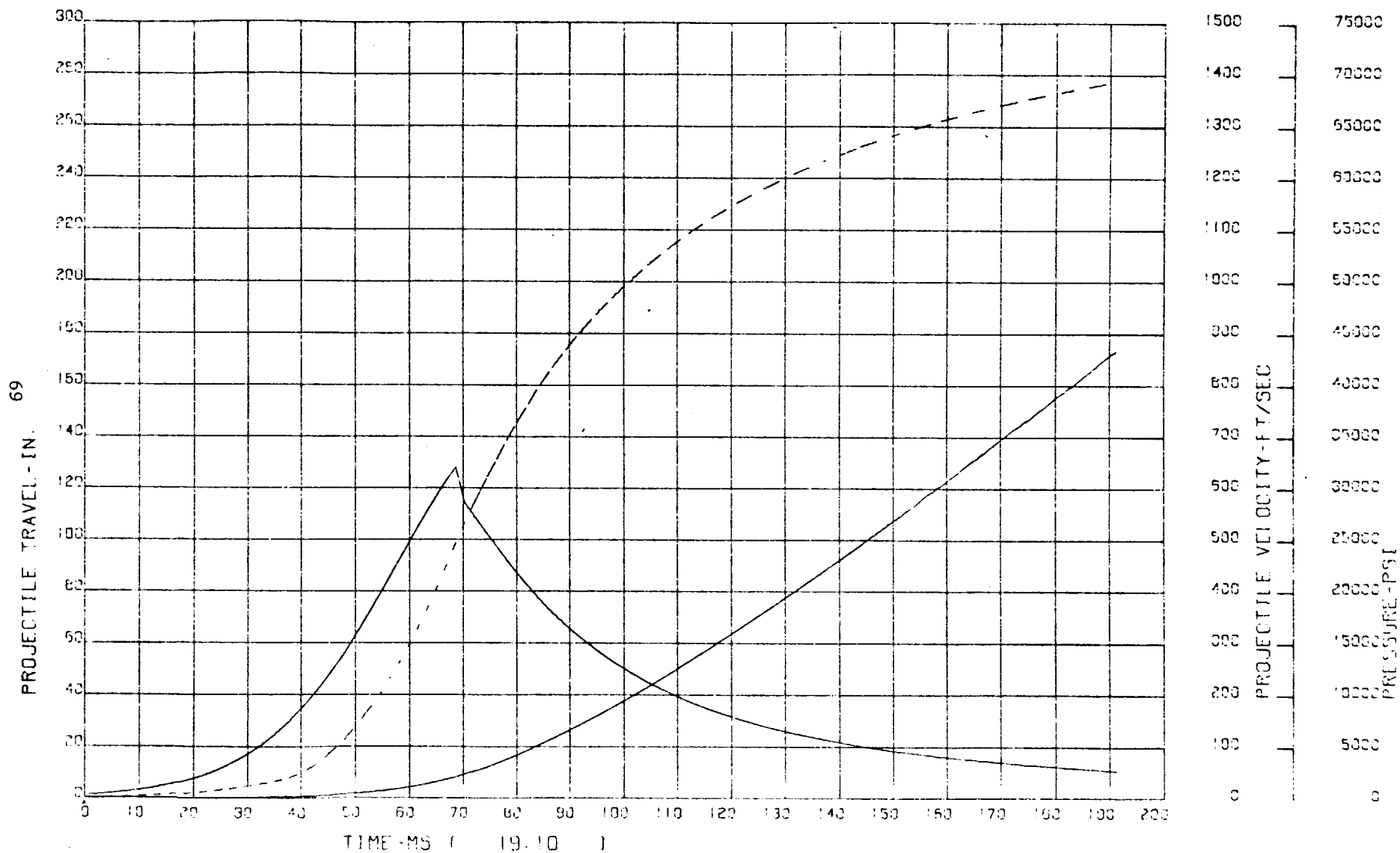


8-INCH HOWITZER, M2 FIRING HE, M106 ZONE 5 (M1)

PR2 = 3650 psi

PR3 = 310 psi

PROJECTILE TRAVEL, VELOCITY, BREACH PRESSURE, VS TIME

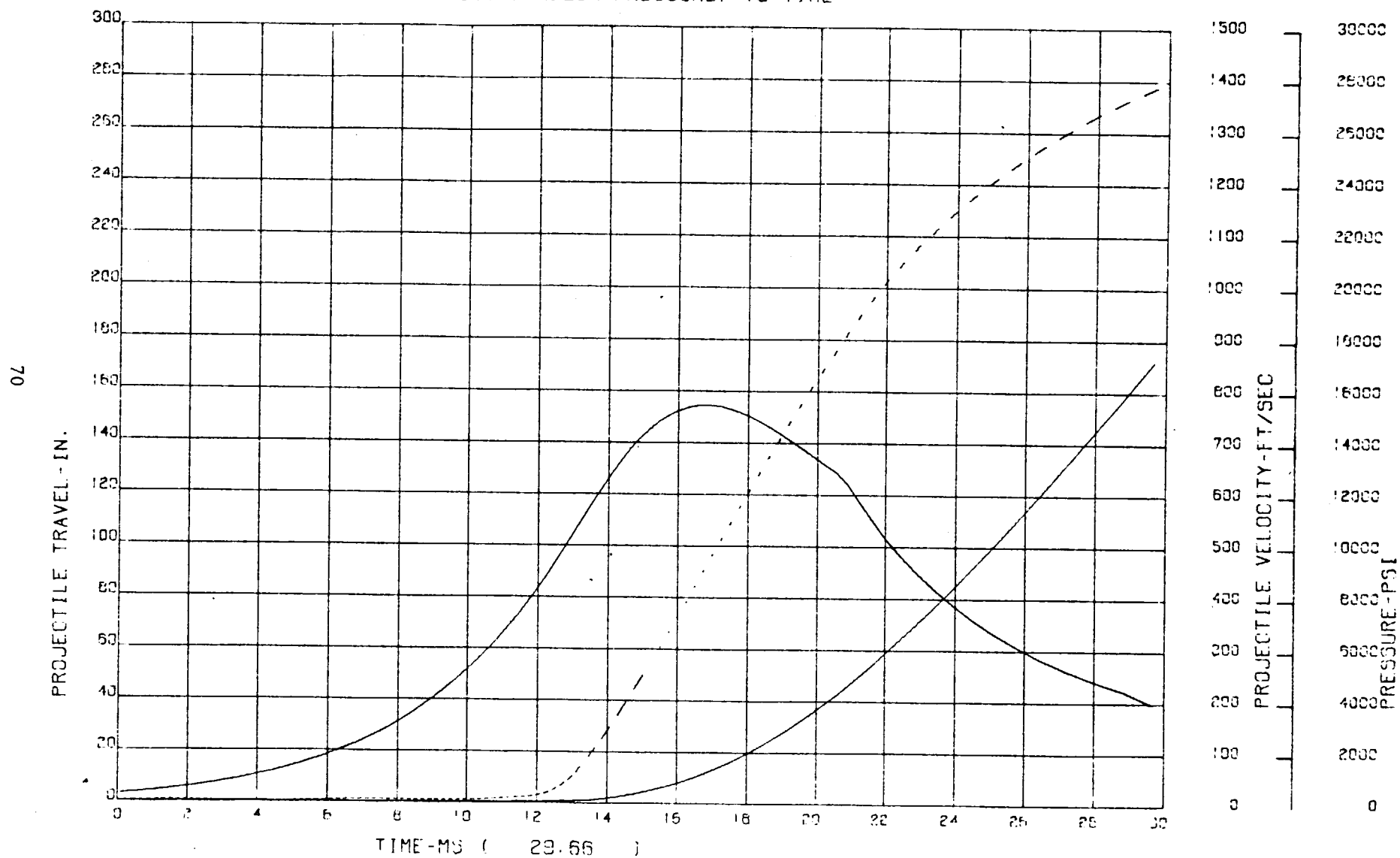


# 8-INCH HOWITZER, M2 FIRING HE, M106 ZONE 5 (M2)

PR2 = 6900 psi

PR3 = 310 psi

PROJECTILE TRAVEL, VELOCITY, BREECH PRESSURE, VS TIME

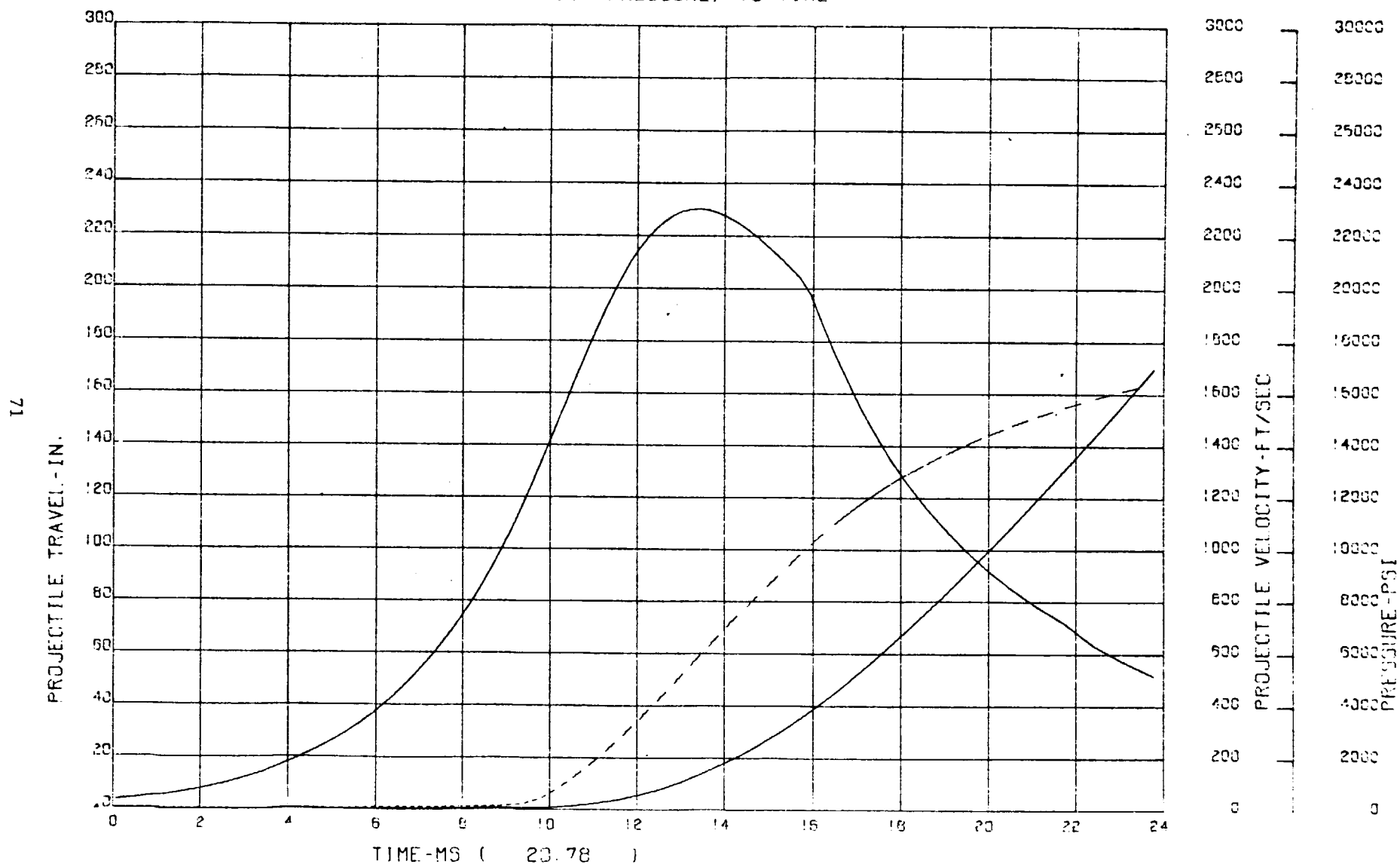


8-INCH HOWITZER, M2 FIRING HE, M106 ZONE 6 (M2)

PR2 = 8550 psi

PR3 = 320 psi

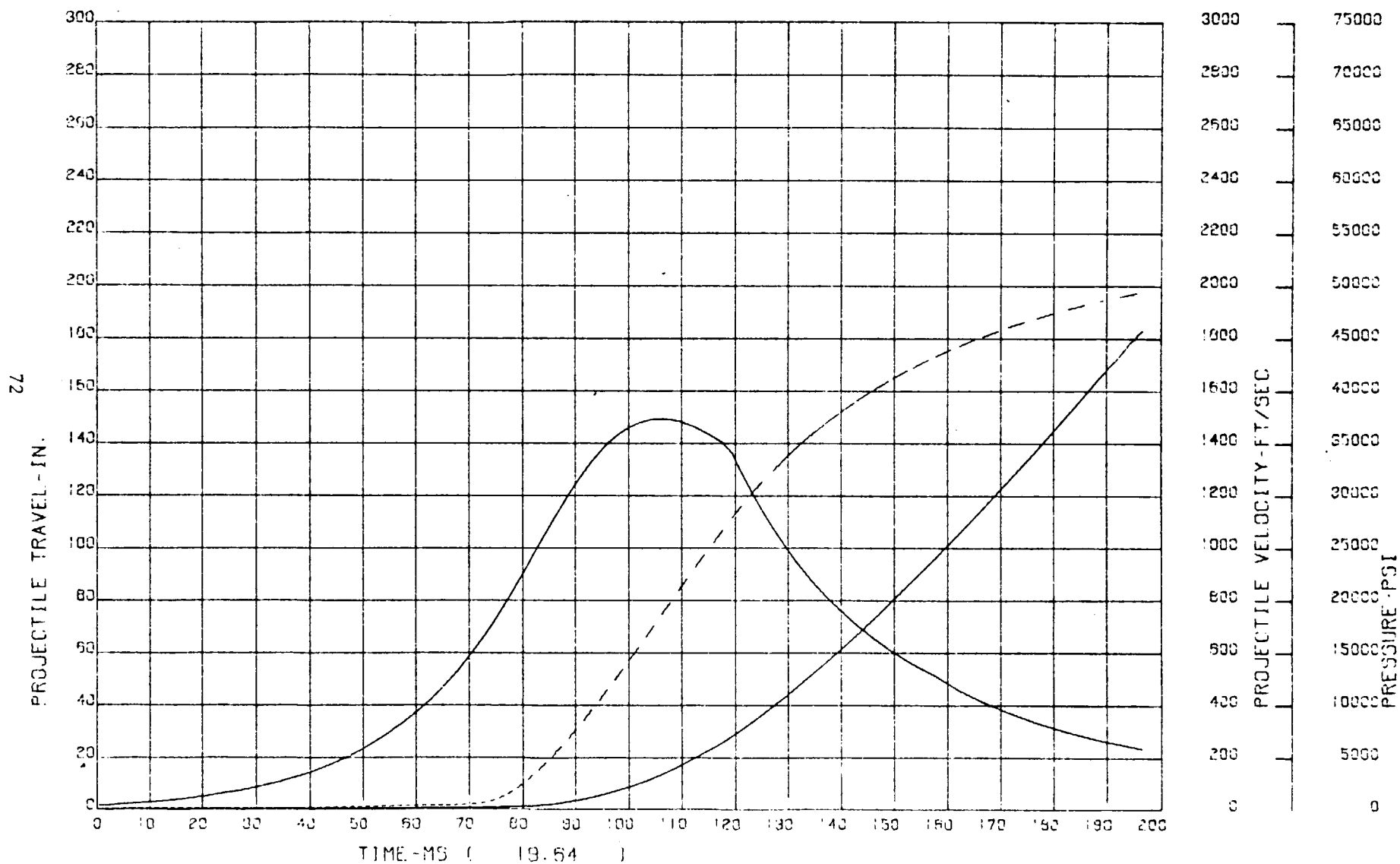
PROJECTILE TRAVEL, VELOCITY, BREECH PRESSURE, VS TIME



# 8-INCH HOWITZER, M2 FIRING HE, M106 ZONE 7 (M2)

PR2 = 12400 psi  
PR3 = 320 psi

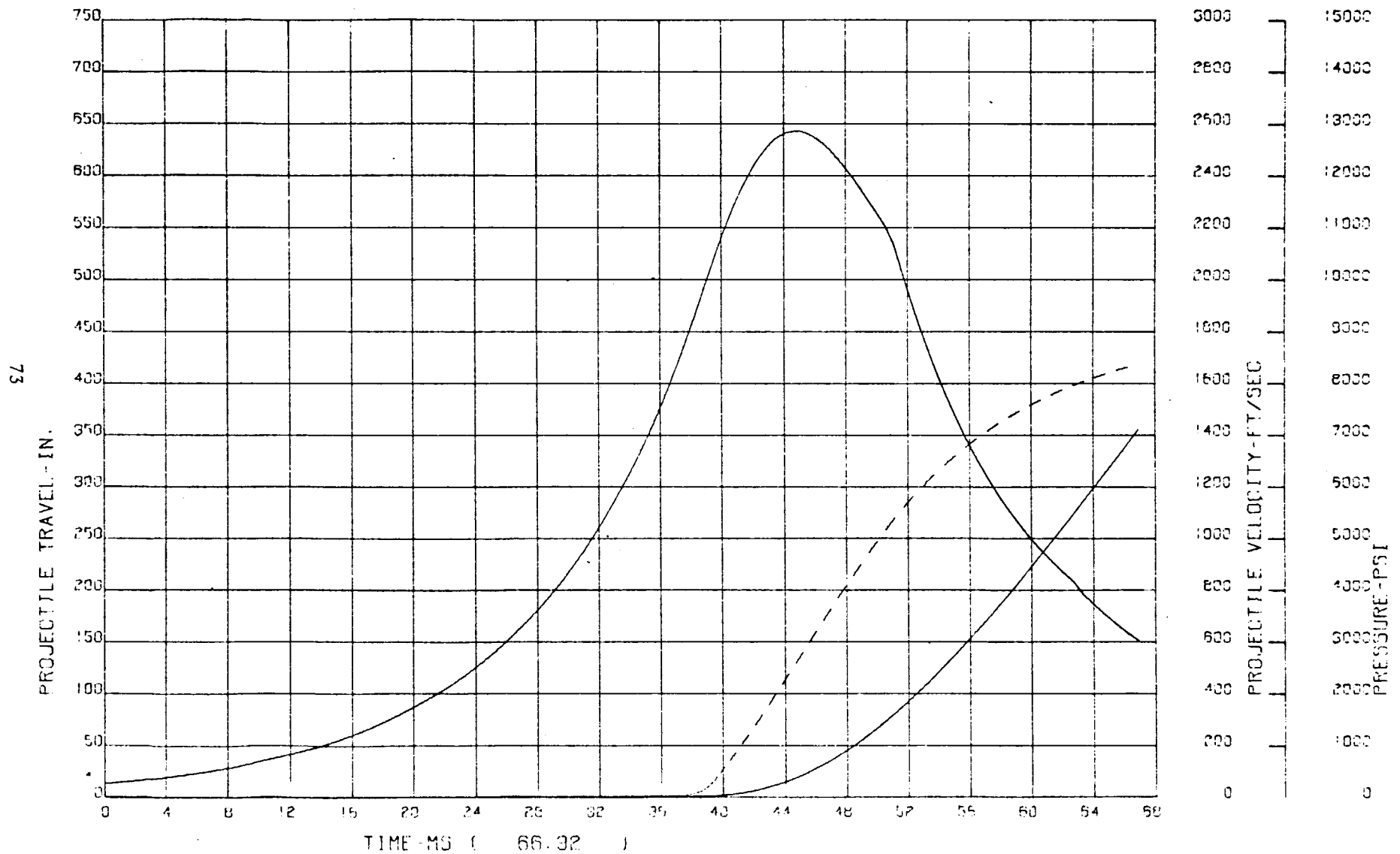
PROJECTILE TRAVEL, VELOCITY, BREECH PRESSURE, VS TIME



175MM GUN, M113 FIRING HE, M437 ZONE 1 (M86)

PR2 = 7740 psi  
PR3 = 890 psi

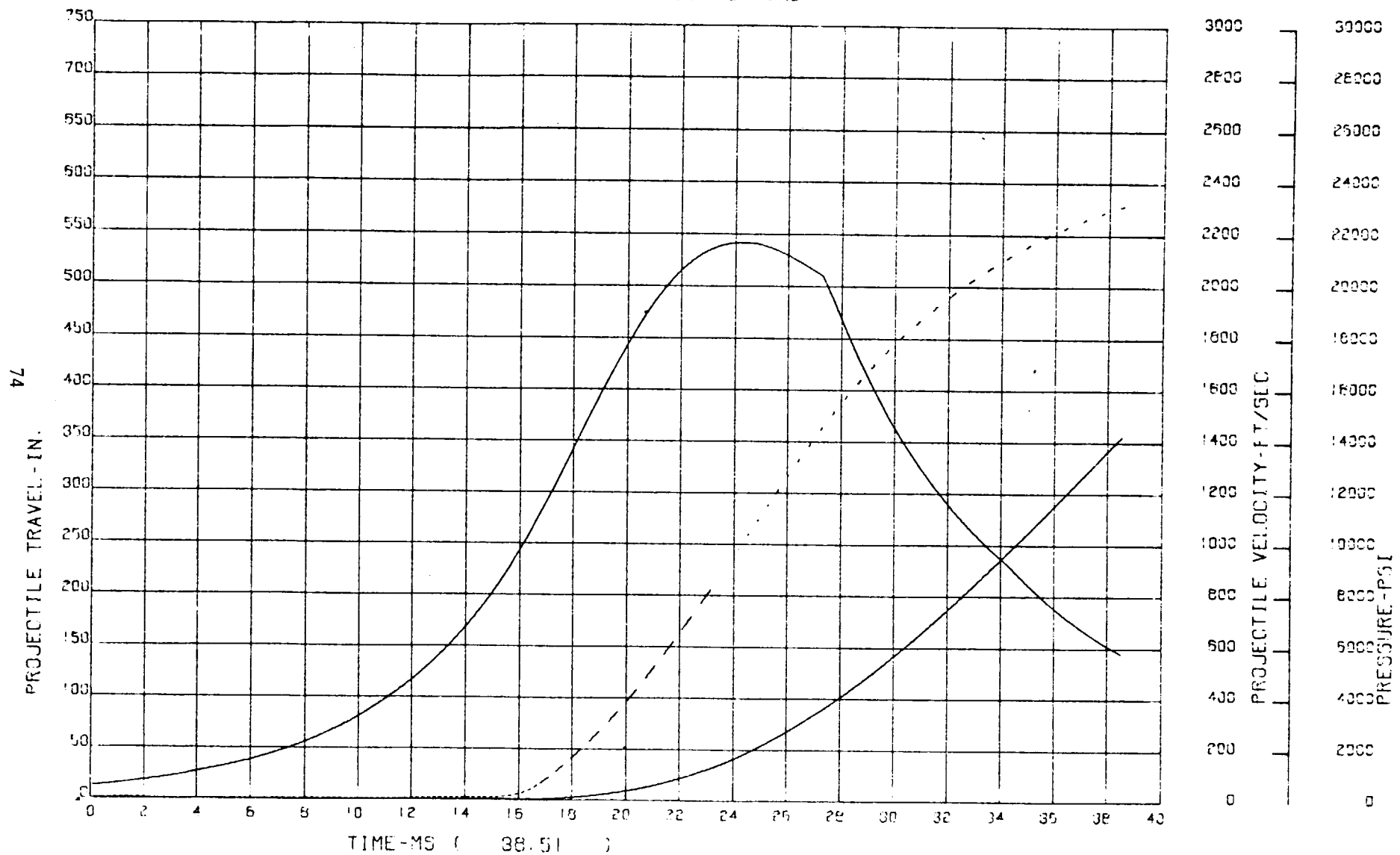
PROJECTILE TRAVEL, VELOCITY, BREECH PRESSURE, VS TIME



175MM GUN, M113 FIRING HE, M437 ZONE 2 (M86)

PR2 = 6975 psi  
PR3 = 910 psi

PROJECTILE TRAVEL, VELOCITY, BREACH PRESSURE, VS TIME

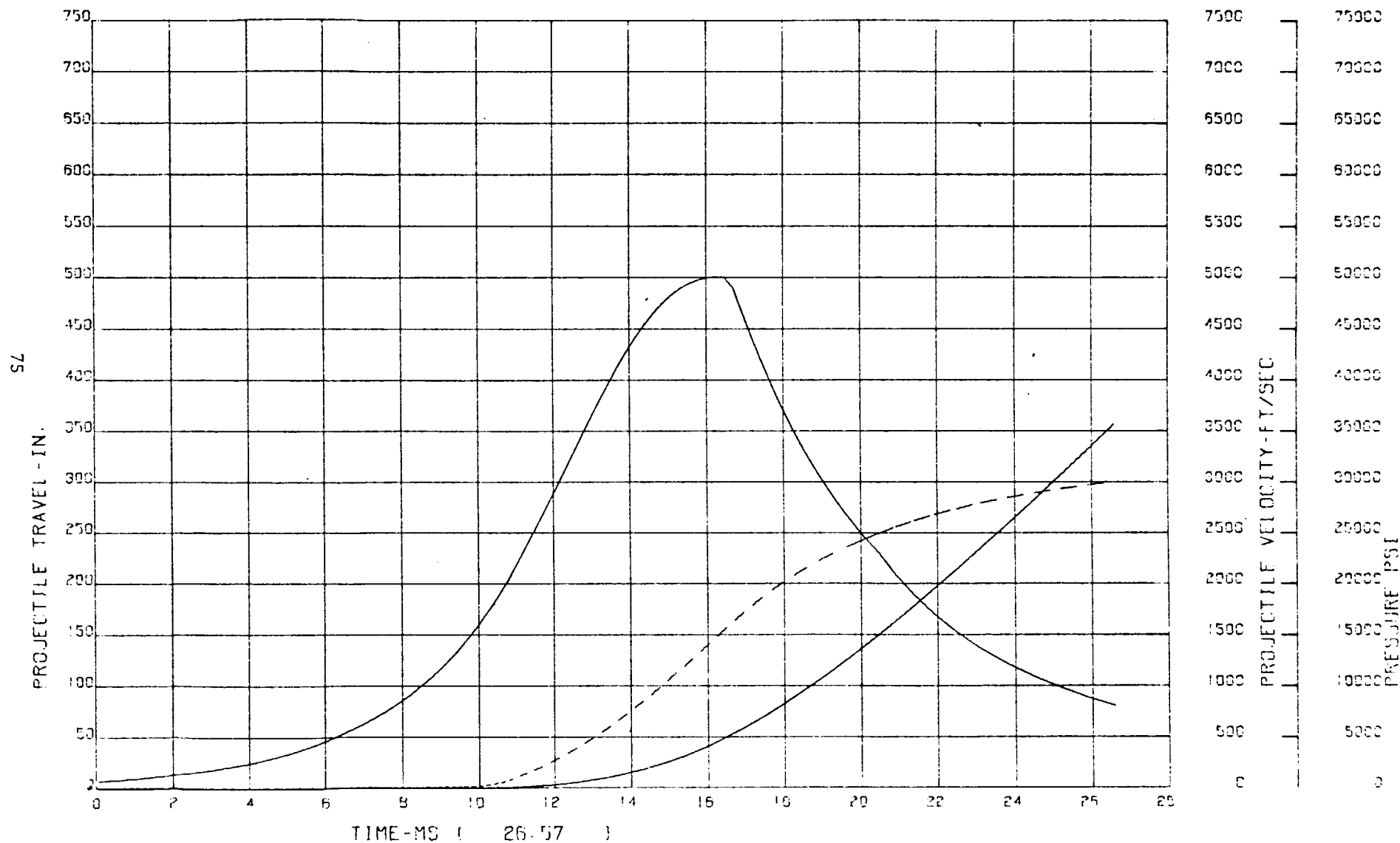


175MM GUN, M113 FIRING HE, M467 ZONE 3

PR2 = 10975 psi

PR3 = 1610 psi

PROJECTILE TRAVEL, VELOCITY, BREECH PRESSURE, VS TIME

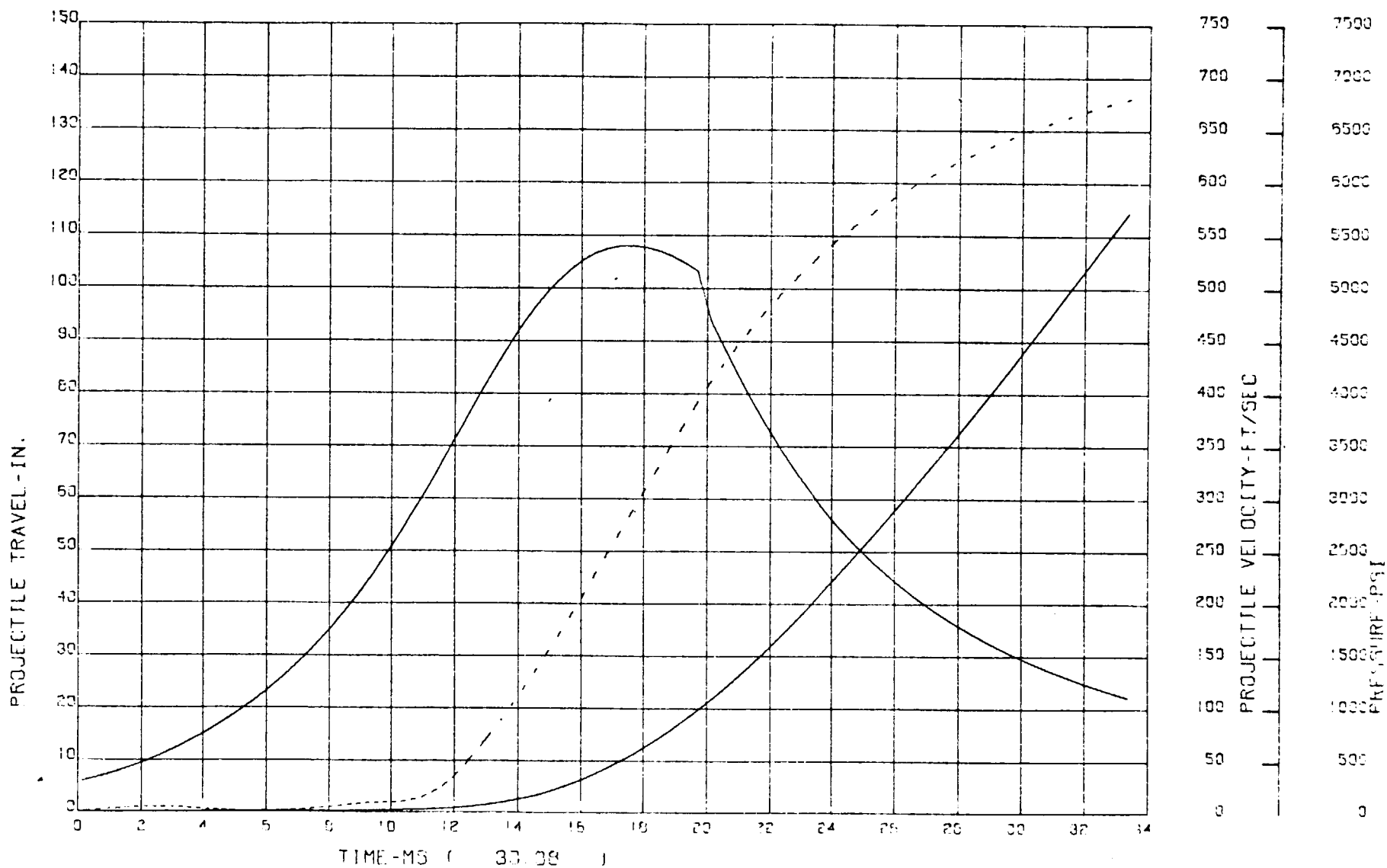


155MM HOWITZER, M1 FIRING HE, M107 ZONE 1 (M3)

PR2 = 2493 psi

PR3 = 279 psi

PROJECTILE TRAVEL, VELOCITY, BREECH PRESSURE, VS TIME

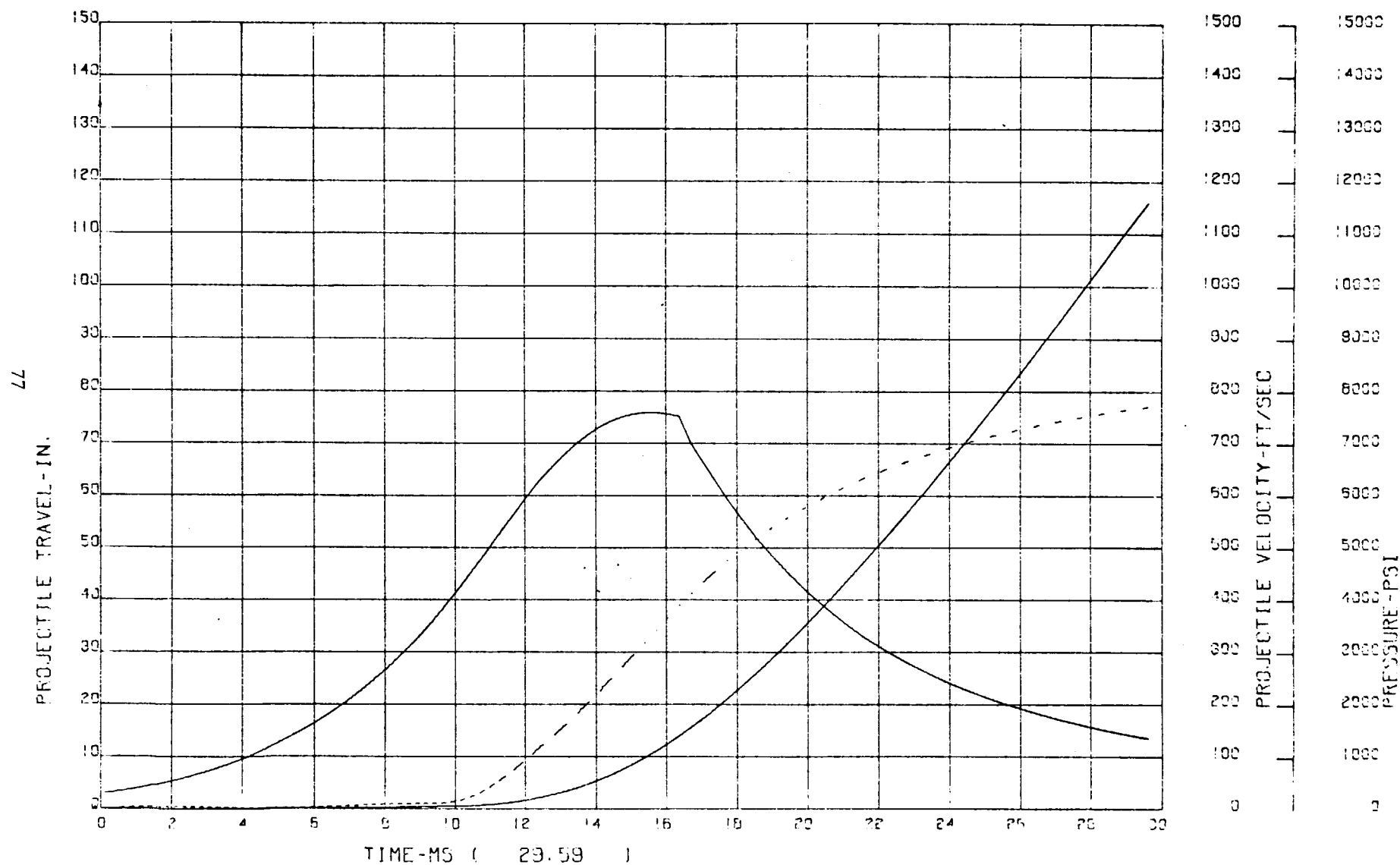


155MM HOWITZER, M1 FIRING HE, M107 ZONE 2 (M3)

PR2 = 3451 psi

PR3 = 349 psi

PROJECTILE TRAVEL, VELOCITY, BREECH PRESSURE, VS TIME



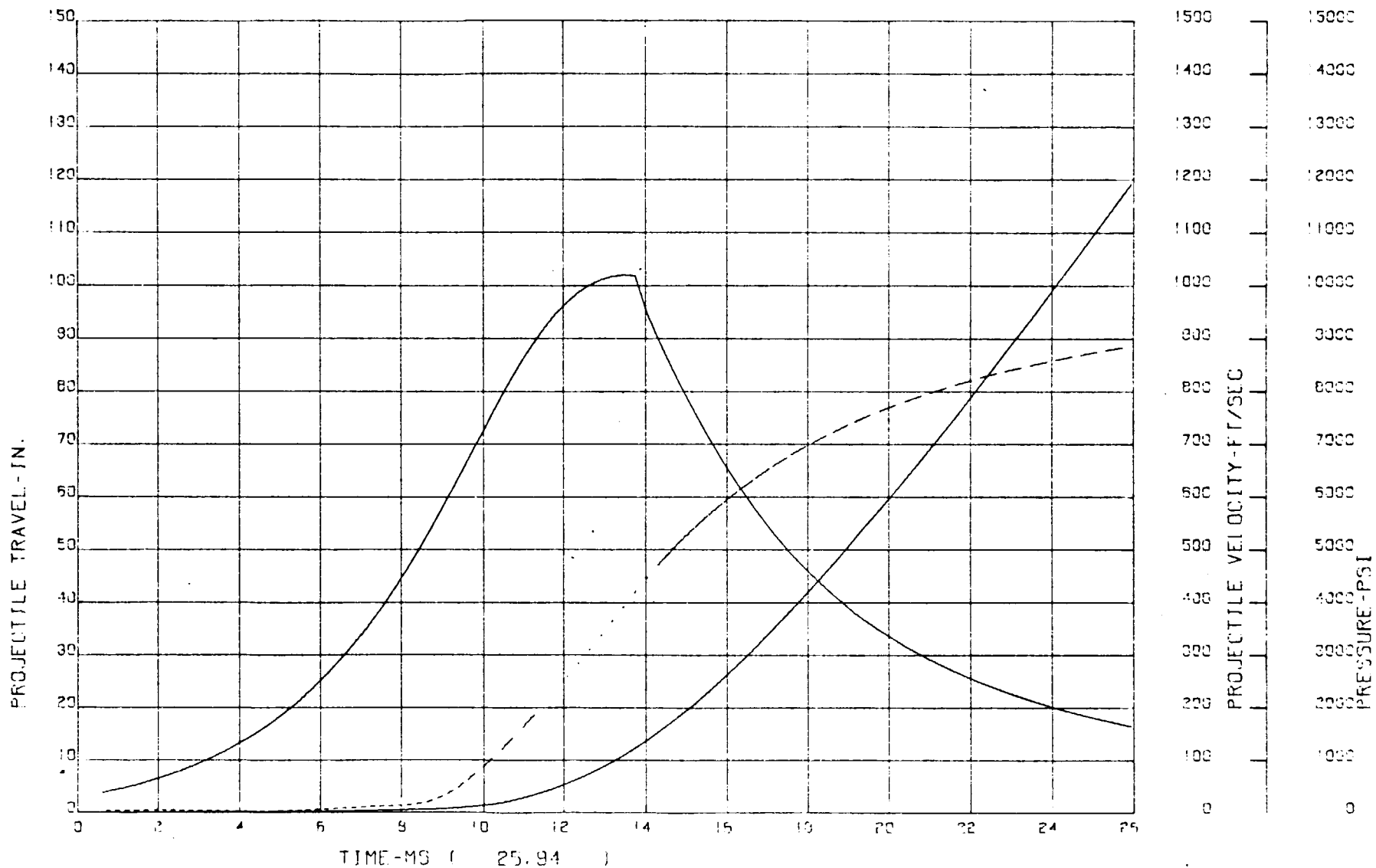
155MM HOWITZER, M1 FIRING HE, M107 ZONE 3 (M3)

PR2 = 4119 psi

PR3 = 346 psi

PROJECTILE TRAVEL, VELOCITY, BREECH PRESSURE, VS TIME

87

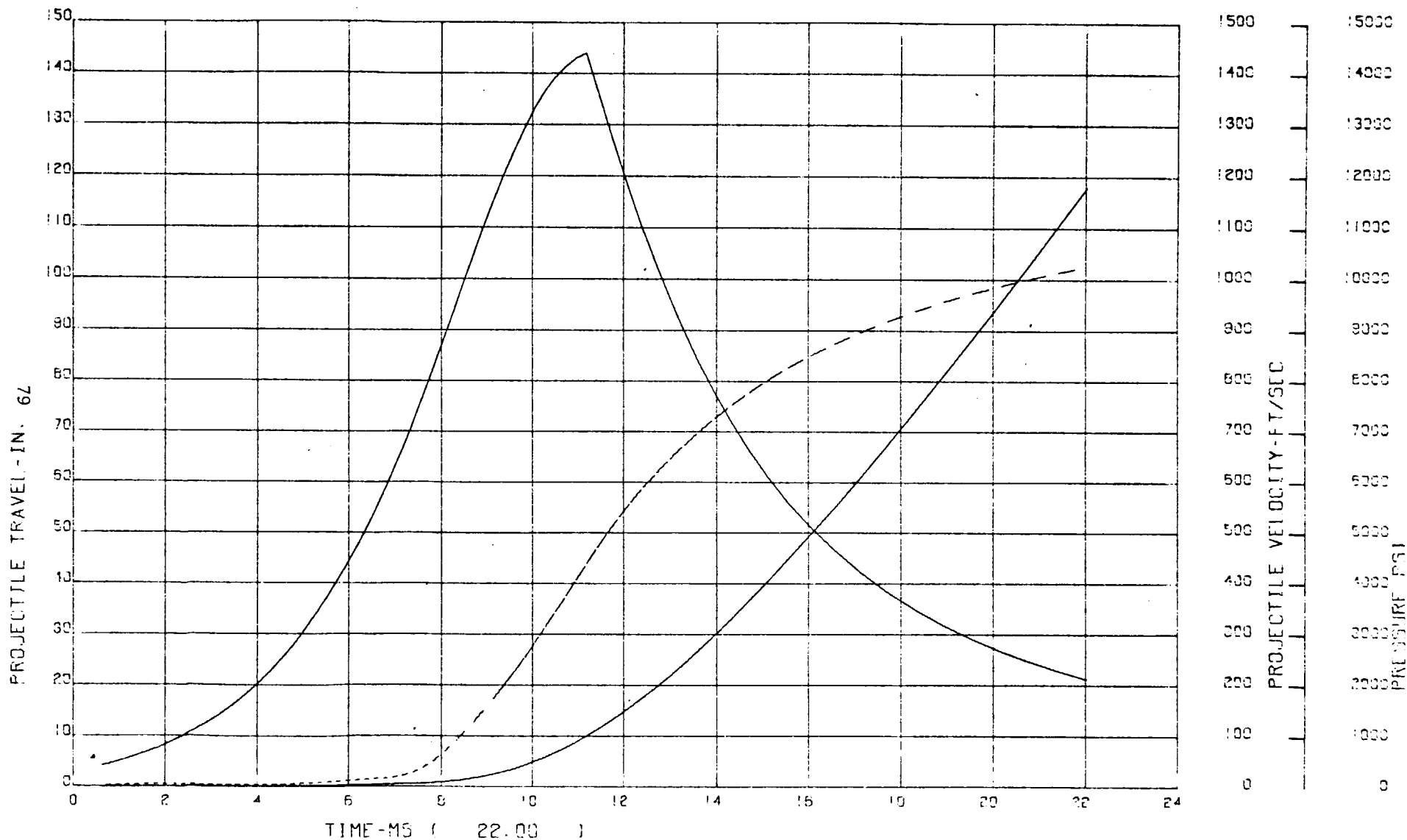


155MM HOWITZER, M1 FIRING HE, M107 ZONE 4 (M3)

PR2 = 5162 psi

PR3 = 311 psi

PROJECTILE TRAVEL, VELOCITY, BREECH PRESSURE, VS TIME

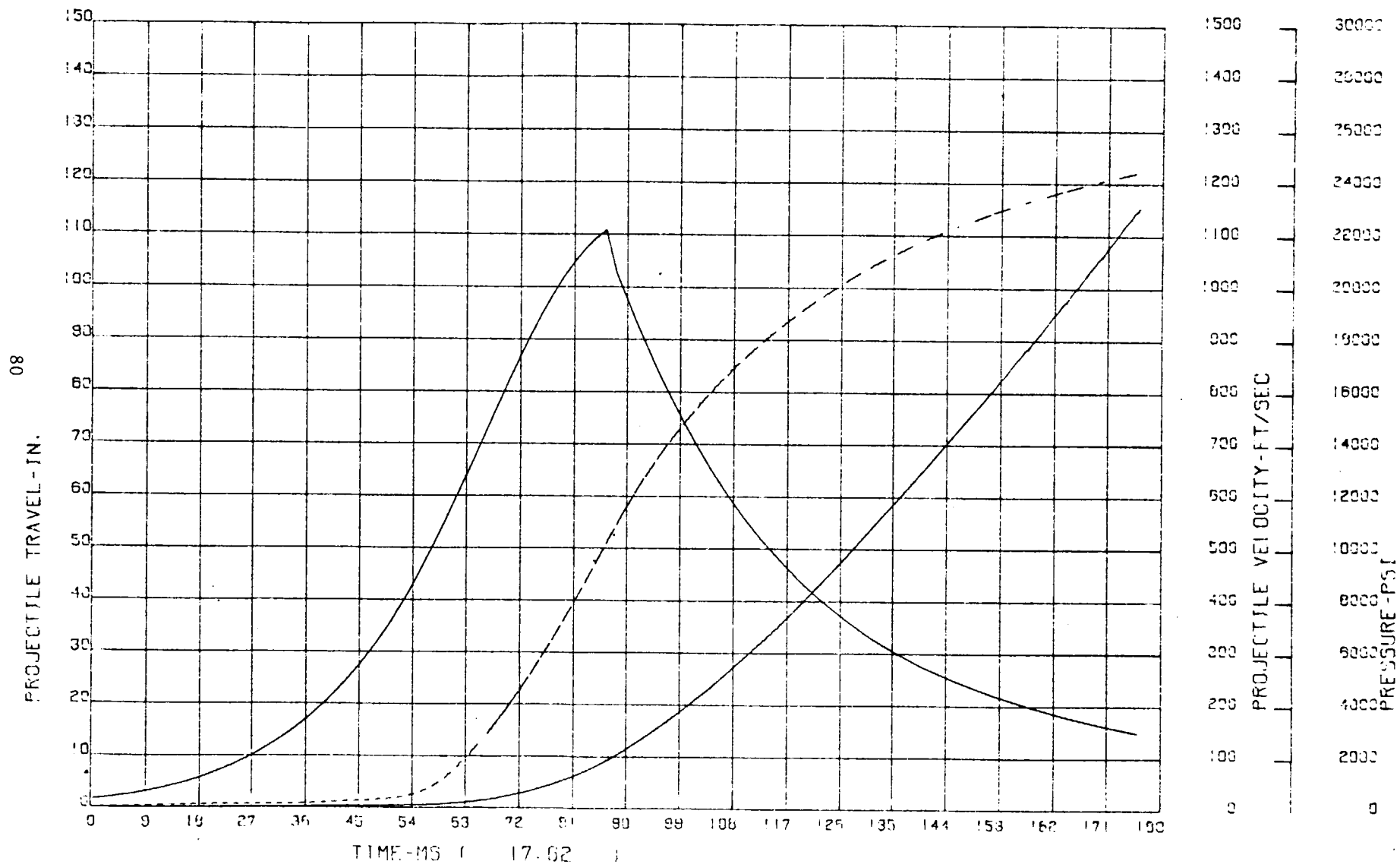


155MM HOWITZER, M1 FIRING HE, M107 ZONE 5 (M3)

PR2 = 6120 psi

PR3 = 330 psi

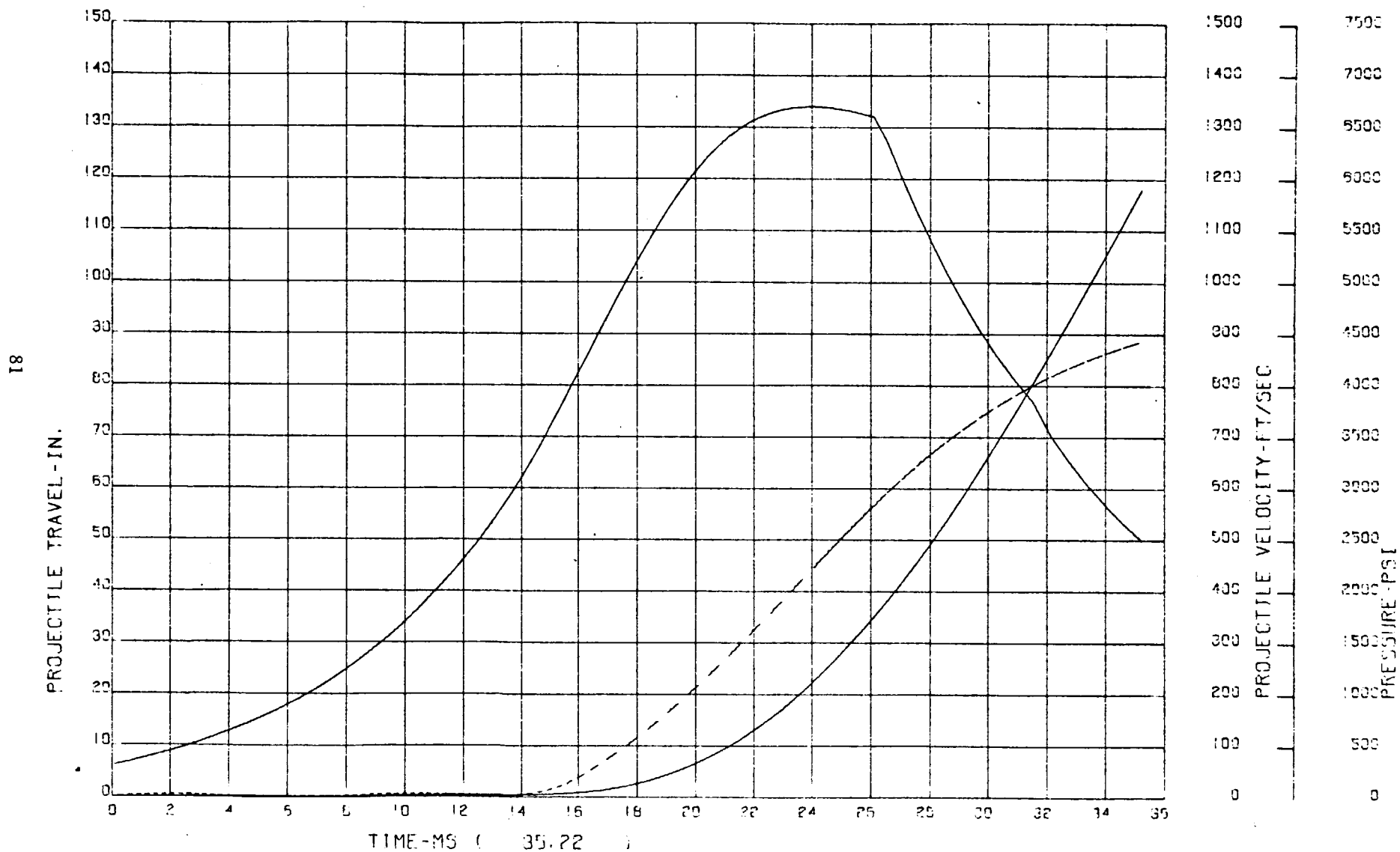
PROJECTILE TRAVEL, VELOCITY, BREECH PRESSURE, VS TIME



155MM HOWITZER, M1 FIRING HE, M107 ZONE 3 (M4A1)

PR2 = 2680 psi  
PR3 = 707 psi

PROJECTILE TRAVEL, VELOCITY, BREACH PRESSURE, VS TIME

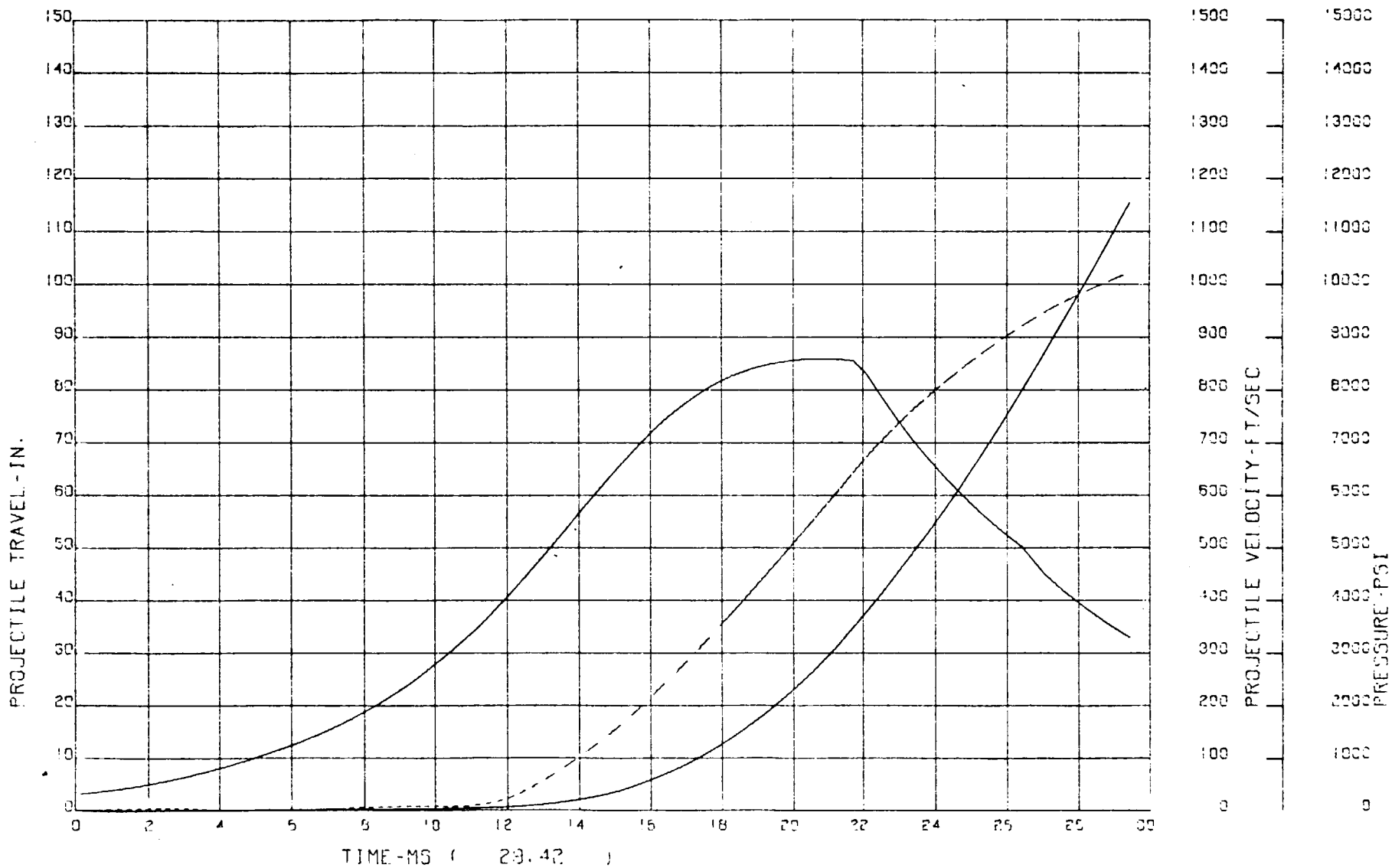


155MM HOWITZER, M1 FIRING HE, MID7 ZONE 4 (M4A1)

PR2 = 2995 psi

PR3 = 623 psi

PROJECTILE TRAVEL, VELOCITY, BREACH PRESSURE, VS TIME

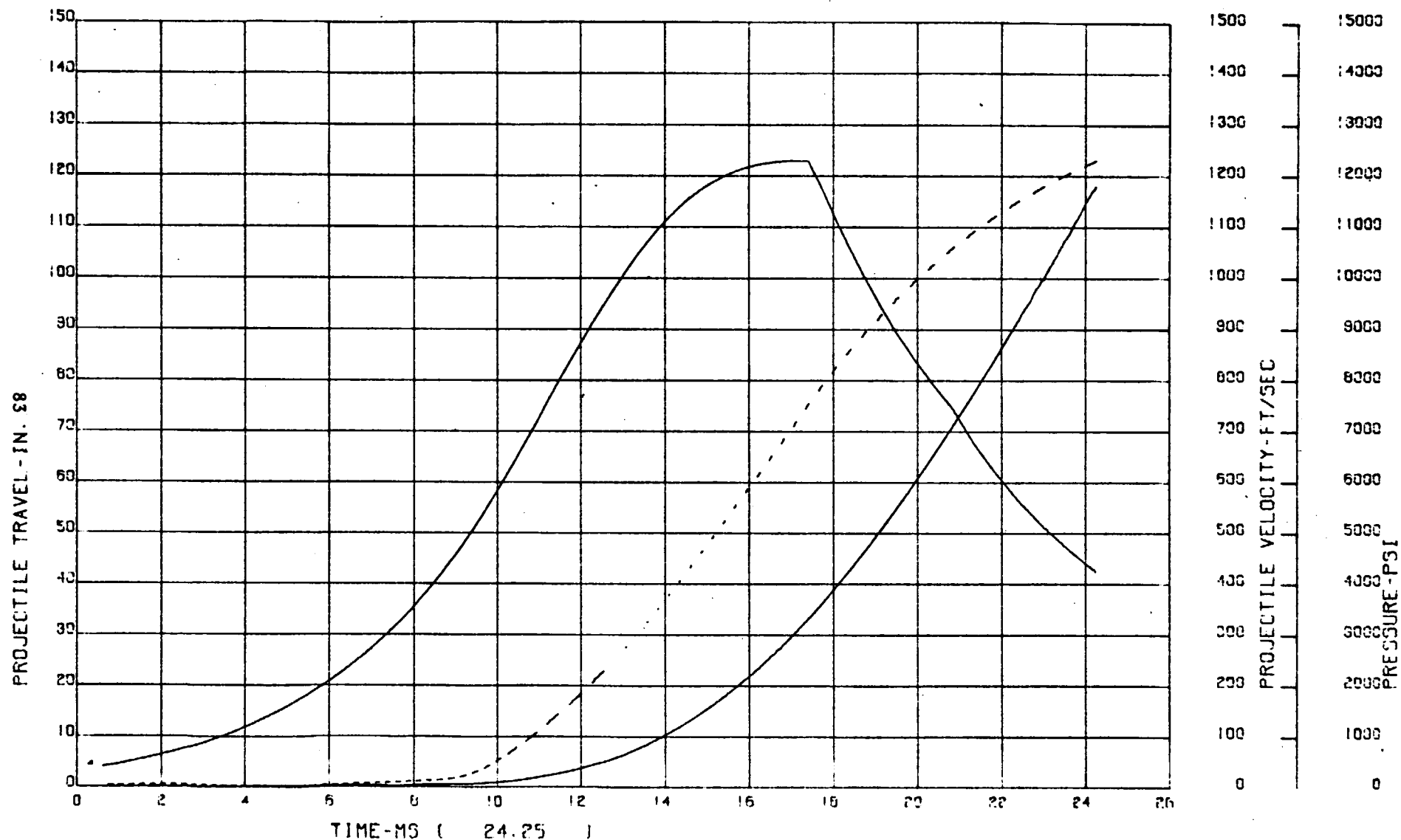


155MM HOWITZER, M1 FIRING HE, M107 ZONE 5 (M4A1)

PR2 = 3446 psi

PR3 = 483 psi

PROJECTILE TRAVEL, VELOCITY, BREECH PRESSURE, VS TIME



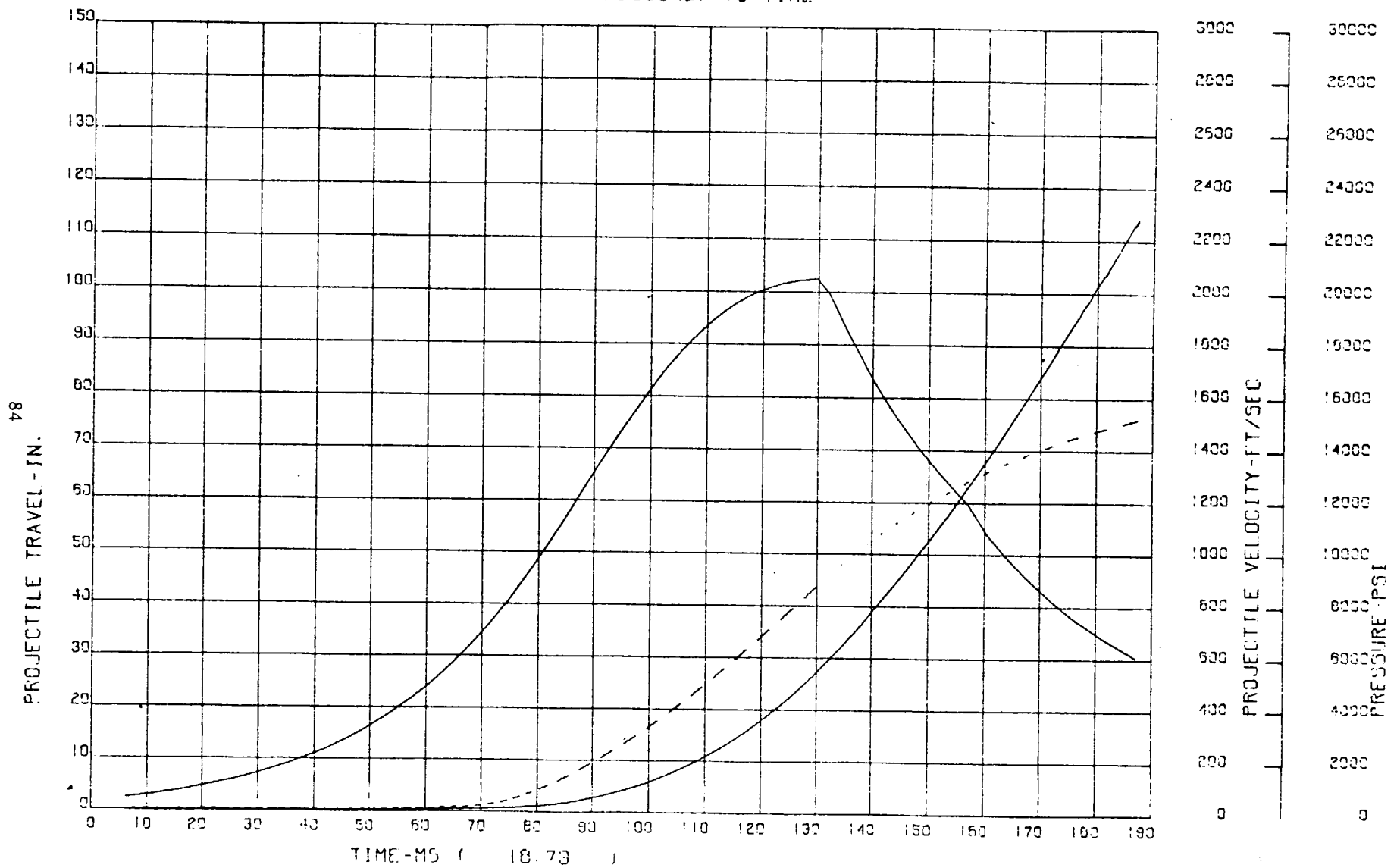
155MM HOWITZER, M1 FIRING HE, M107 ZONE 6 (M4A1)

RUN NO = 1

PR2 = 4904 psi

PR3 = 272 psi

PROJECTILE TRAVEL, VELOCITY, BREECH PRESSURE, VS TIME

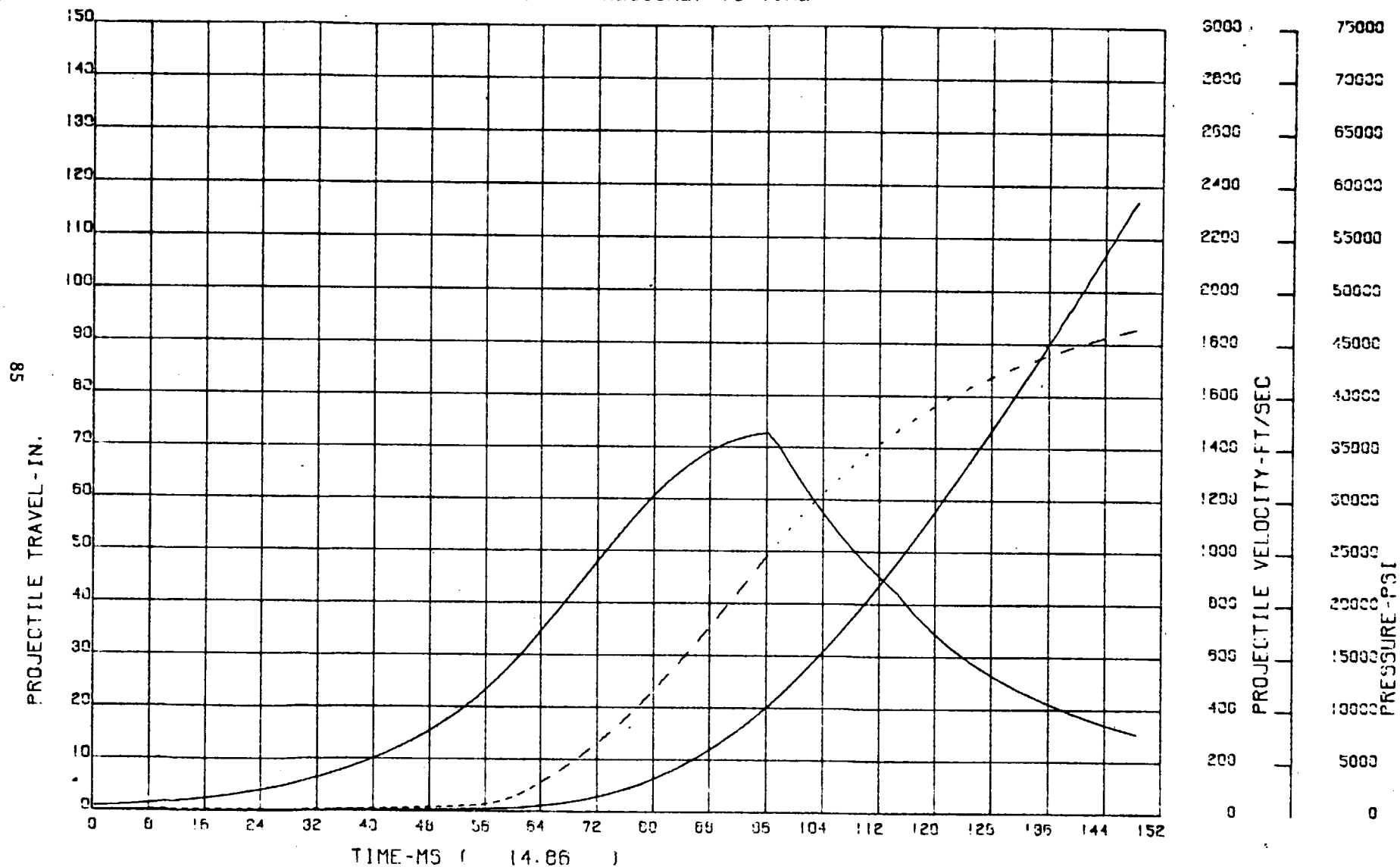


155MM HOWITZER, M1 FIRING HE, M107 ZONE 7 (M4A1)

PR2 = 8288 psi

PR3 = 476 psi

PROJECTILE TRAVEL, VELOCITY, BREECH PRESSURE, VS TIME

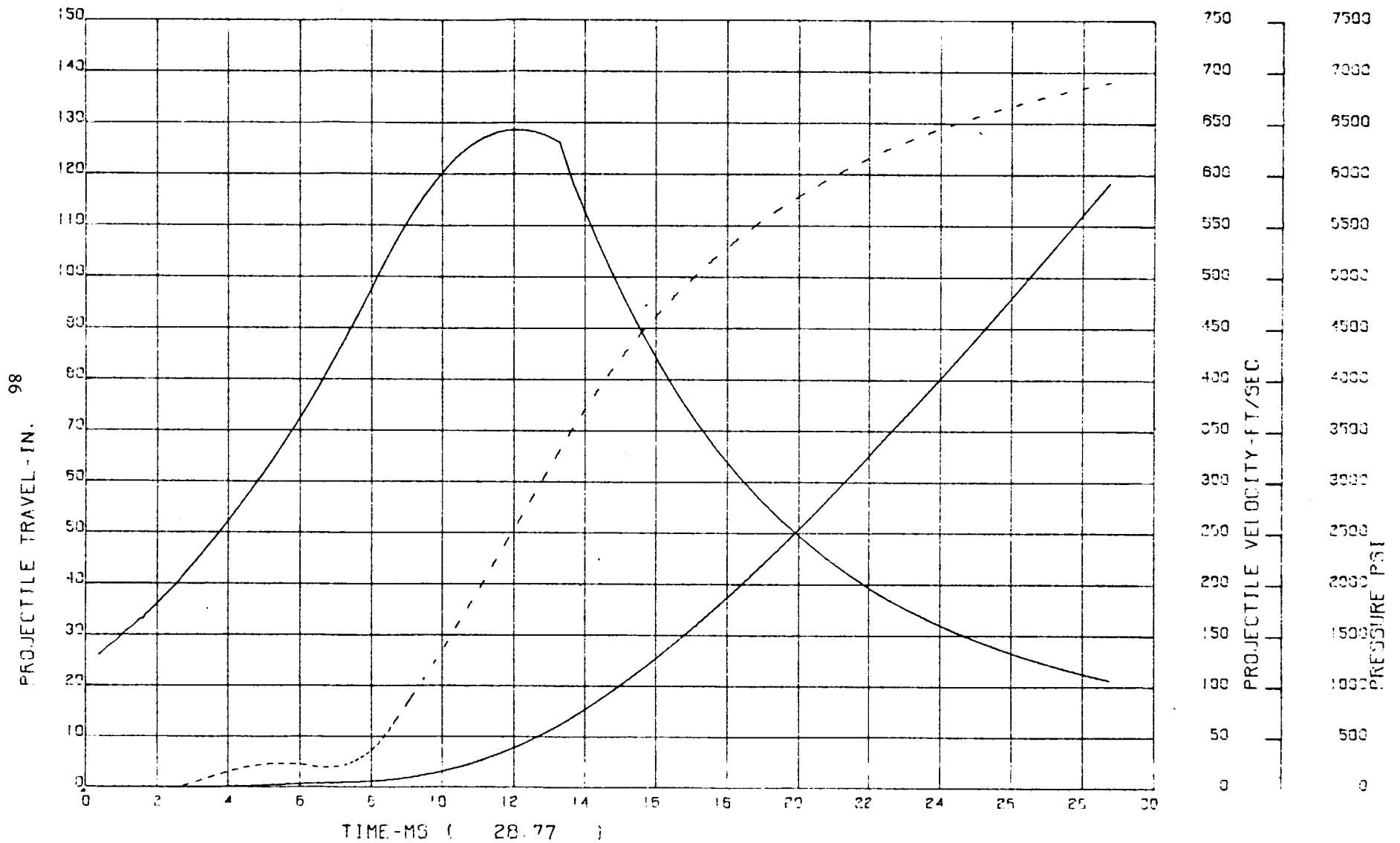


155MM HOWITZER. M125 FIRING HE. RAP. XM549 ZONE 1 (M3A1)

PR2 = 3621 psi

PR3 = 308 psi

PROJECTILE TRAVEL, VELOCITY, BREECH PRESSURE, VS TIME

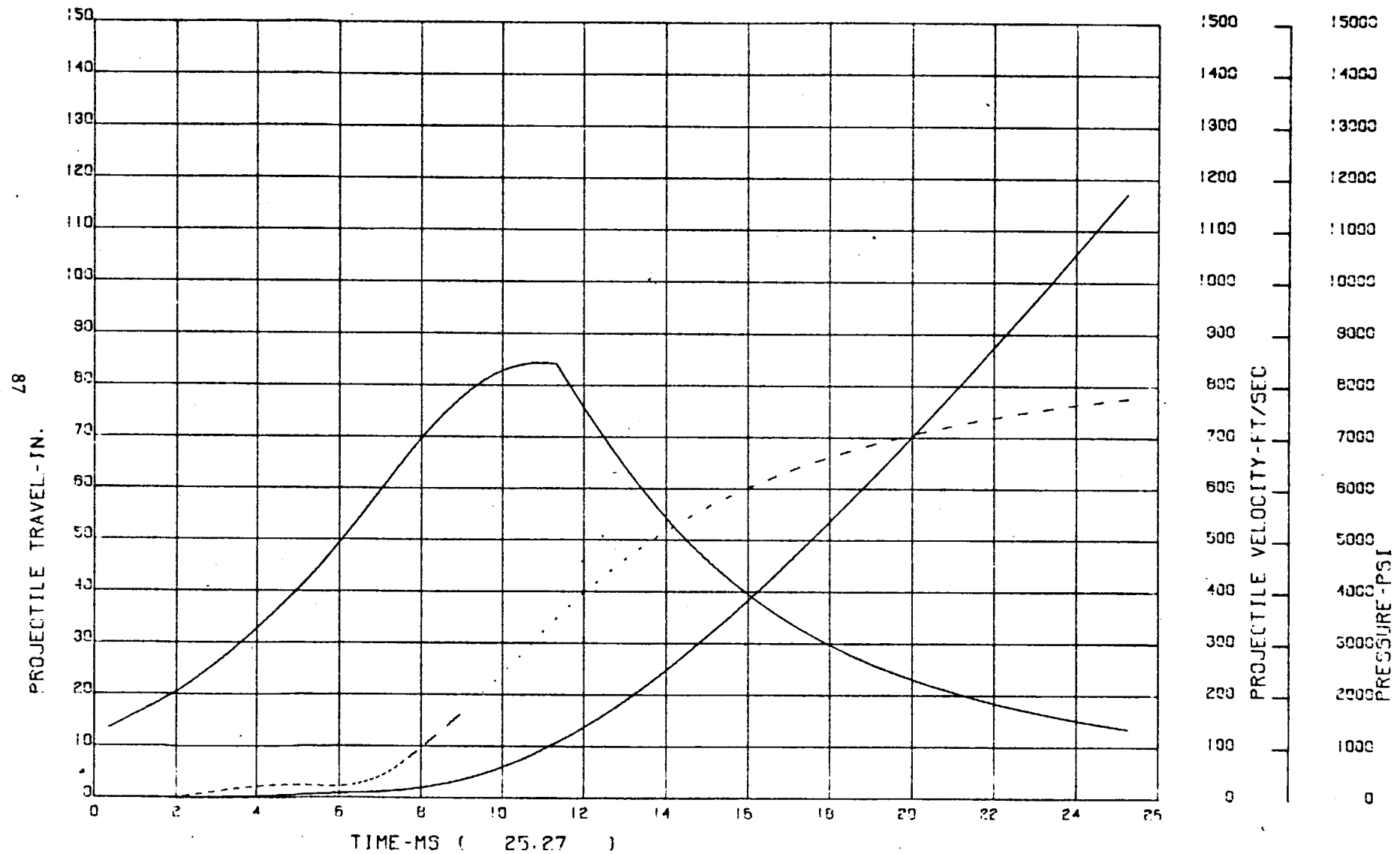


155MM HOWITZER, M126 FIRING HE, RAP, XM549 ZONE 2(M3A1)

PR2 = 4208 psi

PR3 = 388 psi

PROJECTILE TRAVEL, VELOCITY, BREECH PRESSURE, VS TIME



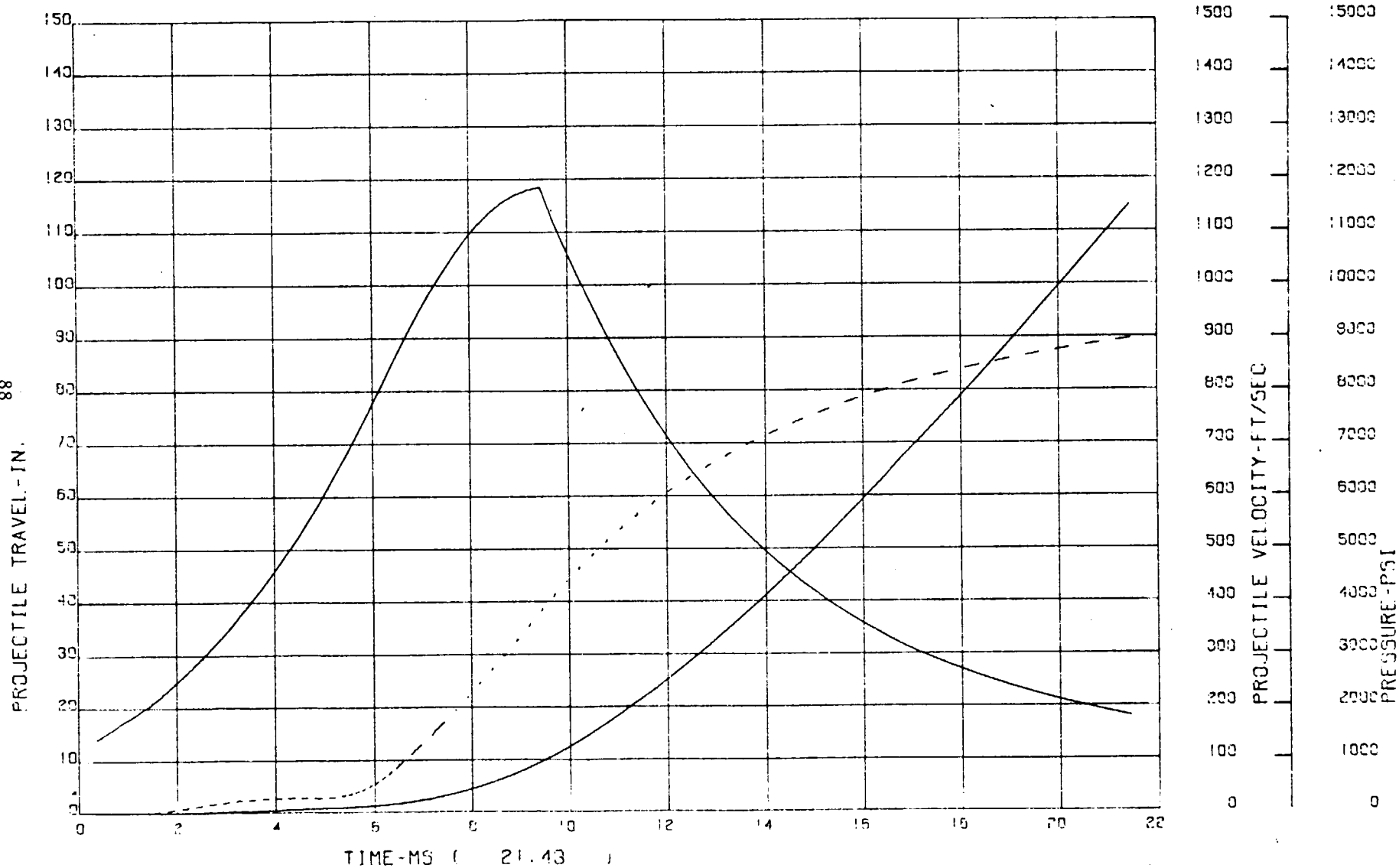
155MM HOWITZER, M126 FIRING HE, RAP, XM549 ZONE 3(M3A1)

PR2 = 5125 psi

PR3 = 487 psi

PROJECTILE TRAVEL, VELOCITY, BREACH PRESSURE, VS TIME

88



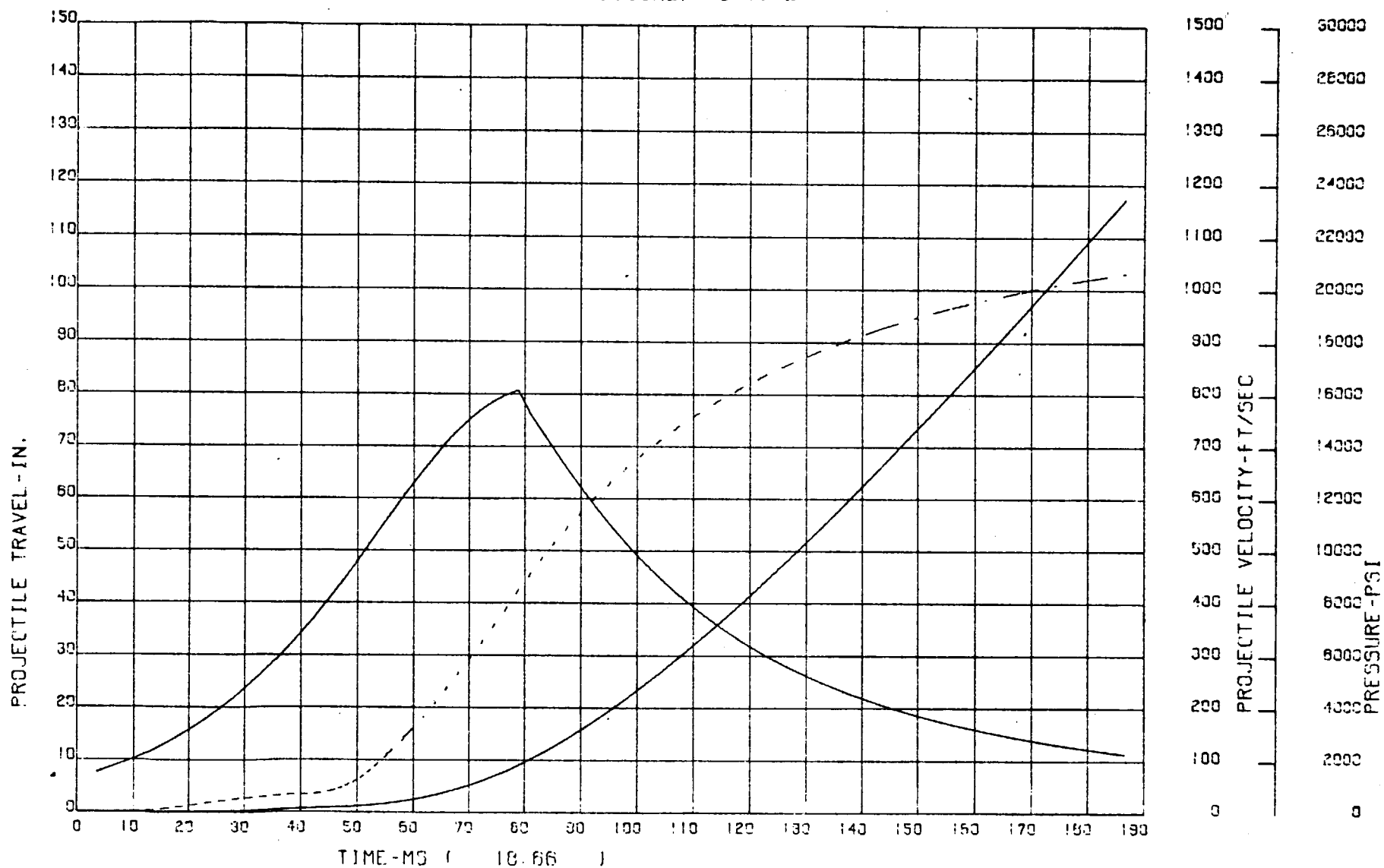
155MM HOWITZER, M126 FIRING HE, RAP, XM549 ZONE 4 (M3A1)

PR2 = 6202 psi

PR3 = 547 psi

PROJECTILE TRAVEL, VELOCITY, BREECH PRESSURE, VS TIME

68



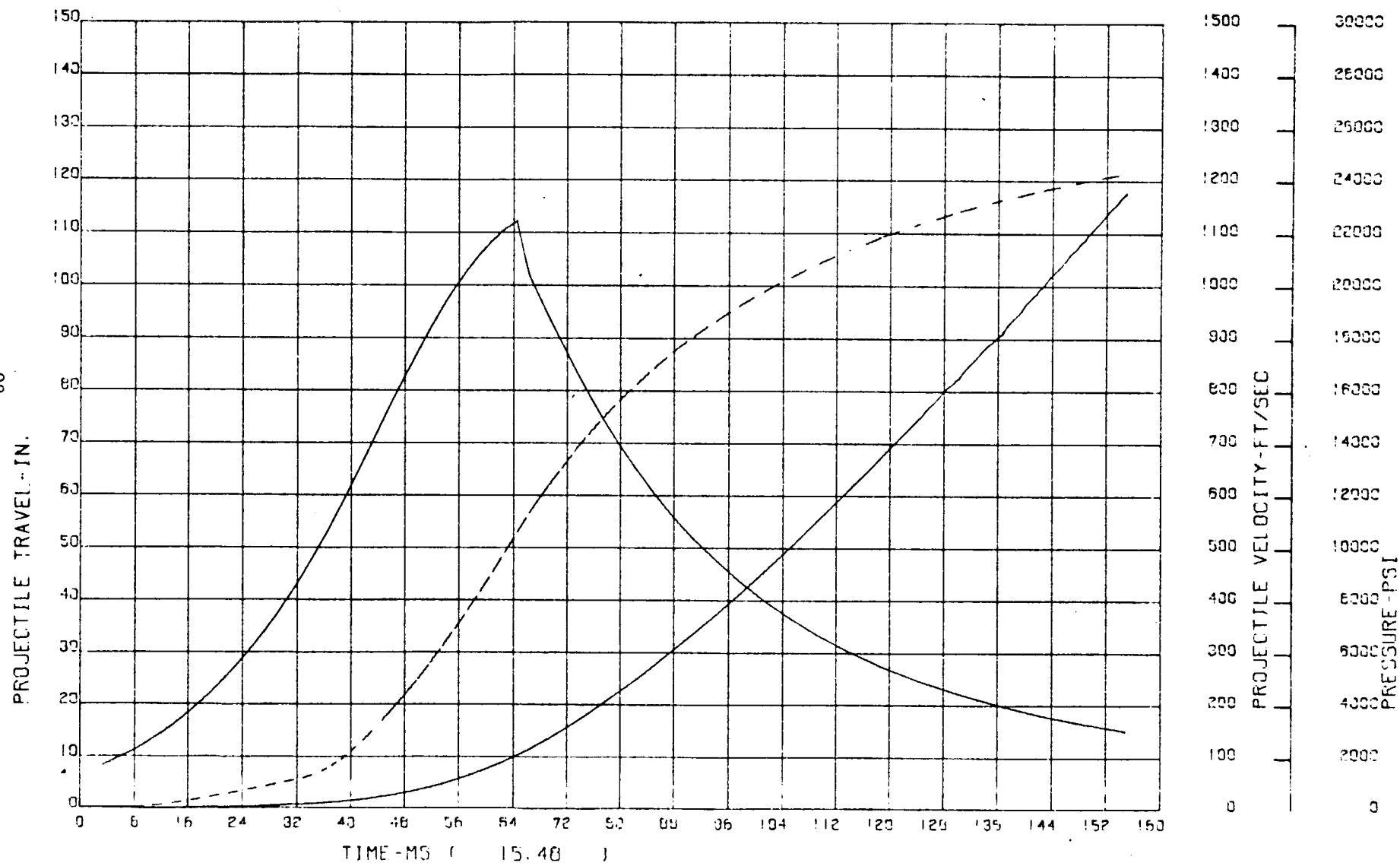
155MM HOWITZER, M126 FIRING HE, RAP, XM549 ZONE 5(M3A1)

PR2 = 6459 psi

PR3 = 595 psi

PROJECTILE TRAVEL, VELOCITY, BREACH PRESSURE, VS TIME

06

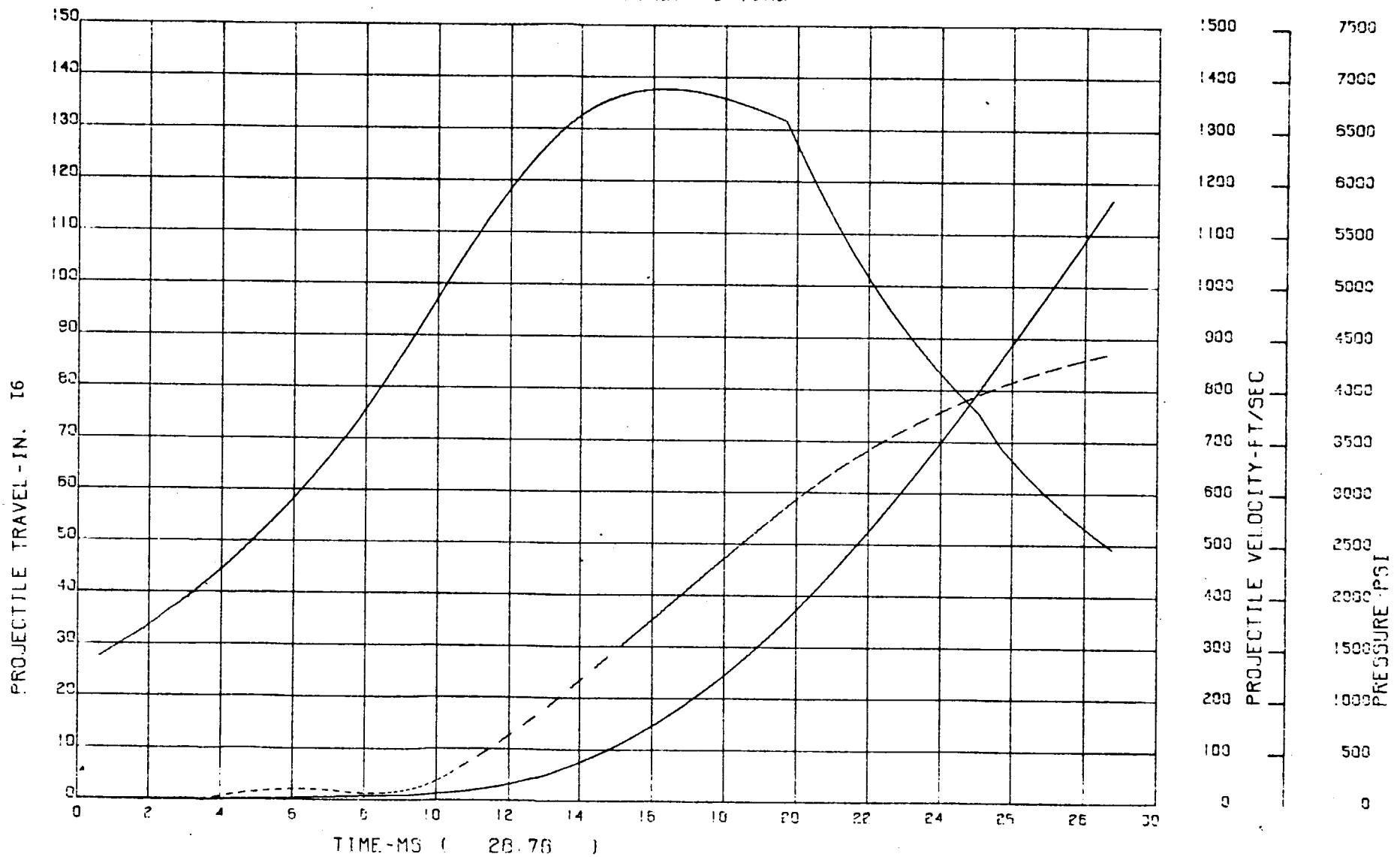


155MM HOWITZER, M126 FIRING HE, RAP, XM549 ZONE 3 (M4A2)

PR2 = 3317 psi

PR3 = 762 psi

PROJECTILE TRAVEL, VELOCITY, BREECH PRESSURE, VS TIME



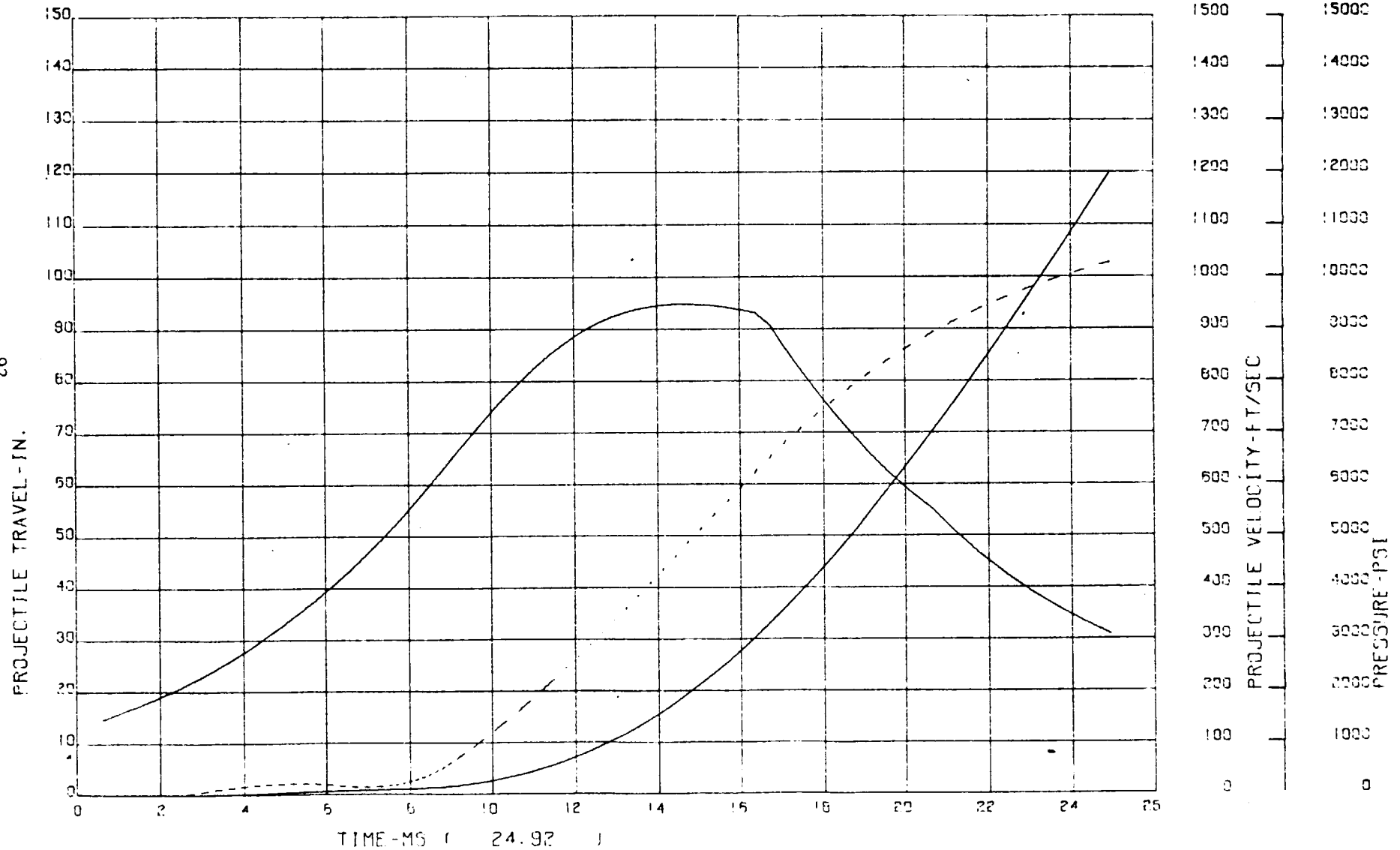
155MM HOWITZER, M125 FIRING HE, RAP, XM549 ZONE 4(M4A2)

PR2 = 3916 psi

PR3 = 827 psi

PROJECTILE TRAVEL, VELOCITY, BREACH PRESSURE, VS TIME

92

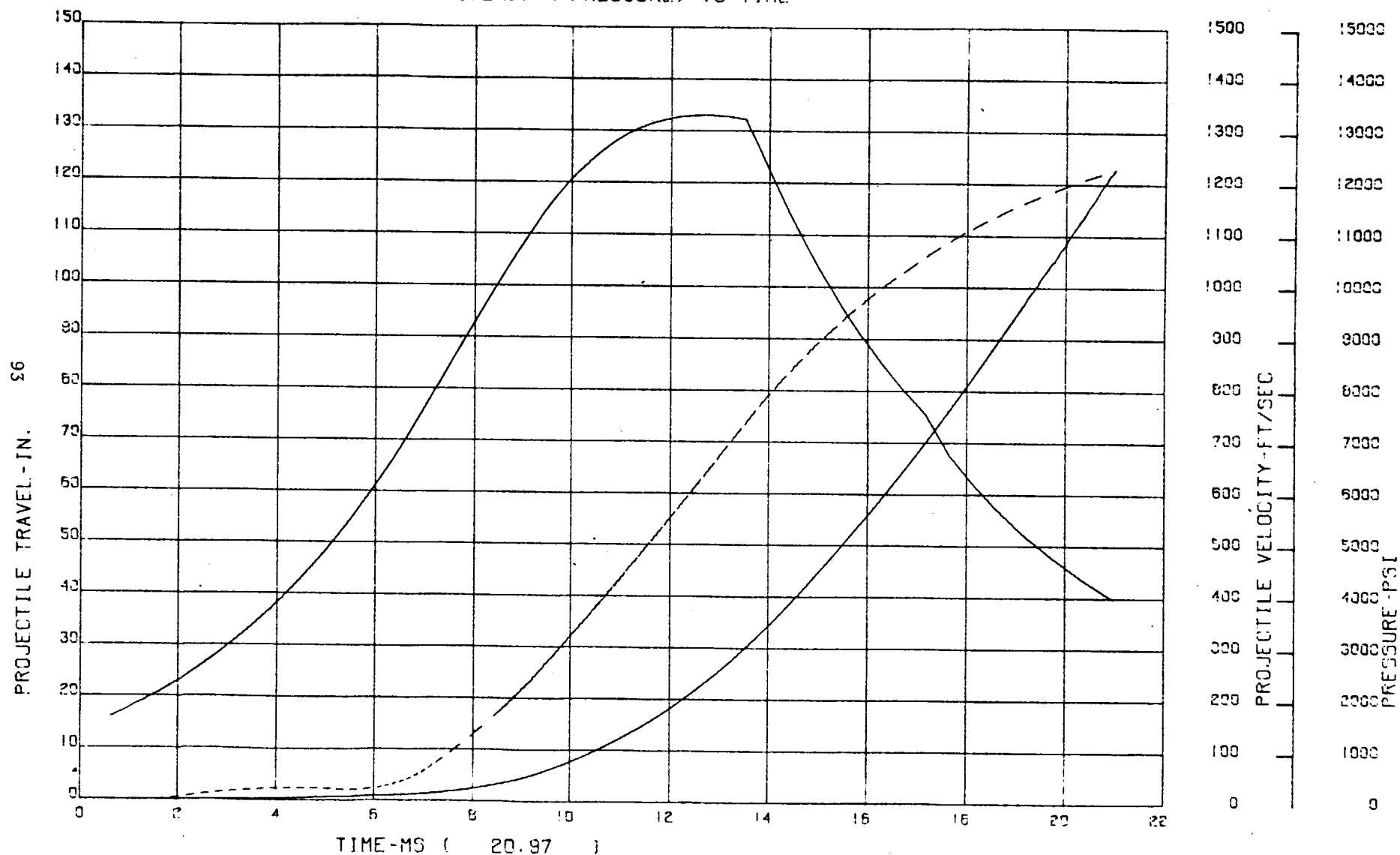


155MM HOWITZER, M126 FIRING HE, RAP, XM549 ZONE 5 (M4A2)

PR2 = 4821 psi

PR3 = 729 psi

PROJECTILE TRAVEL, VELOCITY, BREECH PRESSURE, VS TIME

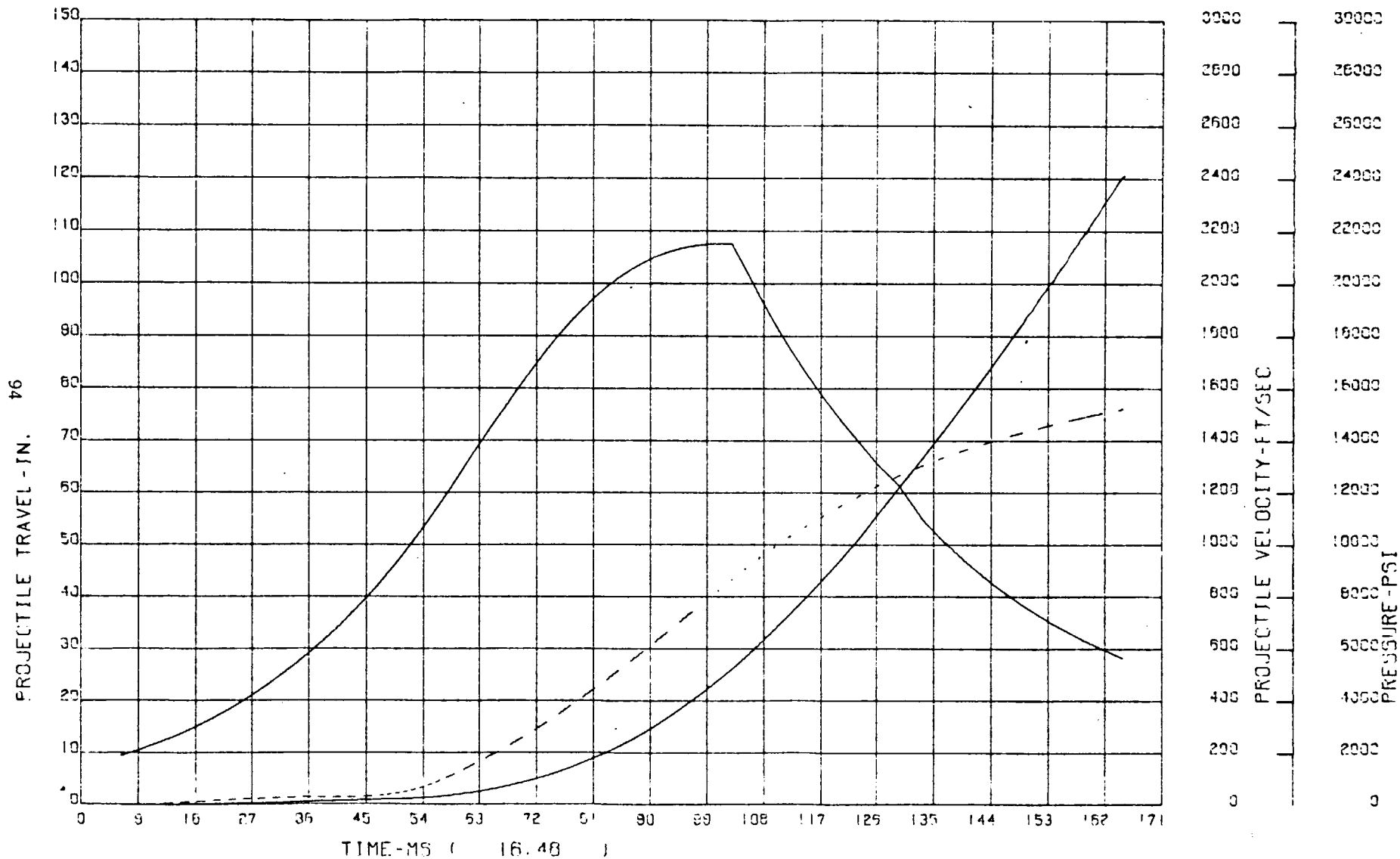


155MM HOWITZER, M126 FIRING HE, RAP, XM549 ZONE 6 (M4A2)

PR2 = 6405 psi

PR3 = 638 psi

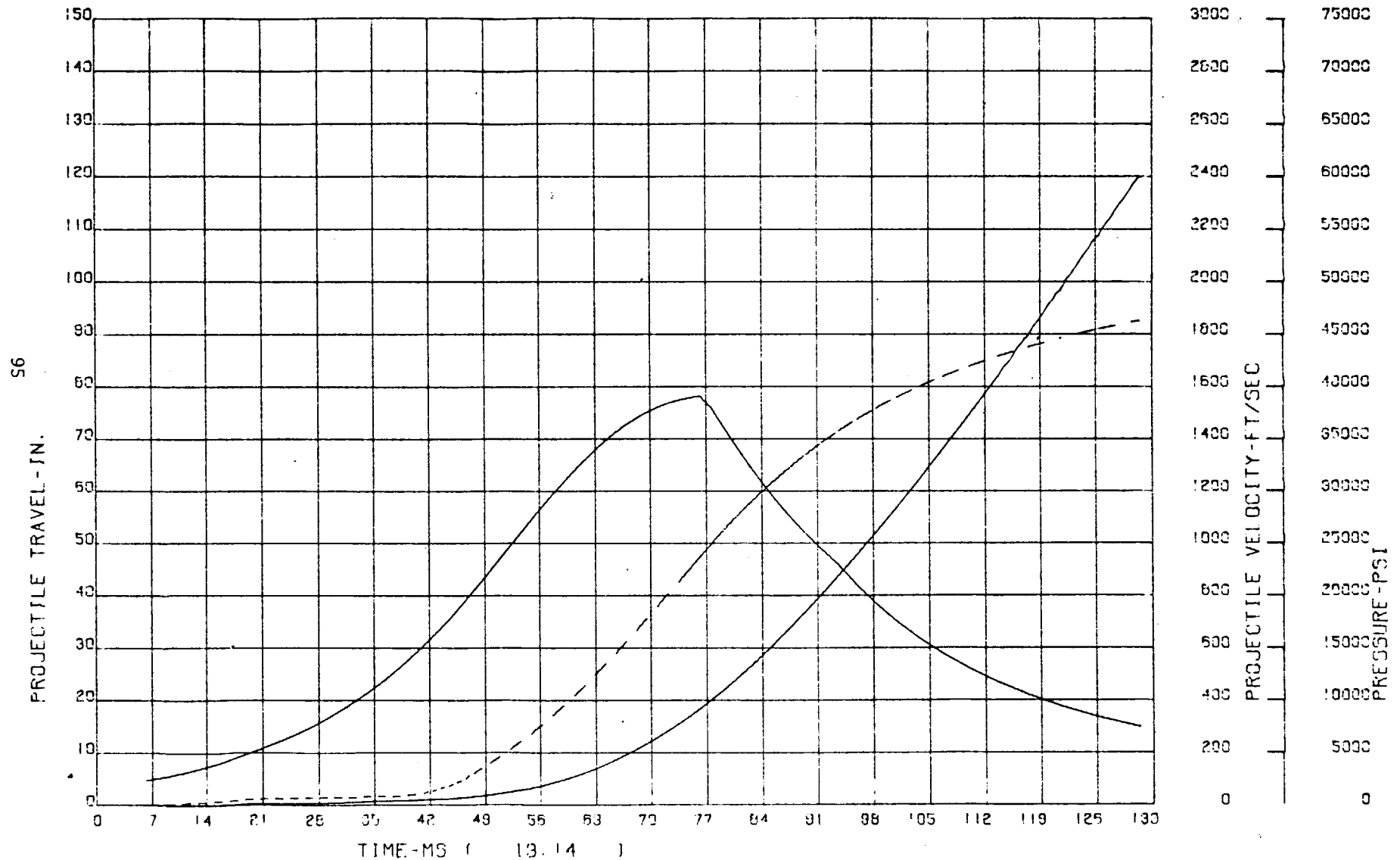
PROJECTILE TRAVEL, VELOCITY, BREACH PRESSURE, VS TIME



155MM HOWITZER, M126 FIRING HE, RAP. XM549 ZONE 7 (M4A2)

PR2 = 9964 psi  
PR3 = 1211 psi

PROJECTILE TRAVEL, VELOCITY, BREACH PRESSURE, VS TIME

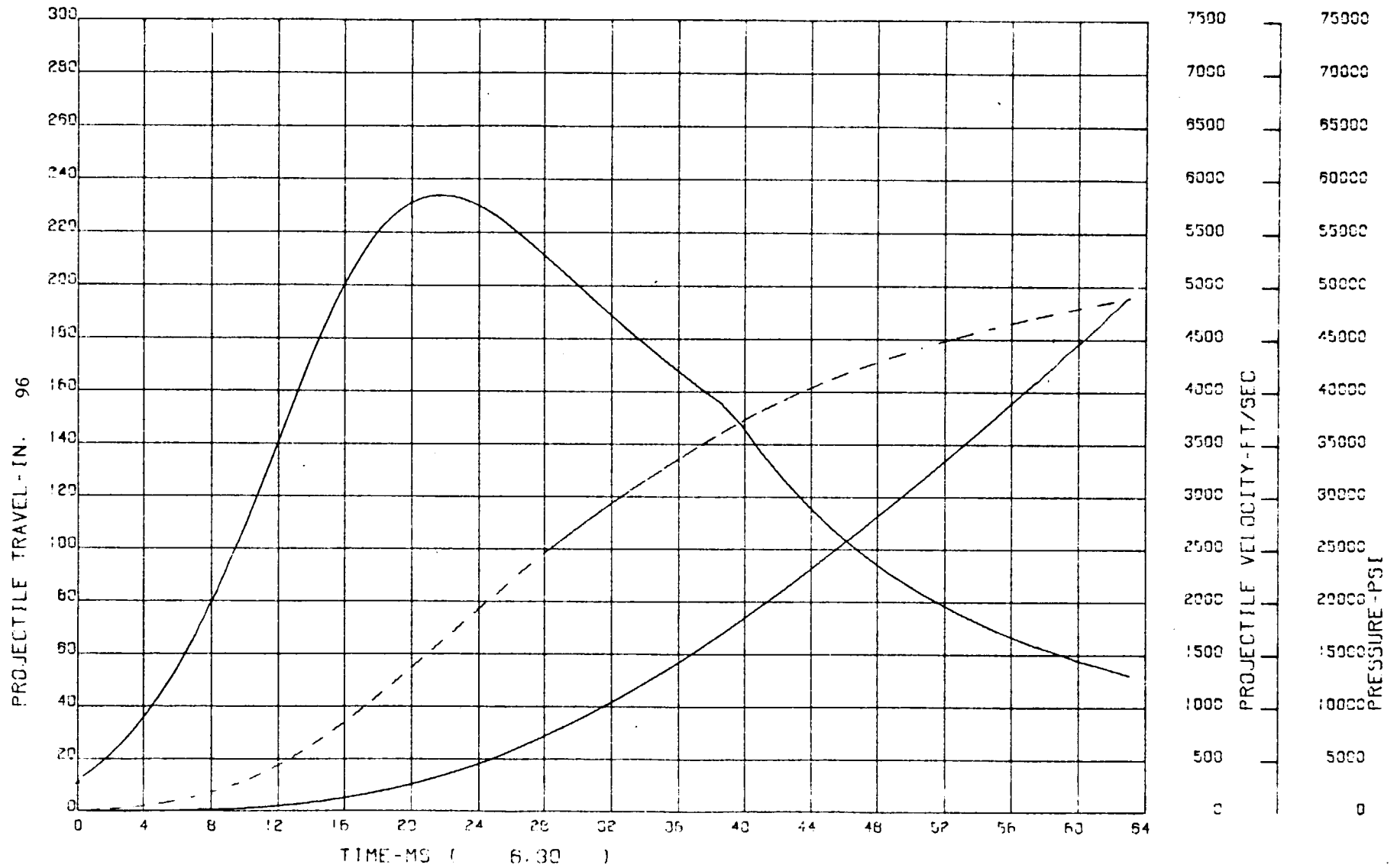


105MM GUN, M68 FIRING APDS, M392A2

PR2 = 566 psi

PR3 = 100 psi

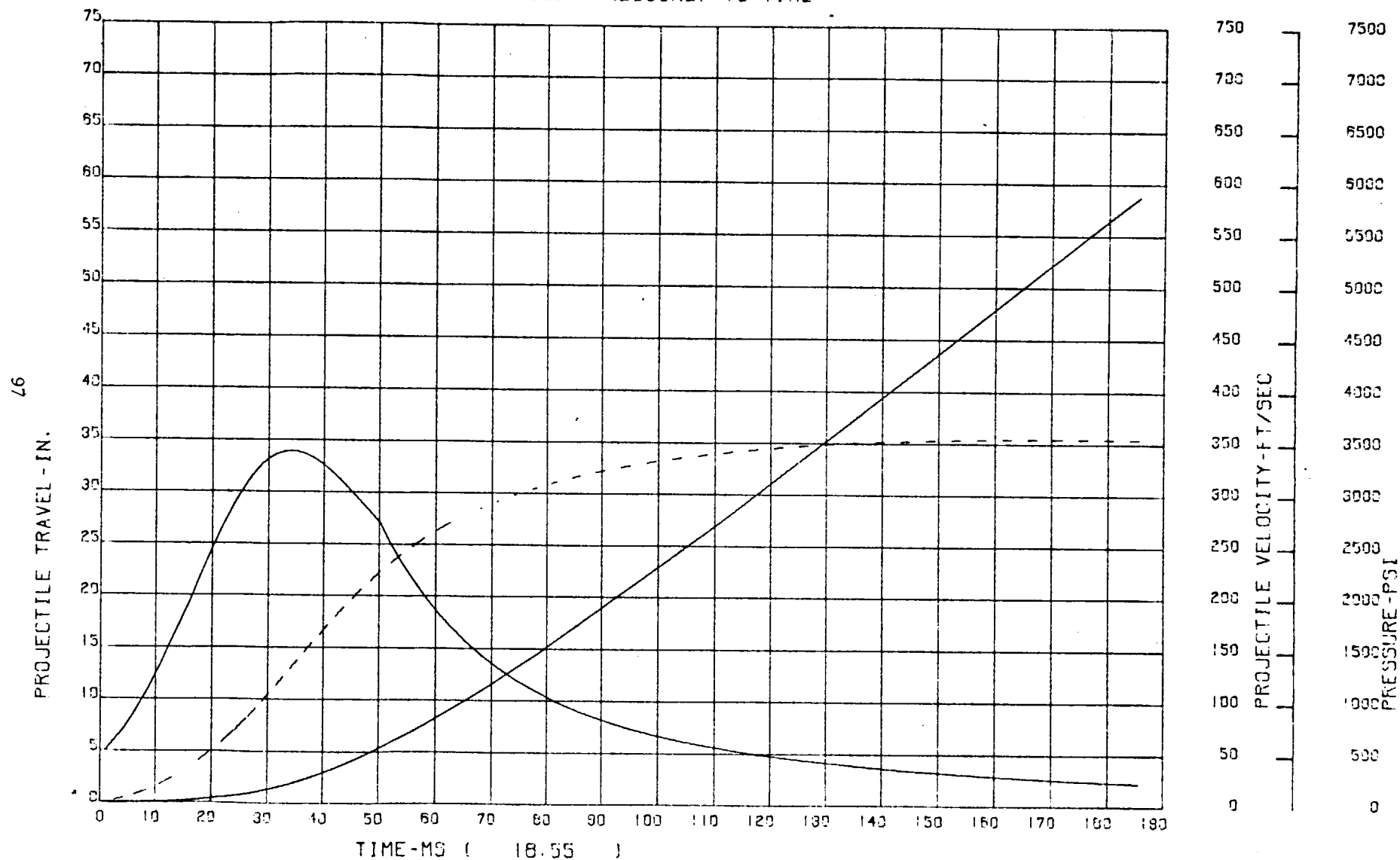
PROJECTILE TRAVEL, VELOCITY, BREECH PRESSURE, VS TIME



# 4.2-INCH MORTAR, M30 FIRING HE, M329A1 5 INC (M36A1)

PR2 = 0 psi  
PR3 = 230 psi

PROJECTILE TRAVEL, VELOCITY, BREACH PRESSURE, VS TIME



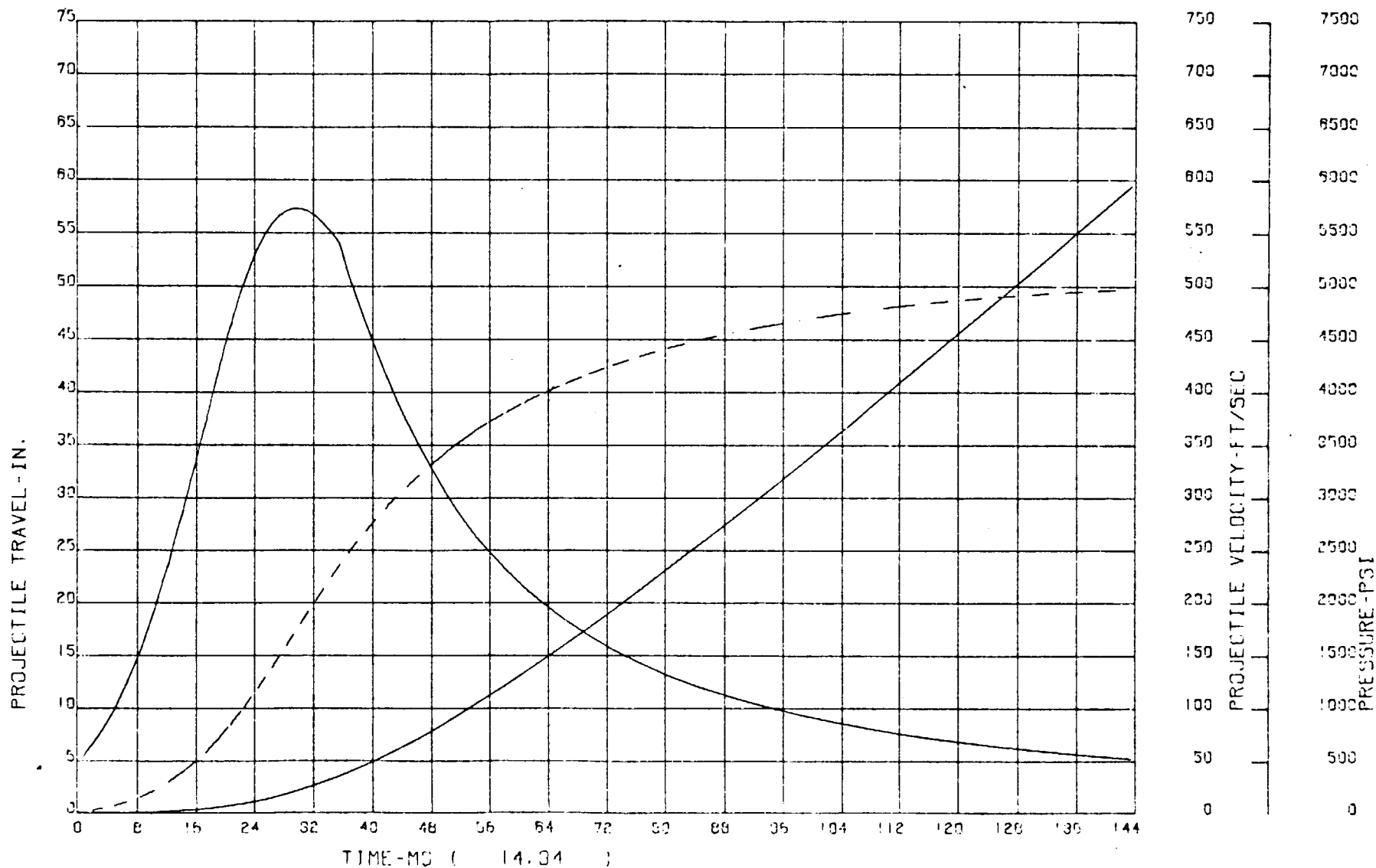
# 4.2-INCH MORTAR, M30 FIRING HE, M329A1 11 INC (M36A1)

PR2 = 0 psi

PR3 = 353 psi

PROJECTILE TRAVEL, VELOCITY, BREECH PRESSURE, VS TIME

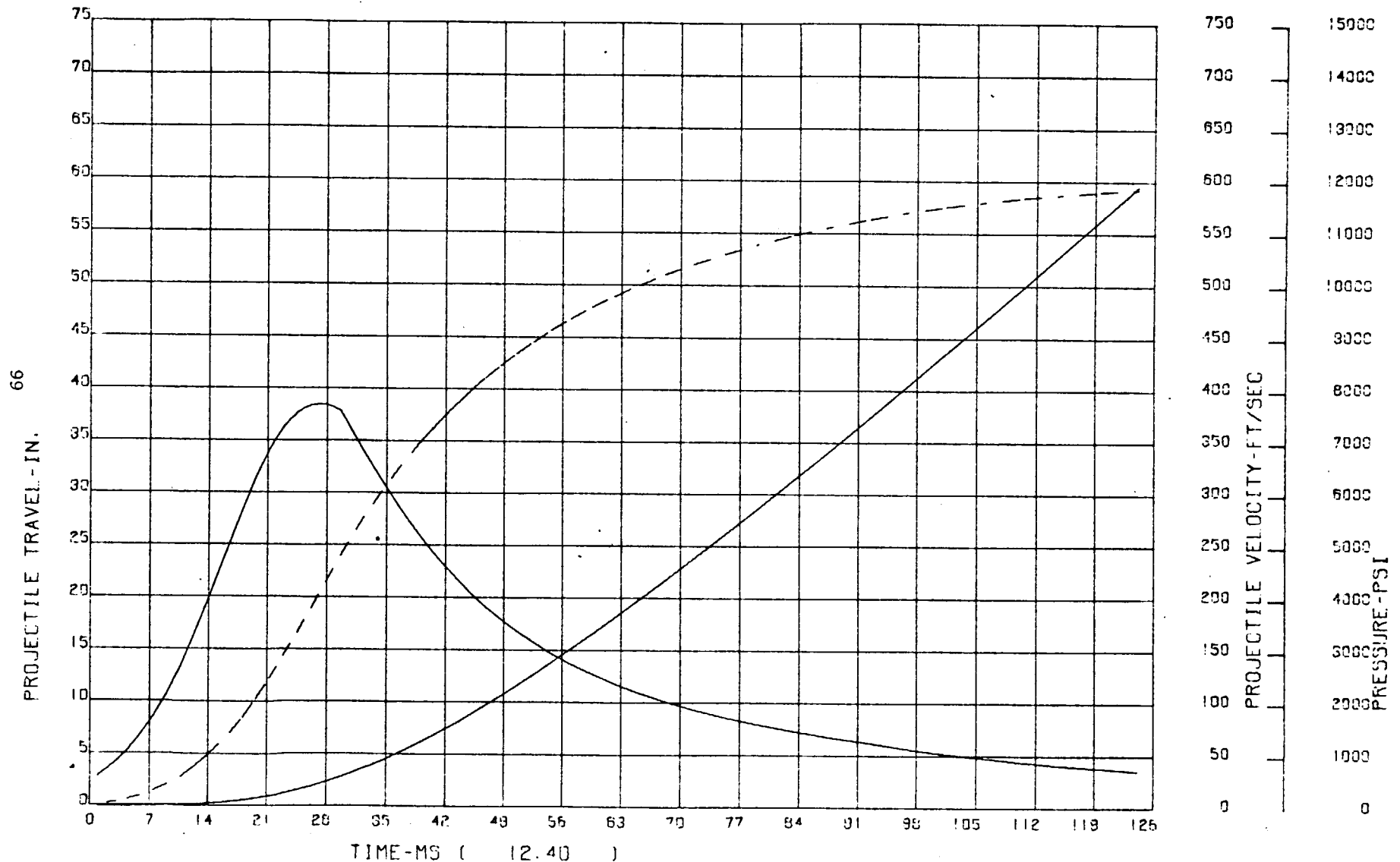
86



4.2-INCH MORTAR, M30 FIRING HE, M329A1 15 INC (M36A1)

PR2 = 0 psi.  
PR3 = 465 psi

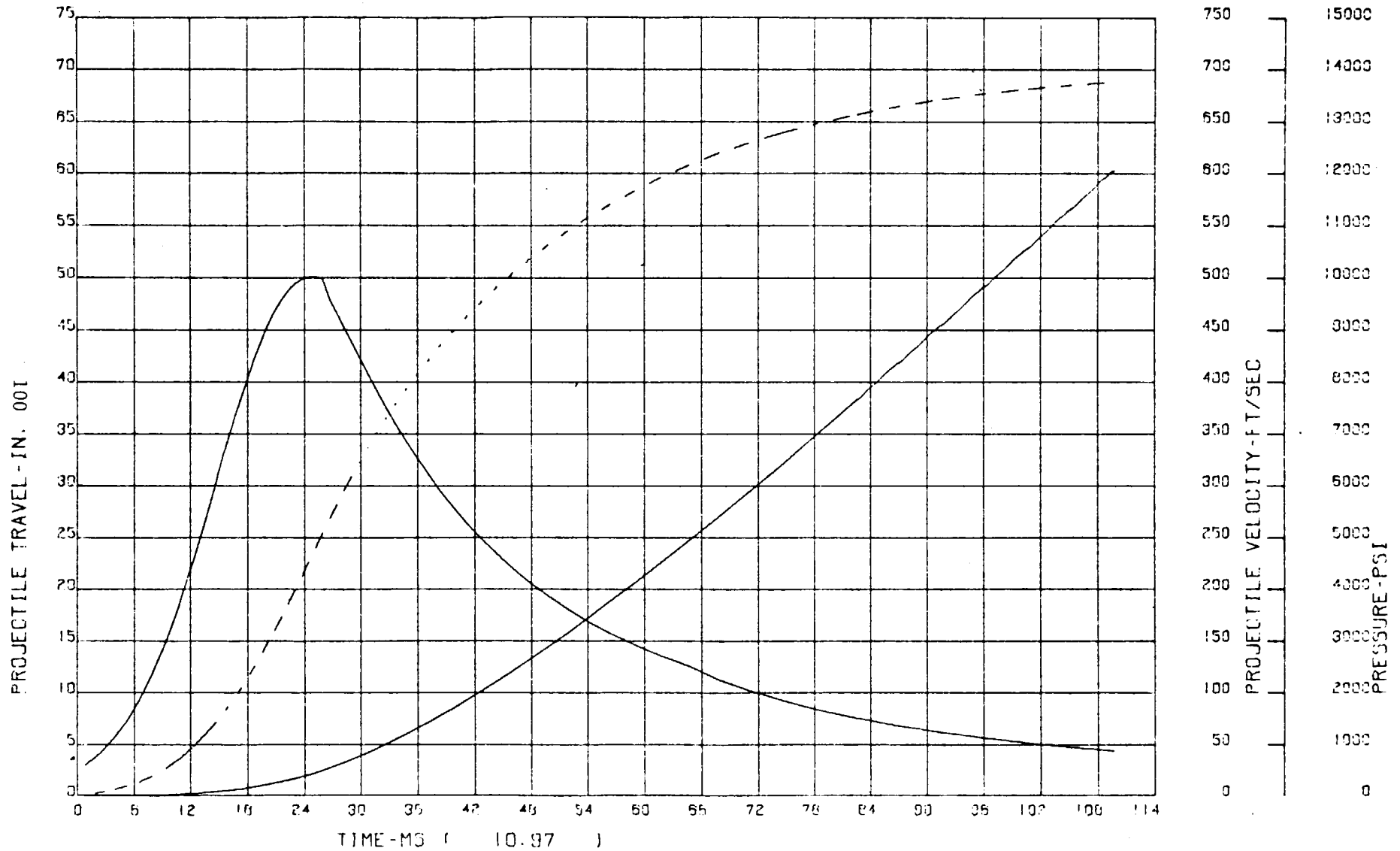
PROJECTILE TRAVEL, VELOCITY, BREECH PRESSURE, VS TIME



4.2-INCH MORTAR, M30 FIRING HE, M329A1 19 INC (M36A1)

PR2 = 0 psi  
PR3 = 540 psi

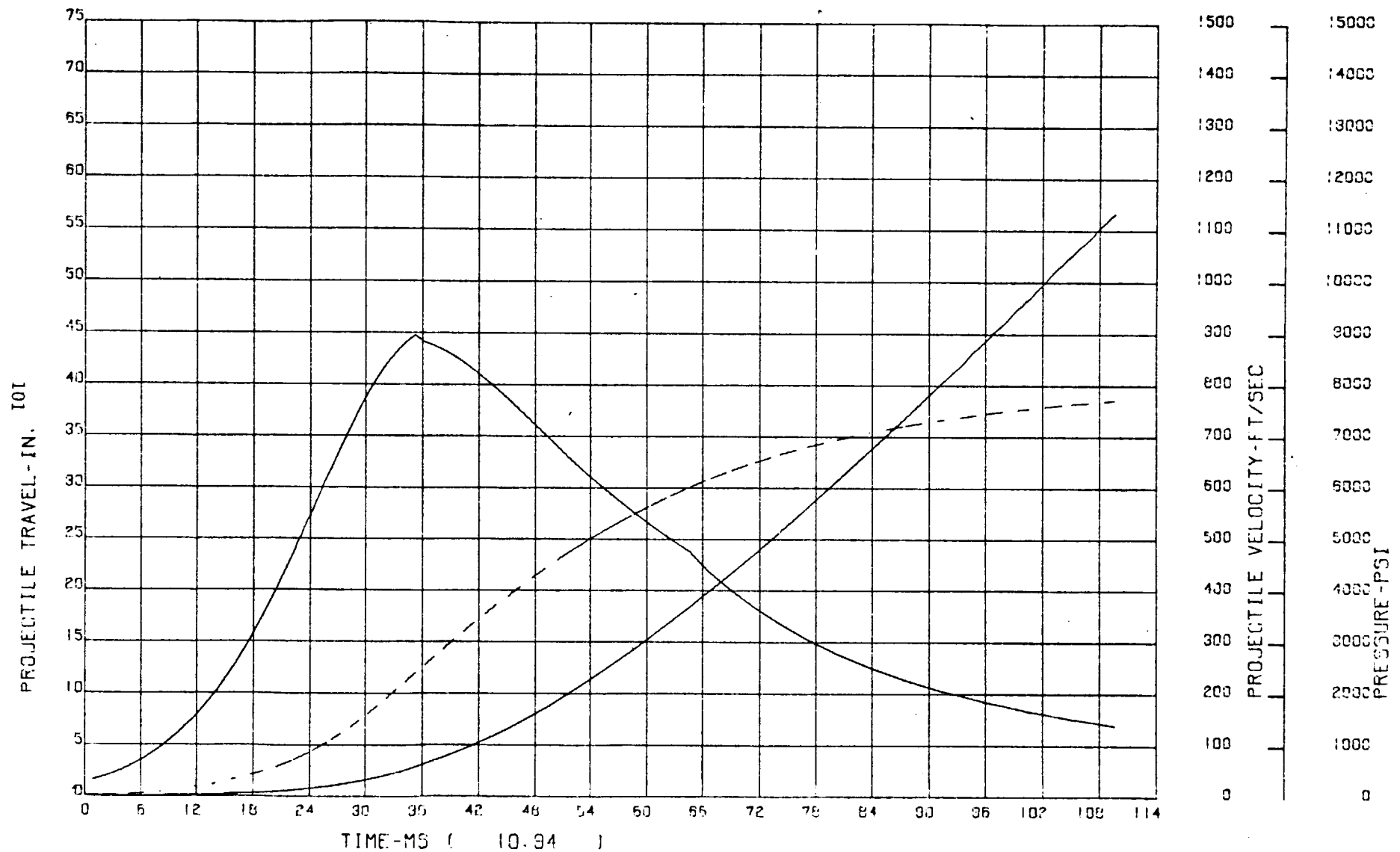
PROJECTILE TRAVEL, VELOCITY, BREECH PRESSURE, VS TIME



# 4.2-INCH MORTAR, M30 FIRING HE, M329A1 27 INC (M36A1)

PR2 = 0 psi  
PR3 = 609 psi

PROJECTILE TRAVEL, VELOCITY, BREECH PRESSURE, VS TIME

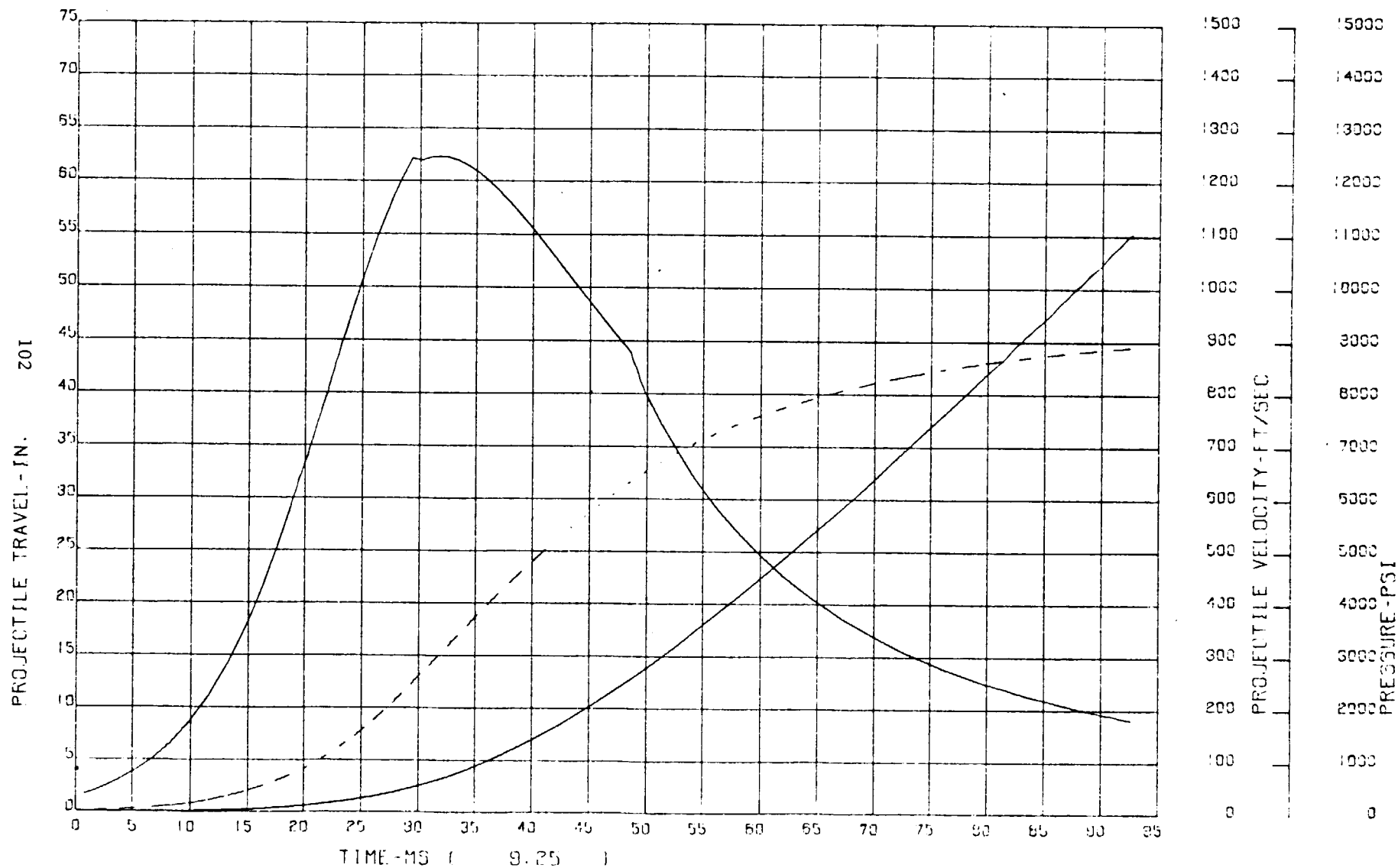


4.2-INCH MORTAR, M30 FIRING HE, M329A1 35 INC (M36A1)

PR2 = 0 psi

PR3 = 889 psi

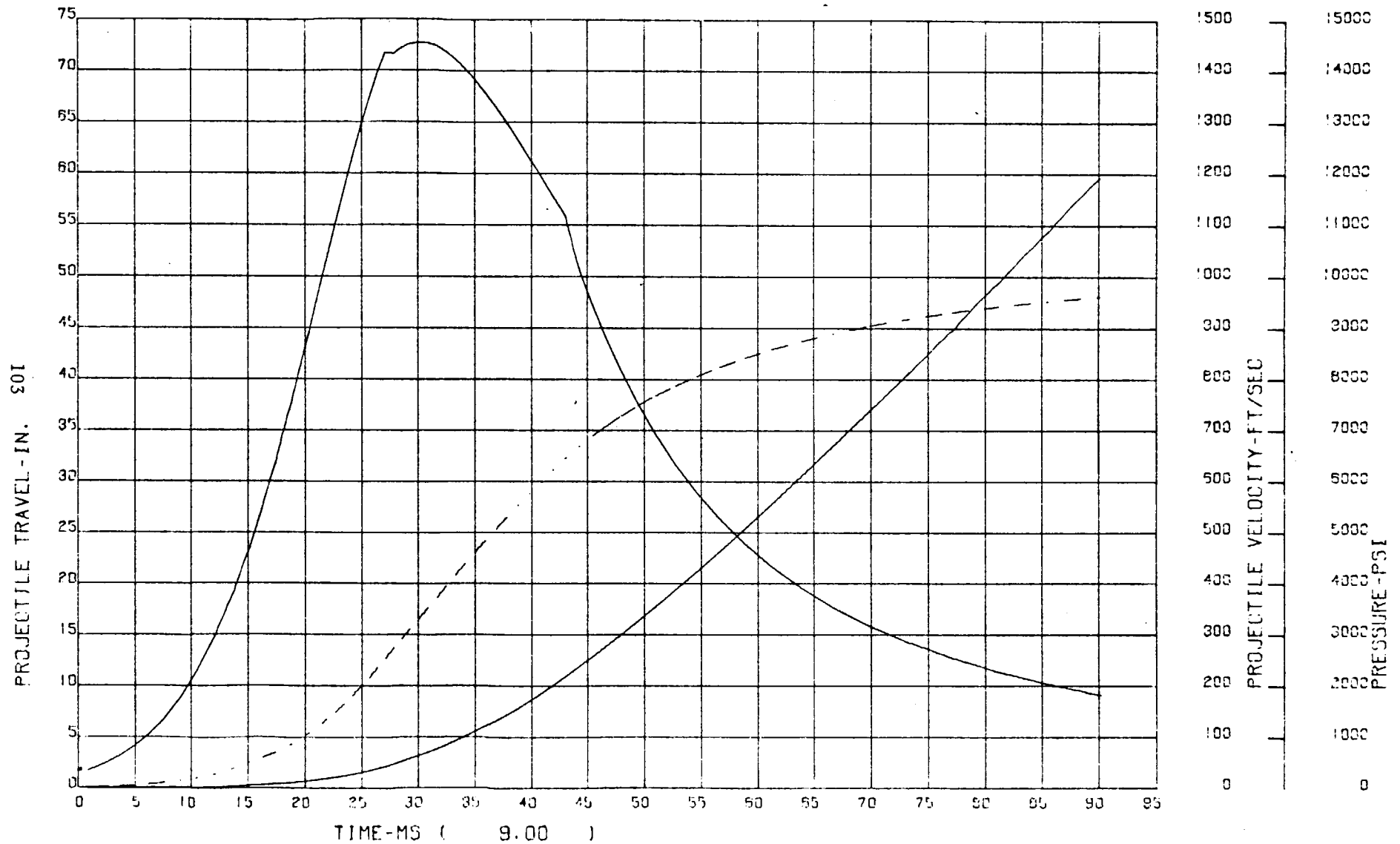
PROJECTILE TRAVEL, VELOCITY, BREACH PRESSURE, VS TIME



4.2-INCH MORTAR, M30 FIRING HE, M329A1 39 INC (M36A1)

PR2 = 0 psi  
PR3 = 951 psi

PROJECTILE TRAVEL, VELOCITY, BREECH PRESSURE, VS TIME

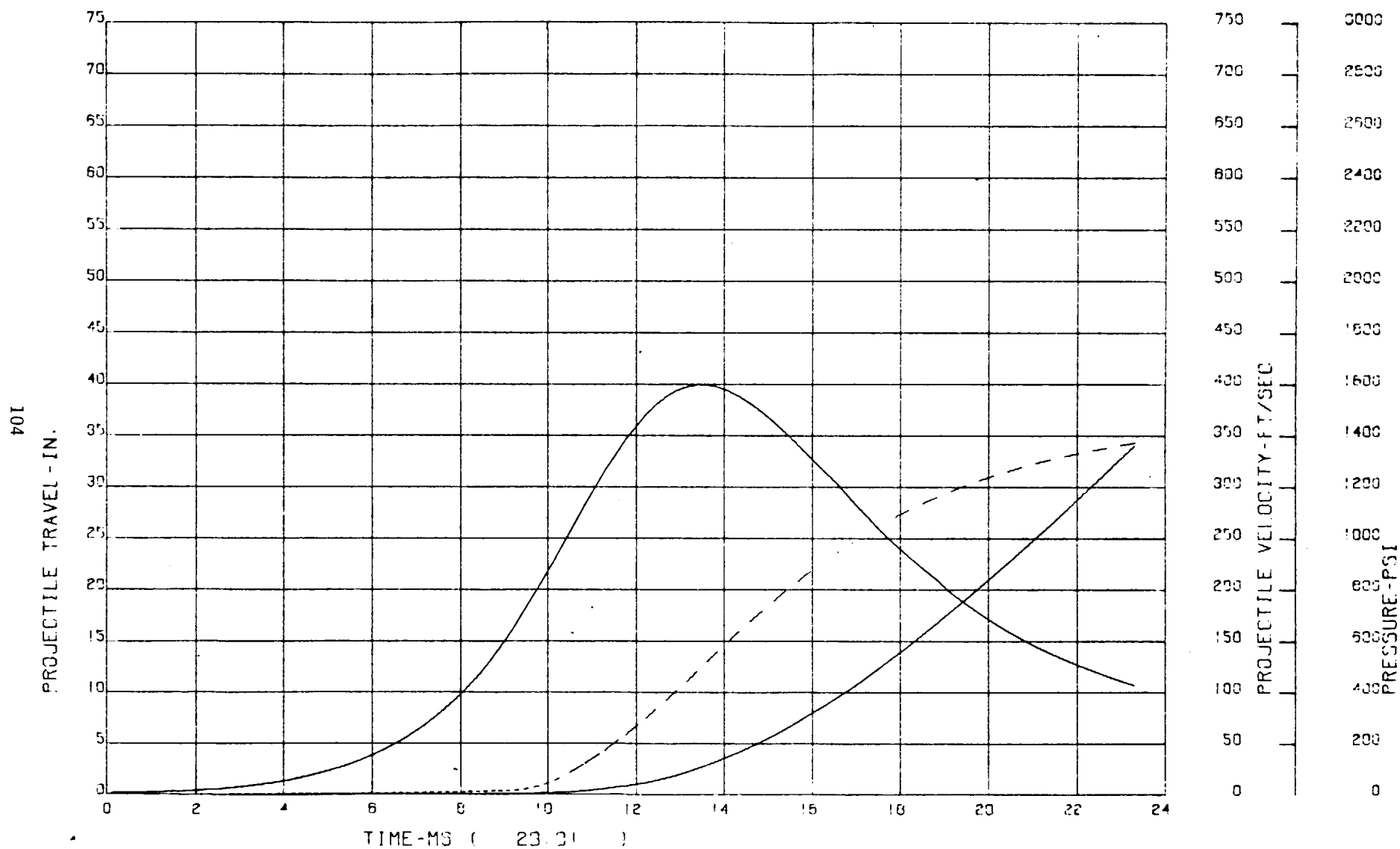


81MM MORTAR, M29 FIRING HE, M374 ZONE I (M30)

PR2 = 553 psi

PR3 = 168 psi

PROJECTILE TRAVEL, VELOCITY, BREACH PRESSURE, VS TIME

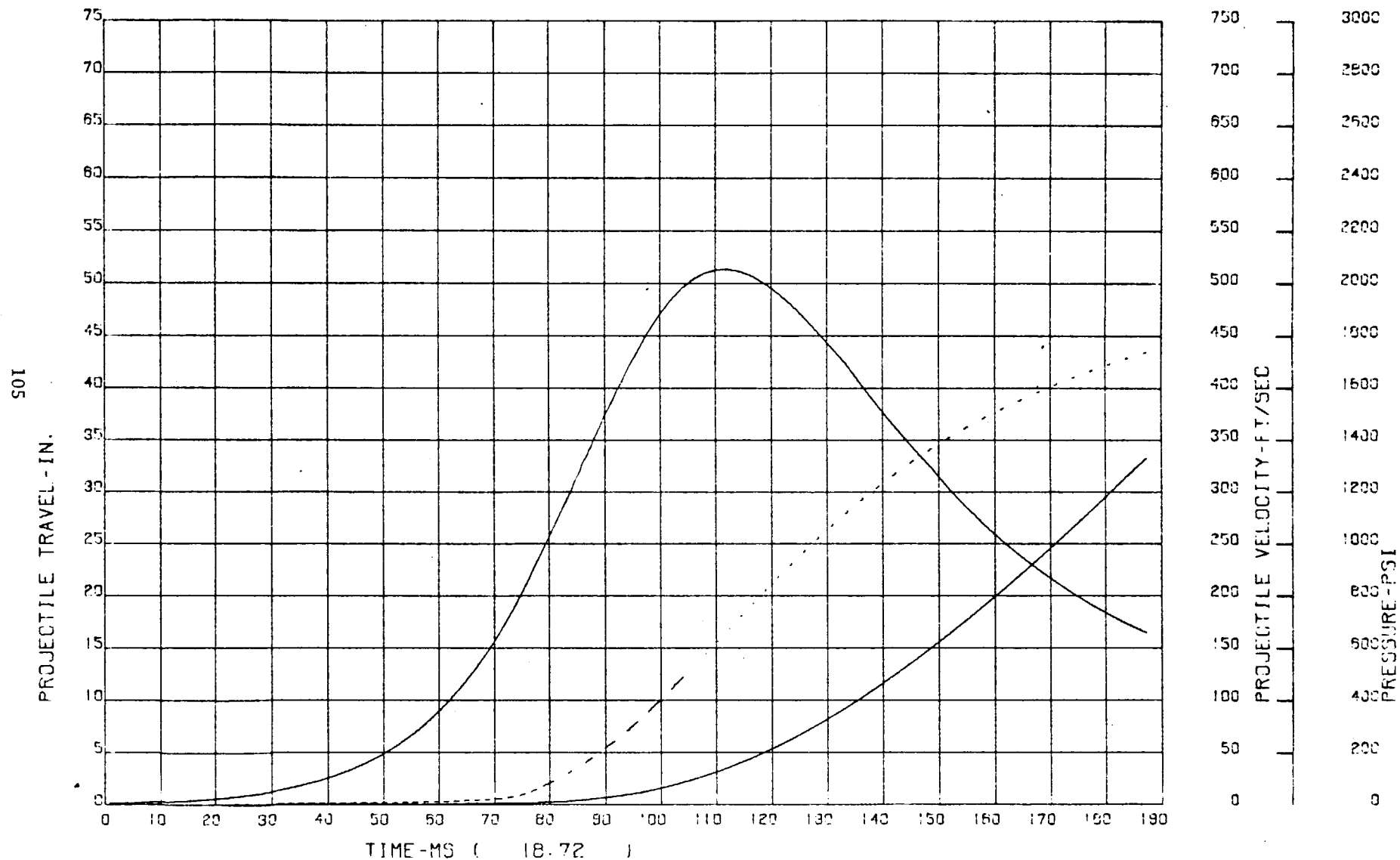


81MM MORTAR, M29 FIRING HE, M374 ZONE 2 (M90)

PR2 = 484 psi

PR3 = 58 psi

PROJECTILE TRAVEL, VELOCITY, BREACH PRESSURE, VS TIME

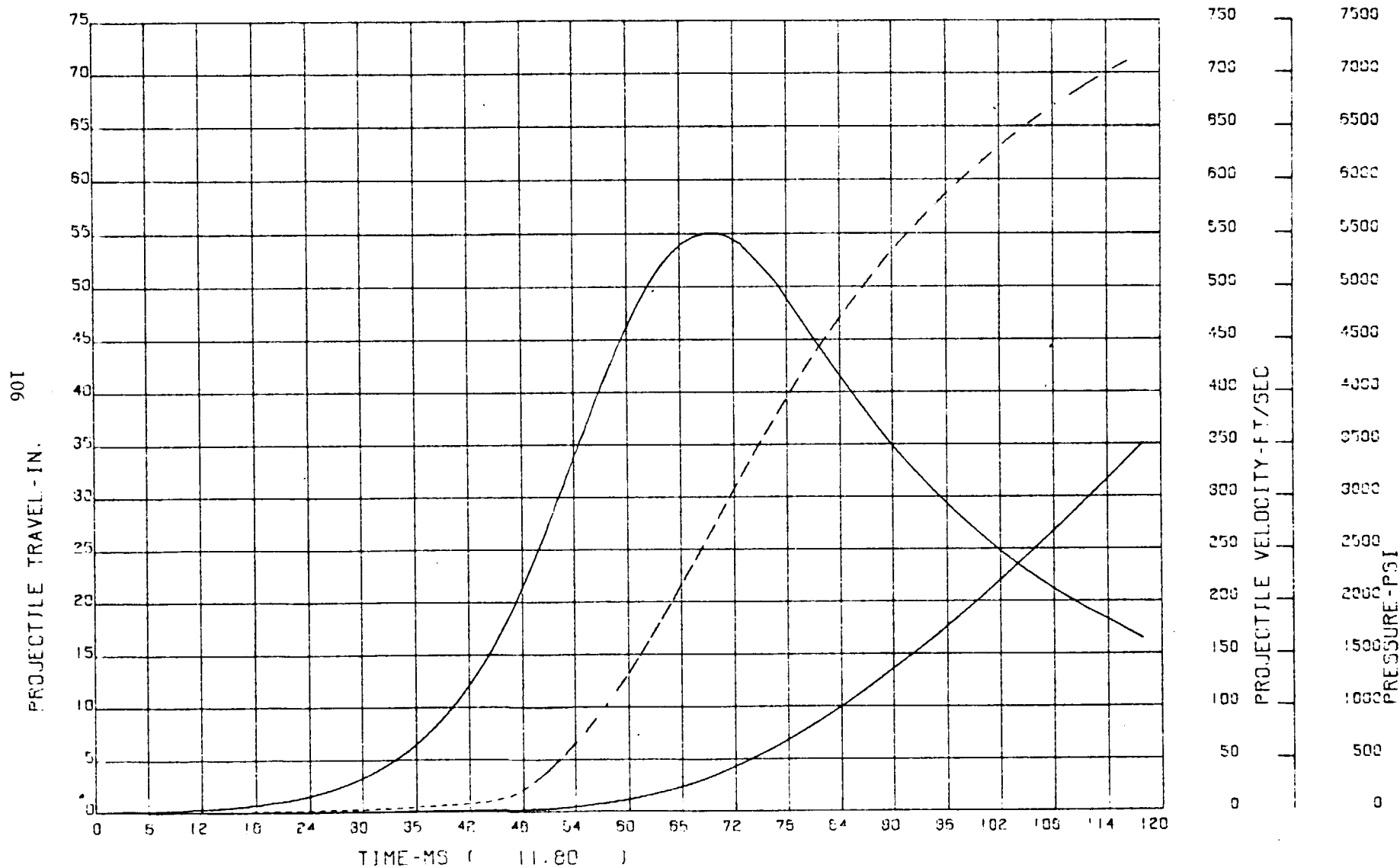


81MM MORTAR, M29 FIRING HE, M374 ZONE 6 (M90)

PR2 = 1079 psi

PR3 = 93 psi

PROJECTILE TRAVEL, VELOCITY, BREECH PRESSURE, VS TIME

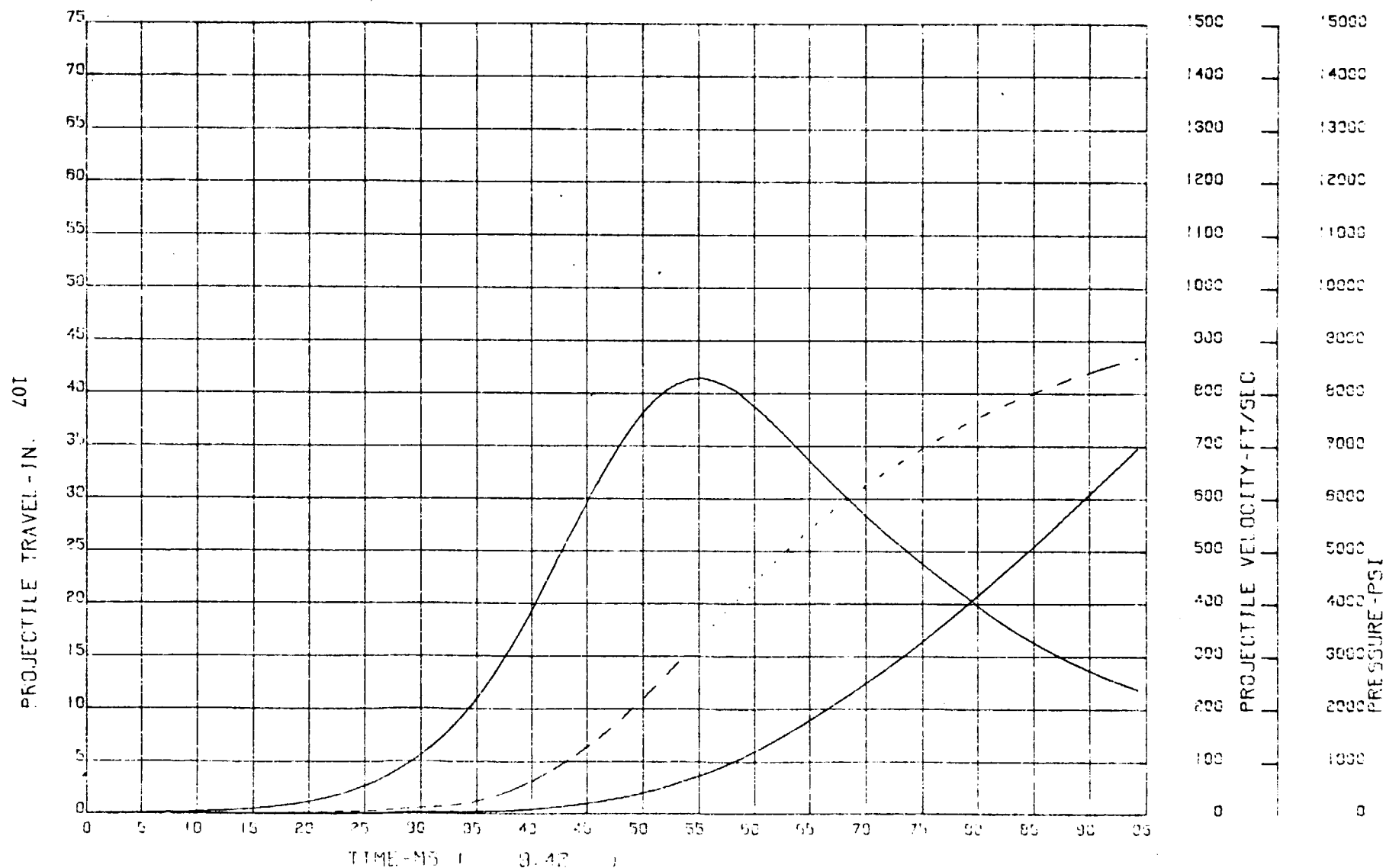


81MM MORTAR, M29 FIRING HE, M374 ZONE 9 (M90)

PR2 = 765 psi

PR3 = 241 psi

PROJECTILE TRAVEL, VELOCITY, BREECH PRESSURE, VS TIME



# APPENDIX C

Propellant Characteristics							
Weapon	Charge Model	Composition	Zone	Web Size Inches	Geometry	Burning Rate Coefficient In/Sec psi	Propellant Force In-Lb/Lb
8-inch Howitzer Firing HE, M106	M1	M1	1 - 5	.0161	SP*	.00050790	3670150.
	M2	M1	5 - 7	.0414	MP	.00050790	3670150.
175mm Gun Firing HE, M437	M86	M6	1 - 3	.0798	MP	.00025620	3813960.
155mm Howitzer M1 Firing HE, M107	M3	M1	1 - 5	.0165	SP	.00050790	3670150.
	M4A1	M1	3 - 7	.0336	MP	.00050790	3670150.
155mm Howitzer M109 Firing HE, XM549 RAP	M3A1	M1	1,3,5	.01	SP	.00050790	3670150.
	M4A2	M1	3,5,7	.0336	MP	.00050790	3670150.
105mm Gun, M68, Firing, APDS, M392A2		M30	-	.0460	MP	.00481900	4734000.
4.2-inch Mortar, M30 Firing HE, M329A1	M36A1	M9	5	.0370	Disc	.00080880	4760820.
	M36A1	M8 + M9	11,15, 19,27, 35,39	.7000	Disc and Sheet		
81mm Mortar, M29 Firing HE, M374	M90	M9	1,2, 6,9	.0330	**Disc	.00080880	4760820.

\*SP = Single Perforation, MP = Multiple Perforation

\*\*Discs are three different sizes

# APPENDIX D

Characteristics of 8-inch Howitzer, M2 Firing Projectile, HE, M106, Propelling Charge M1  
(1-5) Single Perforation and Propelling Charge M2 (5-7) Multiple Perforation

## Gun Parameters

Travel of Projectile - In	168
Chamber Volume In <sup>3</sup>	1545
Bore Area - In <sup>2</sup>	51.32
Bore Diameter - In	8.000
Projectile Weight - Lb	200.0

## Propellant Properties

	Propellant	Igniter
Type	(M1)	Black Powder
Force - In-Lb/Lb	3,670,150	1,152,000
Specific Heat Ratio	1.264	1.25
Covolume - In <sup>3</sup> /Lb	31.080	
Molecular Weight - Lb/Lb-Mole		
Burning Rate Coefficient - In/Sec-psi	.0005079	
Burning Rate Exponent	.8497	

	M1	M2	
Weight - Lb	5.33 (Zone 1)	16.62 (Zone 5)	.3125
	6.28 (Zone 2)	21.84 (Zone 6)	
	7.52 (Zone 3)	28.05 (Zone 7)	
	9.54 (Zone 4)		
	13.16 (Zone 5)		

# APPENDIX D (Continued)

<u>Propellant Dimensions</u>	(M1)	(M2)
Outside Diameter of Grain - In	.050	.230
Diameter of Perforation - In	.020	.020
Length of Grain - In	.220	.530
Web - In	.0161	.0414
Number of Perforations	1	7
Length/Diameter Ratio	4.400	2.304
Outside Diameter/Diameter of Perforation Ratio	2.50	11.50

## Gun Simulation Data

110	Shot Start Pressure - psi	0		
	Engraving Resistance Pressure psi		PR <sub>1</sub>	PR <sub>2</sub>
				PR <sub>3</sub>
	Zone 1 M1	0	2225	370
	Zone 2 M1	0	2575	395
	Zone 3 M1	0	3110	385
	Zone 4 M1	0	3175	310
	Zone 5 M1	0	3650	310
	Zone 5 M2	0	6900	310
	Zone 6 M2	0	8550	320
	Zone 7 M2	0	12400	320
Propellant Erosion Constant		Single Perforation	.00001 (M1)	
		Multiple Perforation	.00004 (M2)	

# DISTRIBUTION LIST

<u>No. of Copies</u>	<u>Organization</u>	<u>No. of Copies</u>	<u>Organization</u>
2	Commander Defense Documentation Center ATTN: TIPCR Cameron Station Alexandria, Virginia 22314	1	Commanding General U.S. Army Tank-Automotive Command ATTN: AMSTA-RIIFL Warren, Michigan 38090
1	Commanding General U.S. Army Materiel Command ATTN: AMCDL Washington, DC 20315	1	Commanding Officer U.S. Army Mobility Equipment Research & Development Center ATTN: Tech Doc Cen, Bldg. 315 AMSME-RZT Fort Belvoir, Virginia 22060
1	Commanding General U.S. Army Materiel Command ATTN: AMCRD, Dr. J.V.R.Kaufman Washington, DC 20315	1	Commanding General U.S. Army Munitions Command ATTN: AMSMU-RE Dover, New Jersey 07801
1	Commanding General U.S. Army Materiel Command ATTN: AMCRD-TE Washington, DC 20315	1	PLASTEC U.S. Army Picatinny Arsenal ATTN: SMUPA-FR-M-D Dover, New Jersey 07801
1	Commanding General U.S. Army Materiel Command ATTN: AMCRD-TP Washington, DC 20315	2	Commanding General U.S. Army Weapons Command ATTN: AMSWE-RE AMSWE-RDF Rock Island, Illinois 61202
1	Commanding General U.S. Army Aviation Systems Command ATTN: AMSAV-E 12th & Spruce Streets St. Louis, Missouri 63166	1	Director U.S. Army Advanced Materiel Concepts Agency 2461 Eisenhower Avenue Alexandria, Virginia 22314
1	Commanding General U.S. Army Electronics Command ATTN: AMSEL-RD Fort Monmouth, New Jersey 07703	1	Director U.S. Army Air Mobility Research & Development Laboratory Ames Research Center Moffett Field, California 94035
1	Commanding General U.S. Army Missile Command ATTN: AMSMI-R Redstone Arsenal, Alabama 35809	1	Commanding Officer U.S. Army Harry Diamond Laboratories ATTN: AMXDO-TD/002 Washington, DC 20438

DISTRIBUTION LIST

<u>No. of</u> <u>Copies</u>	<u>Organization</u>
1	Commanding Officer U.S. Army Materials & Mechanics Research Center ATTN: AMXMR-ATL Watertown, Massachusetts 02172
1	Commanding General U.S. Army Natick Laboratories ATTN: AMXRE, Dr. D. Sieling Natick, Massachusetts 01762
3	Commander U.S. Naval Air Systems Command ATTN: AIR-604 Washington, DC 20360
3	Commander U.S. Naval Ordnance Systems Command ATTN: ORD-0632 ORD-035 ORD-5524 Washington, DC 20360

Aberdeen Proving Ground

Chief, Tech Lib  
Marine Corps Ln Ofc  
CDC Ln Ofc

UNCLASSIFIED

Security Classification

## DOCUMENT CONTROL DATA - R &amp; D

(Security classification of title, body of abstract and indexing annotation must be entered when the overall report is classified)

1. ORIGINATING ACTIVITY (Corporate author) U. S. Army Ballistic Research Laboratories Aberdeen Proving Ground, Maryland		2a. REPORT SECURITY CLASSIFICATION Unclassified	
		2b. GROUP	
3. REPORT TITLE DETERMINATION OF MUZZLE VELOCITY CHANGES DUE TO NONSTANDARD PROPELLANT TEMPERATURE USING AN INTERIOR BALLISTIC COMPUTER SIMULATION			
4. DESCRIPTIVE NOTES (Type of report and inclusive dates)			
5. AUTHOR(S) (First name, middle initial, last name) James F. O'Bryon			
6. REPORT DATE September 1972		7a. TOTAL NO. OF PAGES 112	7b. NO. OF REFS 25
8a. CONTRACT OR GRANT NO.		9a. ORIGINATOR'S REPORT NUMBER(S) BRL Memorandum Report No. 2225	
b. PROJECT NO. RDT&E 1T562603A041			
c.		9b. OTHER REPORT NO(S) (Any other numbers that may be assigned this report)	
d.			
10. DISTRIBUTION STATEMENT Approved for public release; distribution unlimited.			
11. SUPPLEMENTARY NOTES		12. SPONSORING MILITARY ACTIVITY US Army Materiel Command Washington, D. C.	
13. ABSTRACT An interior ballistic computer model is used to study means of simulating the effects of firing weapons using propellants which are not conditioned to 70 degrees F. Functions of burning rate coefficient and propellant force are empirically determined and are used to simulate these effects on muzzle velocity for a wide variety of weapon systems in the current inventory. The simulated velocity changes are compared with data gathered from firings conducted at several discrete propellant temperatures. In the majority of cases, the precision in predicting the changes in muzzle velocity at any given temperature falls within the round-to-round velocity probable error at that same temperature. This method should prove to be sufficiently accurate to permit a significant reduction in the number of rounds fired to determine propellant temperature effects on velocity.			


DD FORM 1473  
1 NOV 65REPLACES DD FORM 1473, 1 JAN 64, WHICH IS  
OBSOLETE FOR ARMY USE.

UNCLASSIFIED

Security Classification

UNCLASSIFIED

Security Classification

14. KEY WORDS	LINK A		LINK B		LINK C	
	ROLE	WT	ROLE	WT	ROLE	WT
Propellant Temperature Interior Ballistics Burning Rate Coefficient Computer Model Temperature Sensitivity Engraving Pressure						
						

UNCLASSIFIED

Security Classification